Design of Rock Socketed Drilled Shafts

September 1998
Final Report

University of Nebraska - Lincoln, W333.2 Nebraska Hall Lincoln, NE 68588-0530

University of Nebraska-Lincoln Iowa State University Kansas State University
University of Kansas University of Missouri-Columbia University of Missouri-Rolla

Design of Rock Socketed Drilled Shafts

September 1998
Final Report

Brett Gunnink and Chad Kiehne
University of Missouri-Columbia
Department of Civil Engineering
Columbia, MO 65211-2200

Mid-America Transportation Center
University of Nebraska-Lincoln
W333.2 Nebraska Hall
Lincoln, NE 68588-0530
Telephone 402-472-1974
Fax 402-472-0859
MATC Project No. MATC UMC96-1

Sponsored by

Hayes Drilling, Inc.
8845 Prospect
Kansas City, MO 64132
Telephone: 816-363-3040
Fax: 816-393-3060

REPORT DOCUMENTATION PAGE

Form Approved
OMB No. 0704-0188

PB98-175110

2. REPORT DATE	3. REPORT TYPE AND DATES COVERED
September 1998	Final Report

4. TITLE AND SUBTITLE

Design of Rock Socketed Drilled Shafts

5. FUNDING NUMBERS

DTRS95-G-0007

6. AUTHOR(S)

Brett Gunnink and Chad Kiehne

7. PERFORMING ORGANIZATION NAME(S) AND ADDRESS(ES)

Mid-America Transportation Center
University of Nebraska-Lincoln
W333.2 Nebraska Hall
Lincoln, NE 68588-0530

8. PERFORMING ORGANIZATION REPORT NUMBER

MATC UMC96-1

9. SPONSORING /MONITORING AGENCY NAME(S) AND ADDRESS(ES

Hayes Drilling, Inc.
8845 Prospect
Kansas City, MO 64132

10. SPONSORING /MONITORING NUMBER

N/A

11. SUPPLEMENTARY NOTES

12a. DISTRIBUTION/AVAILABILITY STATEMENT

This document is available to the public

12b. DISTRIBUTION CODE

13. ABSTRACT ***(Maximum 200 words)***

Three field load tests of drilled shafts socketed in Burlington limestone were conducted using the Osterberg load cell. The objective of these tests was to compare the shaft capacities obtained from the field load tests with capacities predicted using analytical methods and with typical presumptive design capacities. It was believed that the actual capacities of the drilled shafts would be considerably greater than the capacities predicted from presumptive bearing capacity values. Based on the results of this testing the following conclusions were drawn. Observed values of side resistance are comparable to the predicted values obtained from empirical relationships. Observed values of end bearing pressure greatly exceed the presumptive values of allowable bearing capacity commonly used for the design of shafts bearing on Burlington limestone. The test shafts were not failed in end bearing and it is believed that the ultimate end bearing pressures would significantly exceed the observed end bearing pressures.

The actual factors of safety of shafts in Burlington limestone that are designed for end bearing only, using typical presumptive end bearing capacities, will exceed 6. Side resistance will carry a large portion of the load and for service loads, the entire load may be carried by side friction.

14. SUBJECT TERMS

Foundations, Drilled Shafts, Osterberg Cell, Load Test

15. NUMBER OF PAGES

177

16. PRICE CODE

17. SECURITY CLASSIFICATION OF REPORT	18. SECURITY CLASSIFICATION OF THIS PAGE	19. SECURITY CLASSIFICATION OF ABSTRACT	20. LIMITATION OF ABSTRACT
Unclassified	Unclassified	Unclassified	

PREFACE

The following is the final report for the Mid-America Transportation Center (MATC) research project (MATC/UMC95-1) entitled *Design of Rock Socketed Drilled Shafts*. The report is comprised of two sections. The first section is a paper entitled *Capacity of Rock Socketed Drilled Shafts in Burlington Limestone.* This paper has been submitted for consideration for publication in the *ASCE Journal of Geotechnical Engineering*. It is a fairly thorough and somewhat brief summary of the project. The authors suggest that interested parties read this section first. If the reader's depth of interest is greater, the second section of the report is a thesis entitled *Full Scale Load Tests of Rock Socketed Drilled Shafts.* It is a thorough review of the project. The thesis contains, in appendix, a report entitled *Design of Rock Socketed Drilled Shafts.* This is a review of many of the current design procedures available for rock socketed drilled shafts and may be of interest to some readers. Finally, a presentation related to this project will be made at the Crossroads 2000 Transportation Research Conference. The conference will be held August 19-20, 1998 at Iowa State University, Ames Iowa. A paper entitled *Pile Bearing in Burlington Limestone* will appear in the proceedings of this conference.

This research projected was funded by the Mid-America Transportation Center (MATC). MATC is a Department of Transportation (DOT) and Federal Transit Authority (FTA) University Transportation Center (UTC). The research was also supported by the University of Missouri-Columbia (MU); Hayes Drilling of Kansas City, Missouri; LOADTEST Inc., of Gainsville, Florida; and Engineering Surveys and Services (ESS) of Columbia, Missouri. The author's would like to express their thanks to these organizations and the individual within these organizations for their support and help with this research.

TABLE OF CONTENTS

PREFACE ii

TABLE OF CONTENTS iii

SECTION I - *Capacity of Rock Socketed Drilled Shafts in Burlington Limestone* iv

ABSTRACT	2
INTRODUCTION	3
BACKGROUND INFORMATION	3
TEST METHODS AND PROCEDURES	7
RESULTS AND DISCUSSION	9
CONCLUSIONS	15
ACKNOWLEDGEMENTS	15

SECTION II - *Full Scale Load Tests of Rock Socketed Drilled Shafts* v

ACKNOWLEDGEMENTS	ii
ABSTRACT	iii
LIST OF TABLES	iv
LIST OF FIGURES	v
CHAPTER ONE INTRODUCTION	1
CHAPTER TWO LITERATURE REVIEW	3
CHAPTER THREE TEST METHODS AND PROCEDURES	4
CHAPTER FOUR RESULTS AND DISCUSSION	24
CHAPTER FIVE SUMMARY OF CONCLUSIONS	60
REFERENCES	62
APPENDIX A	65
APPENDIX B	110
APPENDIX C	114
APPENDIX D	133

SECTION I

Capacity of Rock Socketed Drilled Shafts in Burlington Limestone

Capacity of Rock Socketed Drilled Shafts in Burlington Limestone

by

Brett Gunnink and Chad Kiehne

Corresponding Author: Brett Gunnink
Department of Civil Engineering
University of Missouri-Columbia
Columbia, MO 65211-2200
(573) 882-3299
FAX (573) 882-4784
E-mail gunnink@risc1.ecn.missouri.edu

Other Authors: Chad Kiehne
Black & Veach Engineers-Architects
P.O. Box 8405
Kansas City, MO 74114
(913) 458-3406

ABSTRACT

Three field load tests of drilled shafts socketed in Burlington limestone were conducted using the Osterberg load cell. The objective of these tests was to compare the shaft capacities obtained from the field load tests with capacities predicted using analytical methods and with typical presumptive design capacities. It was believed that the actual capacities of the drilled shafts would be considerably greater than the capacities predicted from presumptive bearing capacity values. Based on the results of this testing the following conclusions were drawn. Observed values of side resistance are comparable to the predicted values obtained from empirical relationships. Observed values of end bearing pressure greatly exceed the presumptive values of allowable bearing capacity commonly used for the design of shafts bearing on Burlington limestone. The test shafts were not failed in end bearing and it is believed that the ultimate end bearing pressures would significantly exceed the observed end bearing pressures. The actual factors of safety of shafts in Burlington limestone that are designed for end bearing only, using typical presumptive end bearing capacities, will exceed 6. Side resistance will carry a large portion of the load and for service loads, the entire load may be carried by side friction.

Key Words: Foundations, Drilled Shafts, Osterberg Cell, Load Test

INTRODUCTION

It is common engineering practice to design rock-socketed drilled shafts for end bearing only, based on conservative presumptive values of allowable bearing capacity. For example, for the Burlington limestone studied in this paper, a typical allowable bearing capacity is 1914 kPa (40,000 psf). The use of conservative values is due in part to the lack of full scale field load test data that would allow for the validation of less conservative design procedures. Often, site investigations terminate at auger refusal, in which case only the location of the rock is known and very little is known about rock strength. Further, the difficulty and cost of performing full scale load tests of drilled shafts in rock, limits the amount of data available for design procedure validation. Recently, the development of the Osterberg load cell provided a more economical means for conducting load tests. To date, the Osterberg load cell has not been used extensively in Mid-America and particularly it has not been used extensively in limestone.

Three field load tests of drilled shafts socketed in Burlington limestone were conducted. The objective of these tests was to compare the shaft capacities obtained from the field load tests with capacities predicted using analytical methods and with typical presumptive design capacities. It was believed that the actual capacities of the drilled shafts would be considerably greater than the capacities predicted from presumptive bearing capacity values.

BACKGROUND INFORMATION

Design of Rock Socketed Drilled Shafts

A detailed review of rock socketed drilled shaft design procedures is presented by Kiehne (1). The function of a rock socketed drilled shaft is to transfer structural loads through upper non-

competent strata to depths where sound rock can sustain these loads. The load is transmitted to the bedrock through two basic load bearing mechanisms, end bearing and side resistance.

The axial load capacity of a rock socketed drilled shaft is the ultimate load that the shaft may support before failure. This capacity depends on the combination of the end bearing load capacity and the side resistance load capacity. The stress developed along the interface of the rock of the socket and the concrete by the axial load is referred to as side resistance. This stress is a result of the sliding friction along the shaft and the bond between the rock and concrete. The stress developed at the bottom of the socket is referred to as end bearing pressure. The end bearing pressure is a result of the compressive loading between the bottom of the rock socket and the bottom of the shaft. The side resistance load capacity can be found by simply multiplying the area of concrete rock bond by the predicted side resistance. The end bearing load capacity can by found by multiplying the area of the end of the shaft by the predicted end bearing pressure.

Four approaches to the design for rock socketed drilled shafts were presented by Rosenberg and Journeaux (2). A brief description of the four approaches to design follows:

Design For End Bearing Only

When a rock socketed drilled shaft is designed in end bearing only, the socket base must be sized so that the end bearing pressure does not exceed the allowable end bearing capacity of the rock. The side resistance developed between the concrete and the socket walls is ignored with this approach. The approach is based on the assumption that all of the axial load is transferred to the socket base. This is a conservative assumption, resulting in the actual end bearing pressure at the bottom of the socket generally being significantly less than the assumed value. Field tests have

indicated that even in fractured rock the concrete to rock bond is significant (2); therefore, a significant portion of the applied load is carried by side friction, especially at service load levels.

Design for Side Resistance Only

This approach assigns an average side resistance to the entire rock-concrete bond area, but the load carrying capacity developed in end bearing is ignored entirely. This approach is usually employed under extremely poor rock conditions and when the socket base cannot be properly cleaned. This approach generally results in extremely deep sockets.

Design for Allowable End Bearing and Carrying the Remaining Load in Side Resistance

This approach assigns an allowable end bearing capacity for the socket base. The allowable end bearing load capacity is then subtracted from the axial load. The socket length is then designed to carry the remaining load in side resistance. This method does not consider the actual stresses developed in the socket base. Instrumented shafts have shown that the actual stresses developed may be in variance with the assumptions made. Rosenberg and Journeaux, (2) report that the socket base end bearing pressures were lower and the side resistance bond stress higher than anticipated.

Design with Estimated Developed End Bearing and Side Resistance

This approach assumes that part of the applied load is dissipated and carried by side resistance and that the remaining load produces the actual developed end bearing pressure at the socket base. A prediction of the load carried by end bearing is required. Based on this prediction, an allowable end bearing pressure is assigned. It is assumed that the rest of axial load is carried in

side resistance. The socket depth is then adjusted so that the allowable values for end bearing capacity and side resistance are not exceeded. A difference between this method and the other three methods is that the knowledge of the relationship between applied axial stress and the actual developed end bearing stress for various socket embedments and rock properties is required. This information is not readily available nor easily determined.

Osterberg Load Cell

The Osterberg load cell was developed and patented by Dr. Jorj Osterberg (3). The Osterberg load cell is a static load testing device for shafts and piles. An Osterberg cell load test uses an especially designed "pancake-like" hydraulic jack and associated fittings to create pressures in excess of 55 MPa (8,000 psi) at the bottom of the shaft, loading the pile or shaft in end bearing and upward side resistance. The cell is typically slightly smaller in diameter than the shaft or pile and cast in the base during construction of the shaft or placed at the tip of a driven pile.

The Osterberg load cell is lowered into the shaft via the reinforcing cage or if no reinforcement cage is used, a small I-beam or channel can be used to place the load cell. The hydraulic lines and telltale rod casings are also attached to the reinforcement cage. The telltale rods allow for the measurement of the movement of the bottom and the top of the cell. These movements and the movement of the top of the shaft or pile are measured using dial gages supported by an independent reference beam.

The Osterberg cell is pressurized using a compressed air driven pump with diluted automotive antifreeze as the hydraulic fluid. The soil and/or rock surrounding the shaft or pile provides the reaction for the load test. As the cell is pressurized, the bottom of the cell moves downward, testing end bearing, while the top of the cell moves upward, testing side resistance.

The cell is expanded until the expansion force is some desired multiple of the design loading, The O-cell reaches its maximum expansion, or the shaft fails in either end bearing or side resistance. The hydraulic loading can be held at a relatively constant load level allowing for the study of creep. The load may also be cycled to study the effects of repetitive loading. At the completion of the test, the cell may be filled with grout to reestablish its integrity and permit the test shaft or pile to become a component of the structure. Schmertmann, (4), fully discusses the advantages and disadvantages of the use of the use of the Osterberg load cell.

TEST METHODS AND PROCEDURES

Shaft Excavation

Hayes Drilling Inc. of Kansas City, MO, began shaft construction on December 9, 1996. Three shafts were excavated using a truck-mounted rotary drill. An 45.72 cm (18 in.) diameter auger bit with carbide cutting teeth was used to excavate the overburden as well as the rock socket. Water was used as lubrication during the drilling process and to facilitate the removal of the rock cuttings. The base of the socket was cleaned by rapidly spinning the auger bit after the addition of water and then lifting out the rock cuttings.

Osterberg Cell Assembly and Placement

The Osterberg cells used in the base of the three shafts were 33 cm (13 in.) in diameter and approximately 31.75 cm (12.5 in.) high. The cells had a maximum load producing capability of 4000 kN (450 tons). A 40.64 cm (16 in.) diameter 1.27 cm (0.5 in.) thick steel base plate was welded to the bottom of the load cell.

The Osterberg cell was welded to a frame constructed steel channel sections. This frame enabled the cell to be lowered into the shaft safely and also supported two hydraulic lines and four telltale rod casings. Two telltale casings were attached to opposite sides of the base plate and the remaining two casings were attached to opposite sides of the top of the Osterberg cell. Figure 1 illustrates the Osterberg cell assembly.

After the completion of drilling, a small seating layer of concrete was placed by free fall into the base of the shaft. The Osterberg cell base plate was greased to ensure no concrete adhesion. The cell was then lowered into the shaft using the channel frame and seated onto the base layer of concrete. The remaining concrete was then placed by free fall into the shaft. Three concrete test cylinders were made for each shaft so that the strength of the concrete could be measured. The concrete was allowed to cure for 6 days before the load test was performed. The concrete mix was a Missouri DOT state B paving mix with entrained air. The predicted strength was 27.5 Mpa (4000 psi). The average concrete strength at the time of shaft testing was 47.2 Mpa (5300 psi).

Load Test Procedure

A steel channel reference beam was placed near the drilled shaft assembly. Six Ames digital dial gages were attached to the reference beam or steel channel by magnetic stands. The dial gages were designated A through F. Machined steel telltale rods were inserted into the telltale casings. Dial gages A and B measured the downward displacement of the base plate telltale rods and dial gages C and D measured the upward displacement of the top of shaft. Dial gages E and F were attached to the channel frame and measured the displacement between the top of cell telltale rods

and the top of the shaft or otherwise stated they measured the compression of the shaft. The dial gages were connected to a laptop PC to collect the data.

A hydraulic pump driven by a regulated air compressor was used to pressurize the Osterberg cell. The hydraulic fluid was diluted automotive antifreeze. The Osterberg cell was pressurized in increments of approximately 3445 kPa (500 psi). The pressure was held at each loading increment for a total of 4 minutes. The automated data collection system recorded movements at 30 second intervals. Along with the automated data collection system, data was recorded manually at 4 minute intervals with an average of 30 seconds required to adjust the cell pressure to the next load interval. The load increments were increased until side friction shear failure occurred.

RESULTS AND DISCUSSION

Site Geology

The geology of the Boone county Missouri area is characterized by Pleistocene age glacial drift that overlays Pennsylvanian aged limestone and shale which overlay Mississippian aged limestone (5). The glacial drift is moderately to highly overconsolidated and exhibits high shear strength and low compressibility.

Pennsylvanian rock deposits in this area are composed of mainly shale with interbedded limestone. These types of rock deposits occur erratically in the Columbia and Boone County area. The deposits tend to be thickest where they overlie valleys and depressions in the underlying Mississipian surface.

The Mississipian aged rock formations in this area are mostly of the Burlington formation. The Burlington formation is a fairly coarse-grained, massive, clastic limestone. The upper portion

is commonly white to light gray or buff in color, and the lower portion is characteristically buff to reddish brown. The upper portion of the formation is also characterized by an abundance of chert. The limestone has been severely weathered to produce deep solution channels and a pinnacled surface. The Burlington formation also exhibits high shear strength and low compressibility characteristics.

Site Investigation

The initial site investigation consisted of collecting eight previous subsurface investigations that were performed in the general vicinity of the three research shafts. These investigations were performed from 1988 to 1995 by Engineering Surveys and Services of Columbia, Missouri for the purpose of new construction.

The subsurface conditions of the area are highly variable. The overburden consisted of mostly glacial drift. This ranged in depth from zero to over 6 m (20 ft.). The drift consisted of sandy clay, sandy silty clay, gravelly clay and is sometimes underlain by the Pennsylvanian shales. These materials are underlain by massive Mississippian limestone bedrock.

Burlington limestone bedrock depths in the area range between 1.8 and 12.8 m (6 and 42 feet). The surface of the limestone is irregular and weathered in some areas. The weathered layer varied in thickness from a few centimeters to over a meter. Cores of this limestone are tan or light buff to bluish gray. Beds of chert, inclusions of pyrite, and calcite-filled fractures were found within the limestone.

Three unconfined compression strength tests of Burlington limestone core samples show a 43.6 MPa (6,336 psi), 73.8 MPa (10,718 psi) , and 64.7 MPa (9,395 psi) rock strength. Four core samples provided rock quality designations (RQD) and percent recoveries These include a

90 percent recovery with a 78 RQD, a 100 percent recovery with an 80 RQD, a 100 percent recovery with a 100 RQD, and a 100 percent recovery with an 85 RQD.

During the drilling of the shafts glacial till was found at the surface. It was predominantly clay with some silt, sand and gravel. No shale was found during the drilling process. However, a thin layer of weathered limestone was encountered on top of the limestone bedrock..

After completion of the shafts, a feeler gage was used to scrape the sides of the socket in order to find seams or fractures. Small seams were found in shafts 1 and 2 but no seams were detected in shaft 3. No ground water was encountered in any of the shafts. Depth profiles for the shafts are shown in the Table 2.

Downward End Bearing and Upward Side Resistance Load Movement Curves

The downward end bearing load movement curves were obtained directly from dial gages A and B, which measured the difference between the displacement of the reference beam and the telltale rods extending to the base of the cell. The upward side resistance movement was obtained directly from dial gages C and D, which measured the difference between the displacement of the reference beam and the top of the shaft. The pressure corresponding to the above movements was obtained from the pressure transducer. The load was then calculated using the Osterberg cell calibration curves. The side resistance load is the net load calculated by subtracting the weight of the shaft from the cell load. The loads for the downward end bearing movement are the cell loads.

Shafts 1 and 3 were loaded until side resistance failure occurred. Shaft 2 was initially loaded to about 1000 kN (120 tons) and then unloaded due to a an equipment malfunction in the hydraulic pump. Shaft 2 was subsequently reloaded until side resistance failure occurred. Figures

2, 3, and 4 show the Osterberg cell load movement curves for shafts 1, 2, and 3 respectively. The upward shear movement curves are typical of side resistance failure. Side resistance failure occurred at 3500, 1500 and 3800 kN for shafts 1, 2, and 3 respectively. The downward end bearing movement curves, however, show some interesting anomalies. For shaft 3, it appears that the dial gauge B telltale casing became plugged and as a result the telltale rod did not move down with the bottom of the load cell, but rather up with the shaft. The dial gauge B telltale rod also appears to have become stuck in the casing for shaft 1. The downward end bearing movement curve for dial gauge A of shaft 3 shows a much softer response than shafts 1 or 3. This indicates that shaft 3 was not adequately clean prior to concrete placement. Finally, for all three shafts the downward end bearing movements curve show continuing downward displacement of the load cell after side resistance failure has occurred. This is possible only if simultaneous end bearing and side resistance failures occur; which seems highly unlikely. It most likely indicates that after side resistance failure, ground movement at the surface raised the elevation of the reference beam.

Reconstructed, Equivalent Top Load Movement Curve

Reconstructed, equivalent top load movement curves can be developed by adding side resistance movement data and end bearing movement data. Goodwin (6), indicates that the reconstructed curves will represent the load movement of a shaft loaded in the conventional field load test manner if 1)the end bearing load movement in a conventionally loaded shaft is the same as the load movement curve developed by the bottom of the Osterberg cell, 2)the upward side resistance movement curve for the Osterberg cell test is the same as the downward side resistance movement in a conventionally top loaded test and 3) the compression of the shaft is considered negligible and the shaft is assumed rigid.

Equivalent load movement curves were reconstructed up to the maximum test load. The equivalent top load curve for shaft 1 was reconstructed to a load of 6444 kN (724 tons). The top load curve for shaft 2 was reconstructed to a load of 2821 kN (317 tons). The top load curve for shaft 3 was reconstructed to load of 6524 kN (733 tons). The reconstructed equivalent top load movement curves for shafts 1, 2, and 3 are presented in Figures 5, 6, and 7.

Observed End Bearing Pressures and Side Resistance

The maximum side resistance of the three shafts was reached and therefore can be compared directly with predicted side resistance values. Due to the limitations of the bi-directional loading of the Osterberg cell the maximum capacity in end bearing was not reached.

Side resistance is typically predicted using empirical relationships between side resistance and either concrete or rock strength. Williams et al. (7) and Rowe and Armitage (8) provide relationships developed for used with limestone rock. The predicted side resistance capacities were calculated using a concrete strength of 47.2 Mpa (5300 psi) rather than the higher unconfined compressive strength of the rock. The lower value should be used when calculating predicted side resistance because side resistance failure will occur in the lower strength material. The predicted side resistance using the Williams relationship is 1550 kPa (225 psi) and using the Rowe and Armitage relationship it is 1252 kPa (181 psi). The observed side resistance values for shafts 1, 2 and 3 respectively are 2343 kPa (340 psi), 916 kPa (133 psi), and 2278 kPa (330 psi). The predicted values of side resistance are significantly lower than the values of side resistance observed from shafts 1 and 3. The side resistance value observed from shaft 2 is lower than predicted values. Based on this data, the authors conclude that the empirical relationships are adequate if typical design factors of safety are used.

Due to the limitations of the Osterberg cell it was not possible to reach the maximum end bearing capacity. Since the Osterberg cell loads the shaft from the bottom, the applied load can only be as large as the load bearing mechanism with the lowest capacity. In the case of shafts 1, 2, and 3 it was side resistance. The observed end bearing pressures at termination of testing were 21.4 MPa (3112 psi), 9.1 MPa (1320 psi) and 22.9 MPa (3325 psi) for shafts 1, 2, and 3 respectively.

Impact on Design Practice

It is common engineering practice to design rock-socketed drilled shafts for end bearing only, based on conservative presumptive values of allowable bearing capacity. For the Burlington limestone studied in this paper, a typical allowable bearing capacity is 1914 kPa (40,000 psf). It is also typical to specify that shafts be socketed 0.61 m (2 ft) into sound rock. The conservatism of this approach to design can be illustrated with the following example.

Given a design shaft load of 2670 kN (300 tons) and an allowable end bearing pressure of 1914 kPa, the shaft would have a design diameter of 1.37 m (54 in.). Using the lowest observed value of side resistance, 916 kPa (133 psi), the side resistance capacity of the shaft would be 2409 kN (270 tons). Based on the lowest observed value of end bearing pressure, 9.1 MPa (1320 psi) the end bearing capacity would be 13,448 kN (1511 tons) and probably much larger. Therefore, particularly at service loads, the shaft load would be carried almost entirely by side resistance and the actual factor of safety would be greater than 6, possibly much greater.

CONCLUSIONS

Based on the results of this study the following conclusions can be drawn:

1. The observed values of side resistance are comparable to the predicted values obtained from empirical relationships.
2. The observed values of end bearing pressure greatly exceed the presumptive values of allowable bearing capacity commonly used for the design of shafts in bearing on Burlington limestone. The test shafts were not failed in end bearing and it is believed that the ultimate end bearing capacity would significantly exceed the observed end bearing pressures.
3. The actual factor of safety of shafts in Burlington limestone that are designed for end bearing only, using typical presumptive end bearing capacities, will exceed 6. Side resistance will carry a large portion of the load and particularly for service loads, the entire load may be carried by side friction.

ACKNOWLEDGEMENTS

This research projected was funded by the Mid-America Transportation Center (MATC). MATC is a Department of Transportation (DOT) and Federal Transit Authority (FTA) University Transportation Center (UTC). The research was also supported by the University of Missouri-Columbia (MU); Hayes Drilling of Kansas City, Missouri; LOADTEST Inc., of Gainsville, Florida; and Engineering Surveys and Services (ESS) of Columbia, Missouri.

REFERENCES

1. Kiehne, C., Full scale load tests of rock socketed drilled shafts, a thesis completed in partial fulfillment of the degree Master of Science at the University of Missouri-Columbia, MO, USA, 1997, 129 pages.
2. Rosenberg, P., and N. L. Journeaux, Friction and end bearing tests on bedrock for high capacity socket design. *Canadian Geotechnical Journal*, vol.13, 1976, pp. 324-333.
3. Osterberg, J. O., and S. F. Pepper. A new simplified method for load testing drilled shafts. *Foundation Drilling*, Association of Drilled Shaft Contractors, August 1984 pp. 9-11.
4. Schmertmann, J. H. (Unpublished manuscript). The bottom-up, Osterberg cell method for static testing of shafts and piles. Thirteenth Central PA Geotechnical Seminar, Hershey, PA, April 12-14, 1993.
5. Unklesbay, A. G. *Geology of Boone County Missouri,* Vol. 33, State of Missouri Jefferson City, MO, 1952.
6. Goodwin, J. W. (Unpublished manuscript). Bi-directional load testing of shafts to 6000 tons. Presented at the 1993 ASCE Annual Convention, Dallas, TX
7. Williams, A. F., Johnston, I. W., and I.B. Donald, The design of socketed piles in weak rock, *Proceedings of the International Conference on Structural Foundations on Rock*, Sydney, Australia, 1980, pp. 327-347, A. A. Balkema, Rotterdam, Netherlands
8. Rowe, R. K., and H. H. Armitage, Theoretical solutions for axial deformation of drilled shafts in rock. *Canadian Geotechnical Journal*, vol. 24, pp. 114-125.

Table 1 - Shaft depth profiles

Shaft	#1	#2	#3
Top of Rock	13.7'	13.2'	12.4'
Fracture Depth	17.5'	16'	NONE
Bottom of Shaft	18.4'	18.2'	17.5'

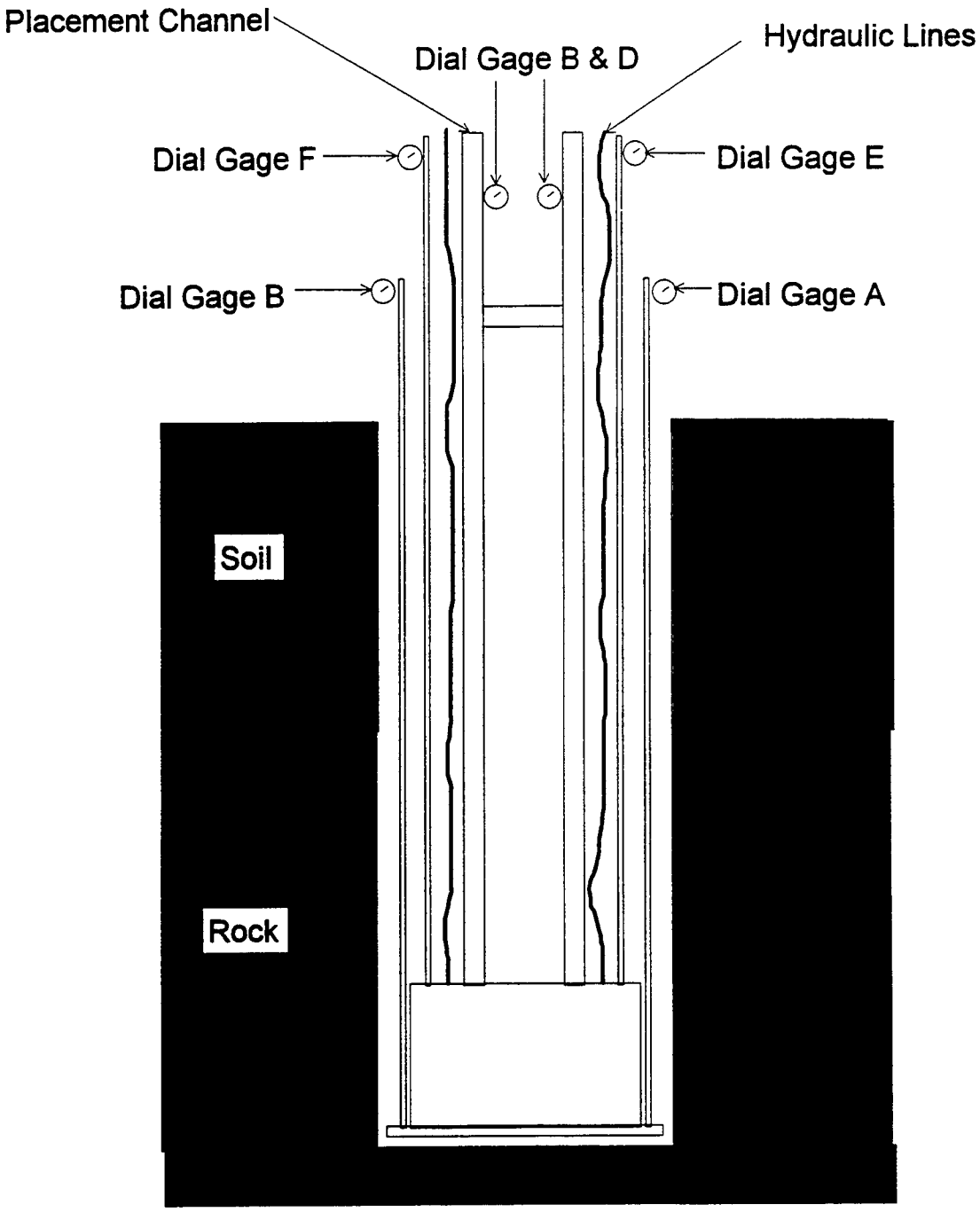

Figure 1 - Osterberg load cell and movement measurement schematic.

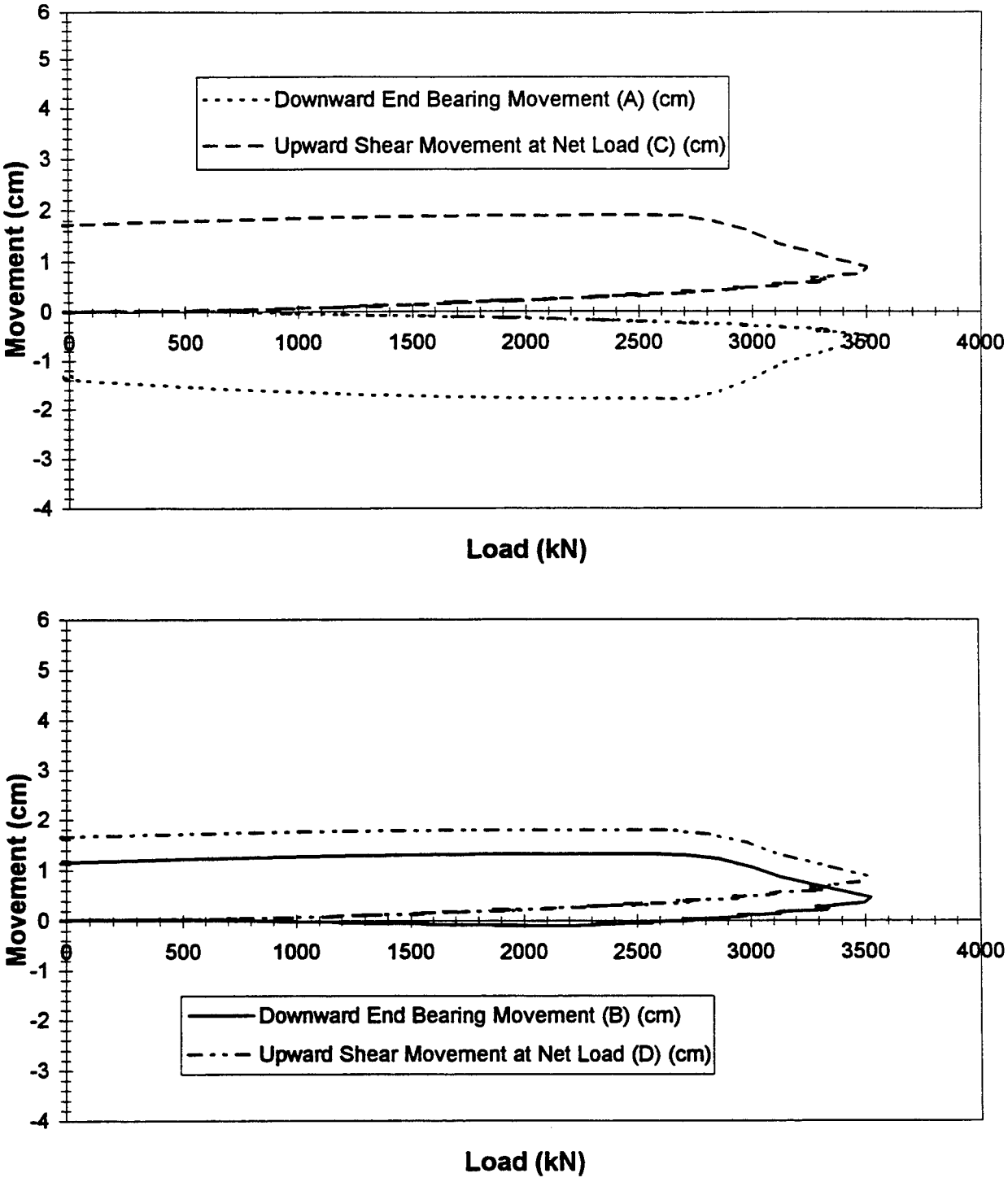

Figure 2 - Osterberg cell load movement curves for shaft #1.

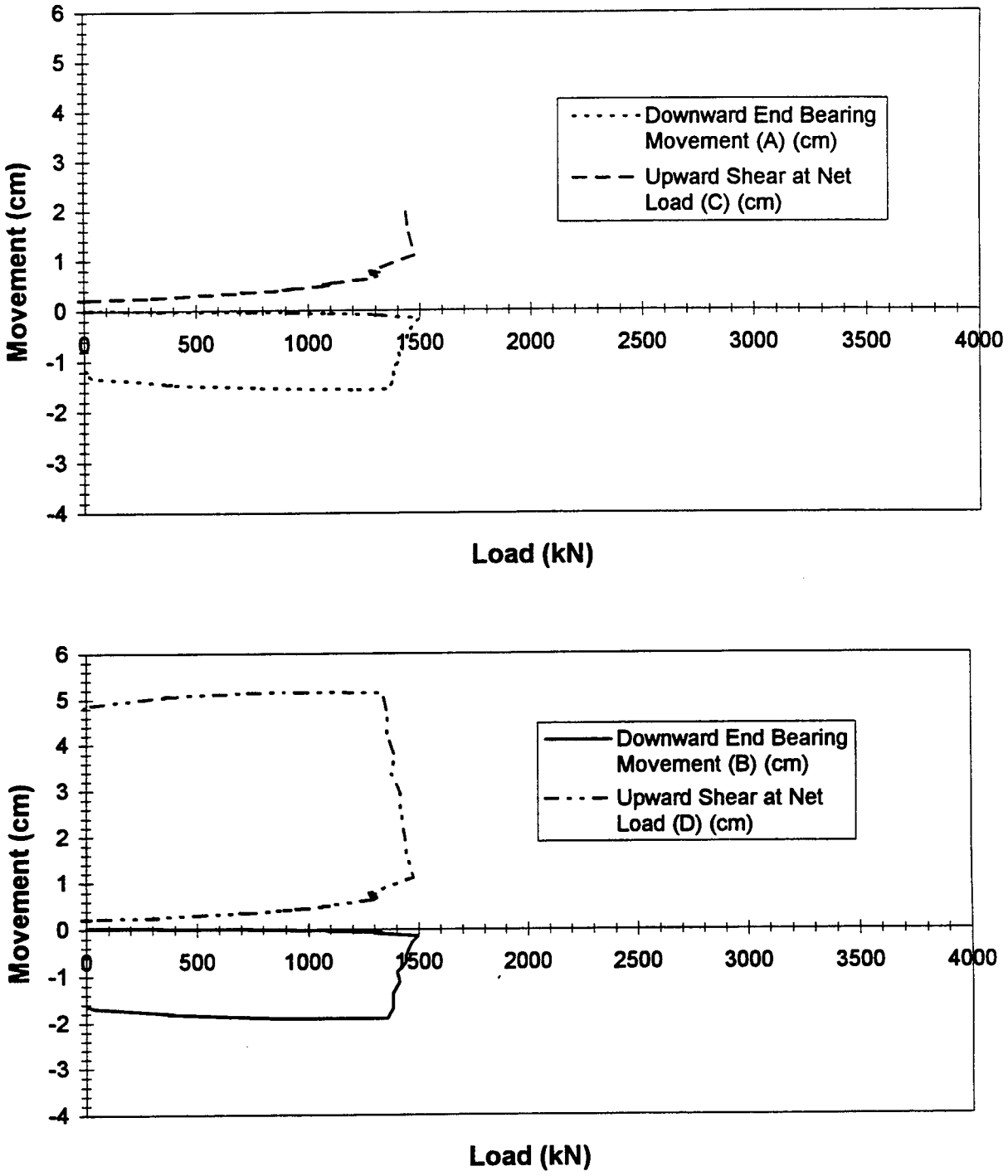

Figure 3 - Osterberg cell load movement curves for shaft #2, 2nd loading.

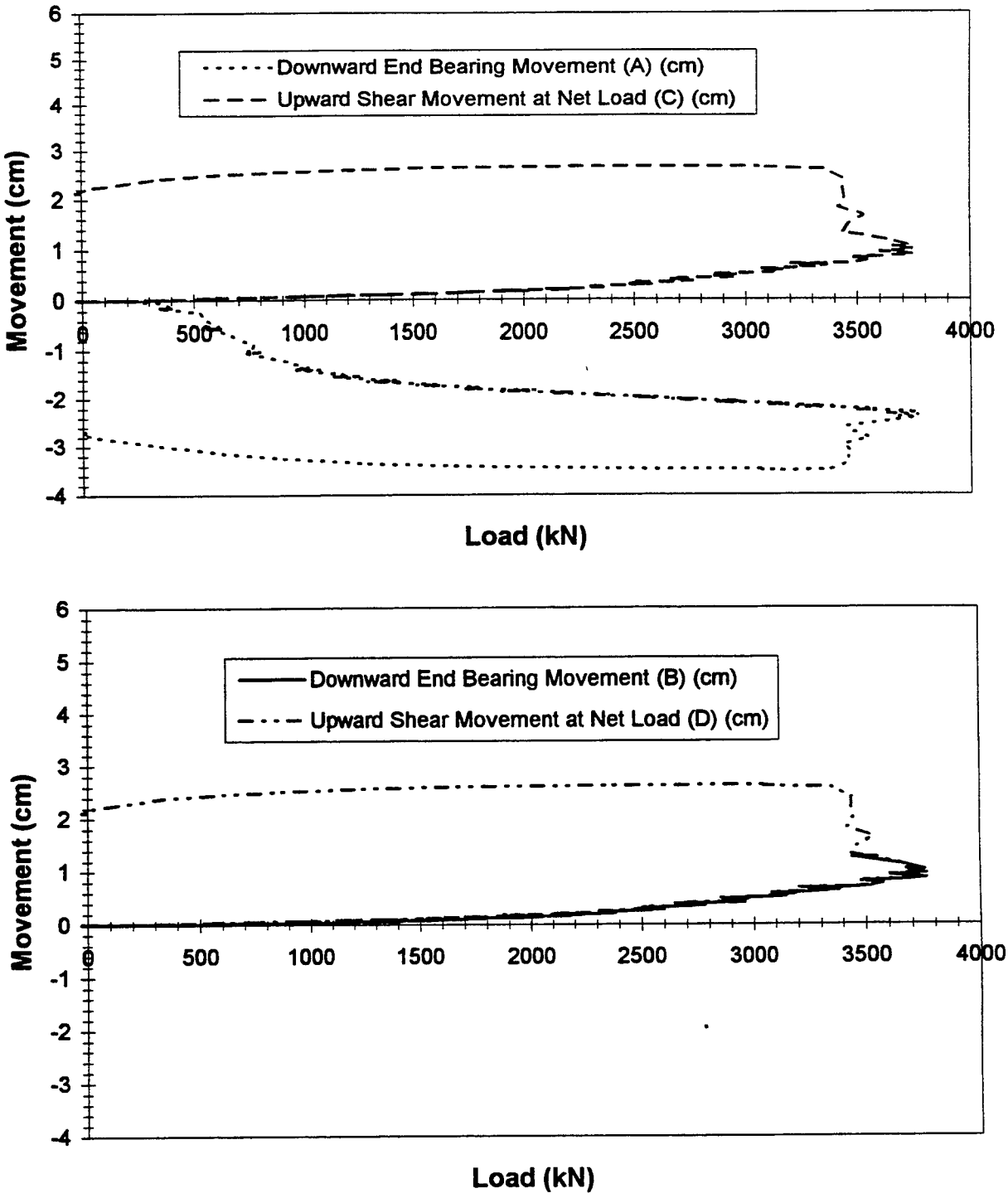

Figure 4 - Osterberg cell load movement curves for shaft #3.

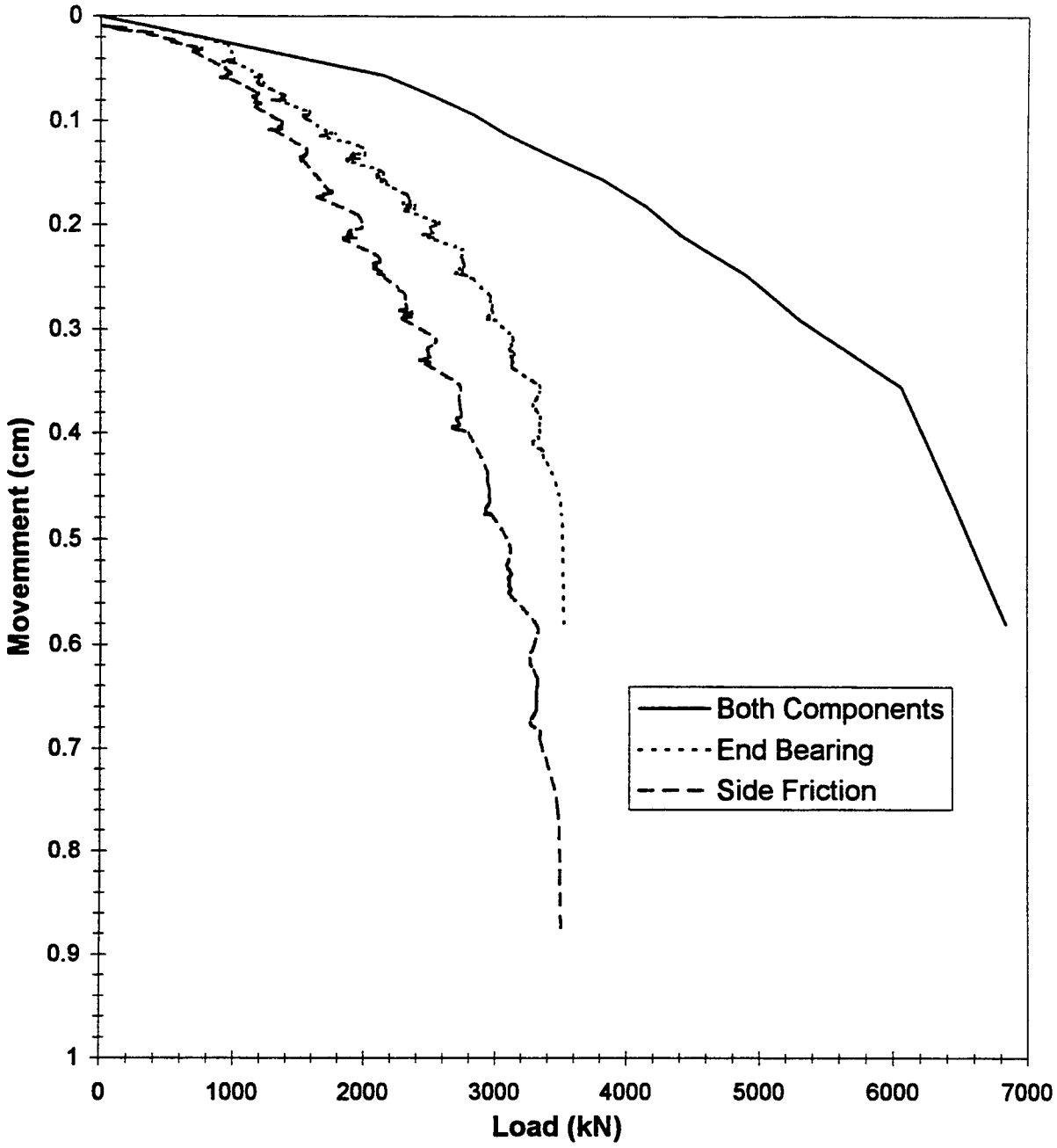

Figure 5 - Equivalent load movement curve for shaft #1.

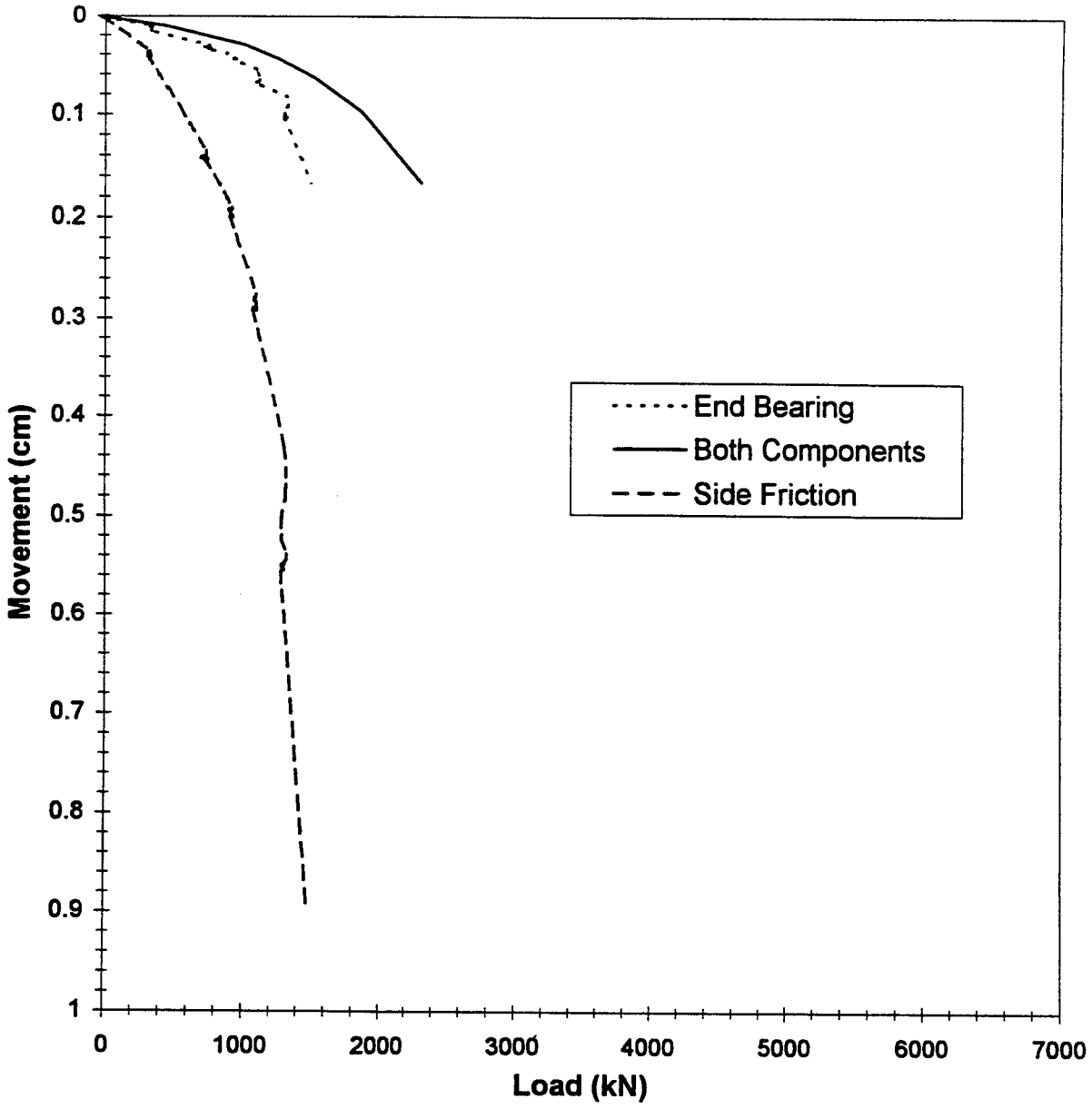

Figure 6 - Equivalent load movement curve for shaft #2.

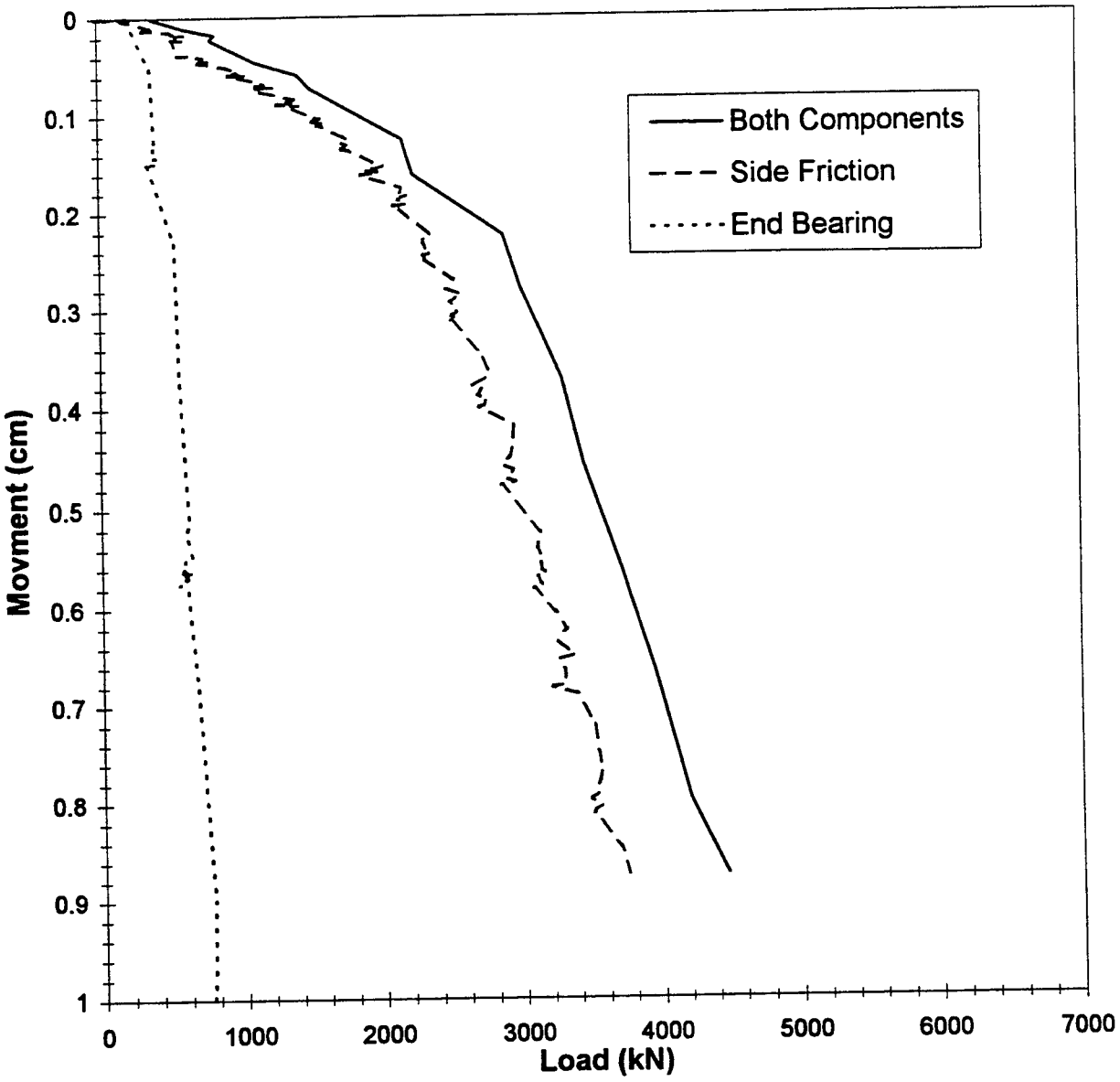

Figure 7 - Equivalent load movement curve for shaft #3.

SECTION II

Full Scale Load Tests of Rock Socketed Drilled Shafts

FULL SCALE LOAD TESTS OF ROCK SOCKETED DRILLED SHAFTS

A Thesis
presented to
the Faculty of the Graduate School
University of Missouri - Columbia

In Partial Fulfillment
of the Requirements for the Degree

Master of Science

---

by
CHAD T. KIEHNE

Dr. Brett Gunnink, Thesis Supervisor

AUGUST 1997

ACKNOWLEDGEMENTS

The author would like to take this opportunity to acknowledge those who helped and supported me during the development and completion of this thesis. First, I would like to thank Dr. Brett Gunnink for giving me the opportunity to take part in this project. His guidance and input is greatly appreciated. Secondly, special thanks go to C.H. Cassil and Rick Wells. Without them the test could not have been completed. Also, the services of Loadtest Inc. and Hayes Drilling, Inc. and the monetary support of the Mid-America Transportation Center enabled the project to be completed.

I would also like to express my immense gratitude to my parents, Tom and Mary Kiehne, for teaching me the value of education and for providing me with the tools to achieve my goals. Finnally, I want to thank Amy Linderer for her guidance, support and love throughout this project.

FULL SCALE LOAD TESTS OF ROCK SOCKETED DRILLED SHAFTS

Chad T. Kiehne

Dr. Brett Gunnink, Thesis Supervisor

ABSTRACT

The designs of rock socketed drilled shafts are often based on building code values of bearing capacity that are generally conservative. It is believed that this commonly employed design procedure for rock socketed drilled shafts is overly conservative when compared to other deep foundation systems. This is due in part to the lack of field load test data for rock socketed drilled shafts. Three full scale load tests were performed using the Osterberg Load Cell. The Osterberg Cell loads the shaft from the bottom, testing both end bearing capacity and upward shear capacity simultaneously. This data will be used to help validate less conservative design procedures.

LIST OF TABLES

Table		Page
4.1	Shaft Profiles	27
4.2	Actual and Predicted Side Resistance Values	55
4.3	Observed End Bearing Loads	57
4.4	Allowable Assumed End Bearing Values for Shafts 1, 2, and 3	58

LIST OF FIGURES

Figure		Page
2.1	Load Bearing Mechanisms of a Rock Socketed Drilled Shaft	4
2.2	Comparison Between Osterberg Cell and Conventional Load Tests	17
3.1	Drilled Shaft Layout	20
3.2	Test Apparatus	22
4.1	Osterberg Cell Load Movement Curve - Drilled Shaft #1	30
4.2	Osterberg Cell Average Load Movement Curve - Drilled Shaft #1	31
4.3	Osterberg Cell Load Movement Curve - Drilled Shaft #2 (1^{st} Loading)	32,33
4.4	Osterberg Cell Load Movement Curve - Drilled Shaft #2 (2^{nd} Loading)	34
4.5	Osterberg Cell Average Load Movement Curve - Drilled Shaft #2 (1^{st} Loading)	35
4.6	Osterberg Cell Average Load Movement Curve - Drilled Shaft #2 (2^{nd} Loading)	36
4.7	Osterberg Cell Load Movement Curve - Drilled Shaft #3	37
4.8	Osterberg Cell Average Load Movement Curve - Drilled Shaft #3	38
4.9	Equivalent Load Movement Curve - Drilled Shaft #1	41
4.10	Equivalent Load Movement Curve - Drilled Shaft #2 (1^{st} Loading)	42
4.11	Equivalent Load Movement Curve - Drilled Shaft #2 (2^{nd} Loading)	43
4.12	Equivalent Load Movement Curve - Drilled Shaft #3	44,45
4.13	Average Bottom of Cell Creep Limit Curve - Drilled Shaft #1	47
4.14	Maximum Bottom of Cell Creep Limit Curve - Drilled Shaft #1	48

4.15 Average Top of Shaft Creep Limit Curve - Drilled Shaft #1 49

4.16 Average Bottom of Cell Creep Limit Curve - Drilled Shaft #2 (2^{nd} Loading) 50

4.17 Average Bottom of Cell Creep Limit Curve - Drilled Shaft #3 51

4.18 Maximum Bottom of Cell Creep Limit Curve - Drilled Shaft #3 52

4.19 Average Top of Shaft Creep Limit Curve - Drilled Shaft #3 53

4.20 Comparison of Actual versus Predicted Side Resistance Values 55

TABLE OF CONTENTS

ACKNOWLEDGEMENTS ii

ABSTRACT iii

LIST OF TABLES iv

LIST OF FIGURES v

CHAPTER ONE INTRODUCTION 1

1.1 Problem Statement 1

1.2 Objectives 1

1.3 Organization of Thesis 2

CHAPTER TWO LITERATURE REVIEW

2.1 Design Procedures for Rock Socketed Drilled Shafts 3

2.1.1 Load Transfer 4

2.1.2 Performance of Rock Socketed Drilled Shafts 5

2.1.3 Side Resistance 10

2.1.4 End Bearing 11

2.1.5 Design Approaches for Rock Socketed Drilled Shafts 13

2.2 Osterberg Load Cell 15

CHAPTER THREE TEST METHODS AND PROCEDURES 20

3.1 Shaft Excavation 20

3.2 Osterberg Cell Assembly and Placement 21

3.3 Concrete Mix 22

3.4 Load Test Procedure 23

CHAPTER FOUR RESULTS AND DISCUSSION 24

4.1 Geology of Area 24

4.2 Site Investigation 25

4.3 Presentation of Field Load Test Results 27

4.3.1 Downward End Bearing and Upward Side Resistance Load Movement Curves 28

4.3.2 Reconstructed Equivalent Top Load Movement Curve 39

4.3.3 Creep Limits 46

4.4 Comparison of Predicted Versus Actual Capacity 54

4.4.1 Comparison of Predicted Versus Actual Side Resistance 54

4.4.2 Comparison of Actual End Bearing Values Versus End Bearing Assumptions 57

4.5 Discussion 59

CHAPTER FIVE SUMMARY OF CONCLUSIONS 60

REFERANCES 62

APPENDIX A 65

APPENDIX B 110

APPENDIX C 114

APPENDIX D 133

CHAPTER ONE

INTRODUCTION

1.1 Problem Statement

The designs of rock socketed drilled shafts are believed to be overly conservative. Often these designs are based on presumptive values of bearing capacity that are very conservative. Less conservative analytical design procedures are available, but these procedures require information about rock properties that are not typically available from routine site investigations. It is common for site investigation to end at auger refusal. Further, the accuracy of analytical design procedures is not well established. This is due in part to the lack of full scale field load test data that would allow for the validation of less conservative designs. The difficulty and cost in performing full scale load tests of drilled shafts in rock is the principal reason for the lack of data for design validation.

1.2 Objectives

The first objective of this research was to review the current design procedures for rock socketed drilled shafts. The second objective was to perform full scale load tests on socket shafts in sedimentary rock. The field load tests would use the Osterberg Load Cell. The final objective was to compare the shaft capacities obtained from the field load testing with capacities predicted using analytical methods and with capacities predicted

from presumptive bearing capacity values. It was believed that the actual capacities of the drilled shafts would be considerably greater than the capacities predicted from presumptive bearing capacity values.

1.3 Organization of Thesis

Chapter 2 includes a discussion of the factors affecting the performance of rock socketed shafts. This chapter also contains a summary of the analytical methods for socketed shaft design. A more detailed review of rock socketed drilled shaft design procedures may be found in Appendix A. The Osterberg cell and how it was used in the full scale load testing of drilled shafts is also described in this chapter.

Chapter 3 describes the test methods and procedures used during the full scale load tests of rock socketed drilled shafts. The method of excavation is described, as well as the test apparatus and concrete mix. The procedures used during load testing are also provided.

Chapter 4 describes the geology the region as well as the results of the field site investigations. Load movement curves for shafts 1, 2, and 3 are presented as well as reconstructed top loading curves and creep limit curves. The observed capacities of end bearing and side resistance are compared with the predicted shaft capacities.

Chapter 5 summarizes the conclusions from the experimental tests and the data analysis.

CHAPTER TWO

LITERATURE REVIEW

2.1 Design Procedures for Rock Socketed Drilled Shafts

The function of a rock socketed drilled shaft is to transfer structural loads through upper non-competent strata to depths where sound rock can sustain these loads. The load is transmitted to the bedrock through two basic load bearing mechanisms, end bearing and side resistance.

The axial load capacity (P) of a rock socketed drilled shaft is the ultimate load that the shaft may support before failure. This capacity depends on the combination of the end bearing capacity (P_e) and the side resistance capacity (P_s). The stress developed along the interface of the rock of the socket and the concrete by the axial load is referred to as side resistance (f_u). This stress is a result of the sliding friction along the shaft and the bond between the rock and concrete. The stress developed at the bottom of the socket is referred to as end bearing (q_e'). The end bearing stress is a result of the compressive loading between the bottom of the rock socket and the bottom of the shaft. The side resistance capacity can be found by simply multiplying the area of concrete rock bond (A_s) by the predicted side resistance (f_u). The end bearing capacity can by found by multiplying the area of the end of the shaft (A_e) by the predicted end bearing (q_e'). The stresses can be found from test data in a similar manner. Figure 2.1 illustrates the load bearing mechanisms of a rock socketed drilled shaft.

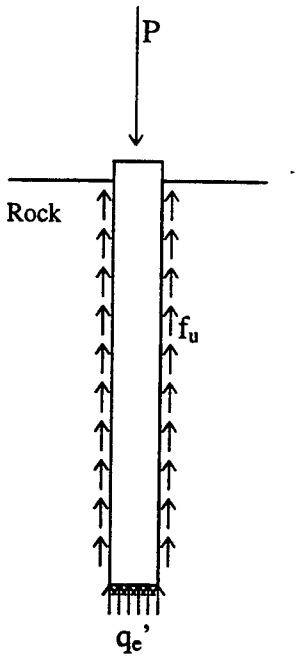

Figure 2.1 Load Bearing Mechanisms of a Rock Socketed Drilled Shaft

2.1.1 Load Transfer

The relative amount of support developed in side resistance and end bearing depends on a number of factors (Wyllie, 1992). First, the distribution of the load is effected by the modulus of the shaft material and the modulus of the rock. The greater the modulus of the socket material the greater the magnitude of the normal force exerted on the shaft in side resistance. Thus, the percentage of load carried in side resistance is increased. Secondly, the load distribution depends on the magnitude of the loading compared to the magnitude of the ultimate side resistance. The residual side resistance,

mobilized after the ultimate side resistance has been exceeded, is less than the ultimate side resistance. The residual side resistance occurs at higher settlements where a larger percentage of the load is carried in end bearing. Finally, the load distribution is effected by the method of construction (Wyllie, 1992). The use of bentonite in the drilling process can drastically reduce the magnitude of side resistance.

2.1.2 Performance of Rock Socketed Drilled Shafts

The load carrying capacity and the settlement of rock socketed drilled shafts are influenced greatly by several factors. The performance, which includes load carrying capacity and settlement, has been studied in laboratory tests, analytical studies using finite element analysis, and in full scale load tests. Ladanyi and Domingue (1980) and Pells et al. (1980) conducted laboratory tests on model piers to determine the behavior of the rock-concrete interface and the factors affecting the side resistance. Rowe et al. (1978), Donald et al. (1980), and Rowe and Pells (1980) have used finite element analysis to study the effect of socket geometry and the relative moduli between the concrete and socket on the performance of socketed shafts. There have also been numerous full scale load tests to determine the portion of load carried in side resistance and end bearing. Seychuck (1970) and Glos and Briggs (1983) accomplished this by placing a soft material on the bottom of the shaft to eliminate end bearing and casing the shaft in order to eliminate side resistance.

Wyllie (1992) surveyed previous rock socketed drilled shaft investigations and summarized the factors affecting their performance. The load carrying capacity and the settlement of socketed shafts depends significantly on the following factors:

(a) ***Effect of Socket Geometry***

The length to diameter ratio has a significant affect on the load capacity of a pier. As the ratio increases from zero, the portion of the load carried in end bearing diminishes, with side resistance carrying an increasing amount of the load. This behavior implies that short sockets require strong rock at the base of the socket to provide sufficient support in end bearing. Conversely, shafts constructed with long sockets have little load reaching the base of the shaft.

End bearing is also affected by socket geometry. When the base of the shaft is at or near the rock surface, a wedge type failure occurs. The shaft will have a rotation as well as a vertical displacement. When the base of the shaft extends to a depth of twice the diameter or greater, a punching type failure will occur. During a punching failure, a truncated cone of rock is formed below the base and there is no rotation.

(b) ***Effect of Rock Modulus***

The magnitude of side resistance is partially dependent on the magnitude of the normal stress acting on the rock surface. The magnitude of the normal stress is directly related to the stiffness of the surrounding rock. When the rock has a higher modulus than the concrete, the socket is confined and high normal stresses are developed. These high

normal stresses cause a major portion of the load to be carried in the upper portion of the socket. Conversely, when the rock has a low modulus compared to the concrete, the normal stresses are low, decreasing the amount of load carried in side resistance. Thus, more of the load is transferred to end bearing.

The modulus of the rock at the base of the socket also affects the percentage of load carried in side resistance and end bearing. If the base of the socket has a very low modulus, little of the load will be supported in end bearing. Socketed shafts with low modulus shaft bases will have lower overall capacity than shafts with sound rock at the base.

(c) ***Effect of Rock Strength***

The magnitude of shear strength and end bearing developed are related to the strength of the rock mass. When the rock is weaker than the concrete, the shear zones develop down the sides of the socket at a diameter slightly greater than the asperities on the walls of the socket. When the rock is stronger than the concrete, the shear strength of the concrete is the limiting shear strength.

(d) ***Condition of the Side Walls***

Side resistance is affected greatly by the condition of the side walls. As the roughness of the side walls increase, the side resistance also increases. The presence of rough side walls also decreases the total settlement of the shaft. The effect of grooving the walls increases the roughness of the shaft. The effect of increased roughness is the

reduction of brittle failure and avoiding the large displacements that occur with brittle failure.

The presence of drill cuttings and bentonite cakes can reduce the side resistance capacity. When bentonite is used to stabilize the walls of the socket, a layer of bentonite is likely to be between the concrete and the rock. This layer can be as thick as 40 mm and as thin as paper. The thin layer is not likely to effect the capacity, but the thick layers can greatly reduce the side resistance capacity.

(e) ***Condition of the End of the Socket***

If there is a low modulus material at the bottom of the socket, considerable displacement will have to occur before end bearing is mobilized. When end bearing is considered in the design of a rock socketed drilled shaft, it is imperative that a socket base be thoroughly cleaned before the concrete is placed, in order to avoid excessive settlement. A possible consequence of excessive settlement is that the peak side resistance could be exceeded, resulting in the reduced capacity of the entire shaft. If it is not possible to clean the socket, or the designer is unsure of the condition of the end of the socket, it may be necessary to design the shaft using side resistance as the sole method of carrying the load.

(f) ***Layering of the Rock***

In some cases, the presence of layers can increase the side resistance capacity by forming grooves that increase the roughness of the socket walls. The presence of weak,

low modulus rock layers in the socket walls and in the base of the socket can reduce the overall capacity of the shaft. In the presence of low modulus layers, the effective side resistance and the effective modulus can be calculated as a weighted average of the strong and weak materials (Thorne, 1980; Rowe and Armitage, 1987):

$$\tau^* = p\tau_s + (1-p)\tau_r \quad (1)$$

$$E^* = pE_s + (1-p)E_r \quad (2)$$

Where τ^* is the effective side resistance, E^* is the effective rock modulus, p is the proportion of the low strength material in the shaft, τ_s is the side resistance of the low strength material, E_s is the modulus of the low strength material, τ_r is the side resistance of the high strength material, and E_r is the modulus of the high strength material.

When end bearing is used as part or all of the load bearing mechanism, the type, size, and location of the layers below the base of the socket must be identified. This can be accomplished by drilling an exploration hole below the base of the socket. Seams of weak material more than three socket diameters below the base of the socket will probably have no effect on the shaft performance. However, areas of weak material at depths less then three socket diameters must be evaluated. The effect of the weak material seams can be evaluated in the same manner as side resistance was previously.

(g) *The Effect of Creep*

The effect of time on the performance of a rock socketed drilled shaft was studied by Landanyi (1977). The load in end bearing of a 35 inch diameter shaft socketed 15 feet into fractured shale was studied over a four year period. The load carried in end bearing increased over the four year period by about 65%. At the end of the four year period about 10% of the total load was carried in end bearing. The probable cause of the increase in load carried in end bearing over time was the gradual reduction of side resistance in the upper high stress portion of the shaft. Thus, this load was transferred to end bearing.

2.1.3 Side Resistance

There have been numerous methods developed to predict the portion of the axial load capacity due to side resistance of rock socketed drilled shafts. Most of these methods relate the side resistance to rock strength. McVay (1992) compiled a list of some of the methods for predicting side resistance. The side resistance (f_{su}) is reported with units of tons per square foot (tsf) and the unconfined compressive strength (q_u) is in pounds per square inch (psi).

$f_{su} = 1.842\ q_u^{0.367}$ (Williams, *et al.* 1980) (3)

$f_{su} = 1.45\ q_u^{0.5}$ (for clean sockets) (Rowe and Armitage, 1987) (4)

$f_{su} = 1.94\ q_u^{0.5}$ (for rough sockets) (Rowe and Armitage, 1987) (5)

$f_{su} = 0.67\ q_u^{0.5}$ (Horvath and Kenny, 1979) (6)

$f_{su} = 0.63\ q_u^{0.5}$ (Carter and Kulhawy, 1988) (7)

$f_{su} = 0.3\ q_u$ (Reynolds and Kaderabek, 1980) (8)

$f_{su} = 0.2\ q_u$ (Gupton and Logan, 1984) (9)

$f_{su} = 0.15\ q_u$ (Reese and O'Neill, 1987) (10)

Equations 3 through 7 are non-linear relationships, whereas equations 8 through 10 are simple constants multiplied by the unconfined compressive strength. Equations 4, 5, 8, 9, and 10 are for soft rock. These relationships are all empirical and are generally based on limited data.

2.1.4 End Bearing

Most methods of determining end bearing capacity relate bearing capacity to unconfined compressive strength. However, unconfined compressive strength based on laboratory tests may not accurately represent the quality of the rock mass. End bearing capacity is determined most reliably by a thorough site investigation. The previously mentioned factors affecting shaft performance, rock strength, presence of rock layers, etc., must be considered. In the absence of an adequate site investigation, many building codes allow presumptive value of end bearing capacity to be used for design purposes.

The National Building Code of Canada (1970) as reported by Rosenberg and Journeaux (1976) permits 10 tons per square foot of bearing pressure on the surface of

limestone. This value allows for the existence of voids, open joints, and soil filled seams that may occur in the bearing material. The Chicago Building code as reported by Baker and Khan (1971) allows 100 tons per square foot of bearing pressure on sound limestone. It also allows a 20 percent increase for each foot of confinement up to a maximum of 200 tons per square foot at a depth of 5 feet. The Uniform Building Code (1985) allows 2 tons per square foot for shafts bearing on "massive crystalline bedrock" with a minimum shaft diameter of 1 foot and a minimum depth of 1 foot. These values may be increased by 20 percent for each additional foot of width and/or depth, up to a maximum value of three times the designated value. The UBC also allows for a side resistance value of 1/6th of the bearing value, but not to exceed 500 pounds per square foot. The side resistance and end bearing cannot be considered to act simultaneously unless warranted by a proper site investigation. The previous values given by the UBC can be increased after proper site investigations. The Building Officials and Code Administrators Basic Building Code (BOCA) (1981) recommends, in the absence of proper site investigations, a presumptive bearing value of "massive crystalline bedrock" of 100 tons per square foot. This may be increased with proper site exploration. BOCA also allows for the increase of allowable end bearing with increasing socket length and the use of side resistance in design, but the amounts of end bearing increase and side resistance are left up to the design engineer.

The high variability of rock formations over relative small distances make the prediction of end bearing capacity difficult. This is one of the causes of overall conservatism inherent in building code predictions of end bearing. Engineers with local

experience and knowledge of the geological characteristics often produce the least conservative presumptive end bearing predictions.

2.1.5 Design Approaches for Rock Socketed Drilled Shafts

Four approaches to the design for rock socketed drilled shafts were reviewed by Freeman et al. (1972) and presented by Rosenberg and Journeaux (1976). A detailed review of rock socketed drilled shaft design procedures can be found in Appendix A - Design of Rock Socketed Drilled Shafts. A description of the four approaches to design follows:

(a) ***Design For End Bearing Only***

When a rock socketed drilled shaft is designed in end bearing only, the socket base must be extended to a sufficient depth so that the end bearing pressure does not exceed the allowable bearing capacity of the rock. As the socket depth increases, the confining pressure of the surrounding rock also increases. This in turn increases the end bearing capacity.

The side resistance developed between the concrete and the socket walls is ignored with this approach. The approach is based on the assumption that all of the axial load is transferred to the socket base. This is a conservative assumption, resulting in the actual end bearing pressure at the bottom of the socket generally being significantly less than the assumed values. Field tests have indicated that even in fractured rock the

concrete to rock bond is significant (Rosenberg and Journeaux, 1976); therefore, a significant portion of the applied load is carried due to side friction, especially at service load levels.

(b) ***Design for Side Resistance Only***

This approach assigns an average side resistance to the entire rock-concrete bond area, but the load carrying capacity developed in end bearing is ignored entirely. This approach is usually employed under extremely poor rock conditions and when the socket base cannot be properly cleaned. This approach usually results in extremely deep sockets (Rosenberg and Journeaux, 1976).

(c) ***Design for Allowable End Bearing and Carrying the Remaining Load in Side Resistance***

This approach assigns an allowable end bearing capacity for the socket base. The allowable end bearing capacity is then subtracted from the axial load. The socket length is then designed to carry the remaining load in side resistance. This method does not consider the actual stresses developed in the socket base. Instrumented shafts have shown that the actual stresses developed may be in variance with the assumptions made. Jackson *et al.* (1974) found that the socket base end bearing pressures were lower and the side resistance bond stress higher than initially anticipated (Rosenberg and Journeaux, 1976).

(d) ***Design with Estimated Developed End Bearing and Side Resistance***

This approach assumes that part of the applied load is dissipated and carried by side resistance and that the remaining load produces the actual developed end bearing pressure at the socket base. A prediction of the load carried by end bearing is required. Based on this prediction, an allowable end bearing pressure is assigned. It is assumed that the rest of axial load is carried in side resistance. The socket depth is then adjusted so that the allowable values for end bearing capacity and side resistance are not exceeded.

The main difference between this method and the other three methods is that the relation between applied axial stress and the actual developed end bearing stress for various socket embedments and rock properties is required (Rosenberg and Journeaux, 1976).

2.2 Osterberg Load Cell

The Osterberg load cell was developed and patented by Dr. Jorj Osterberg (1986), Emeritus Professor of Civil Engineering at Northwestern University. The Osterberg load cell is a static load testing device for shafts and piles. An Osterberg cell load test uses an especially designed "pancake-like" hydraulic jack and associated fittings to create pressures in excess of 8,000 psi at the bottom of the shaft, loading the pile or shaft in end bearing and upward side resistance. The cell is typically slightly smaller in diameter than the shaft or pile and cast in the base during construction of the shaft or placed at the tip of

a driven pile (Osterberg, 1984). A schematic comparison of conventional testing and testing with the Osterberg load cell is illustrated in Figure 2.1.

The Osterberg load cell is lowered into the shaft via reinforcing cage or if no reinforcement cage is used, a small I-beam or channel can be used to place the load cell. The hydraulic lines and telltale rod casings are also attached to the reinforcement cage. The telltale rods allow for the measurement of the movement of the bottom and the top of the cell. These movements and the movement of the top of the shaft or pile are measured using dial gages that are supported by an independent reference beam.

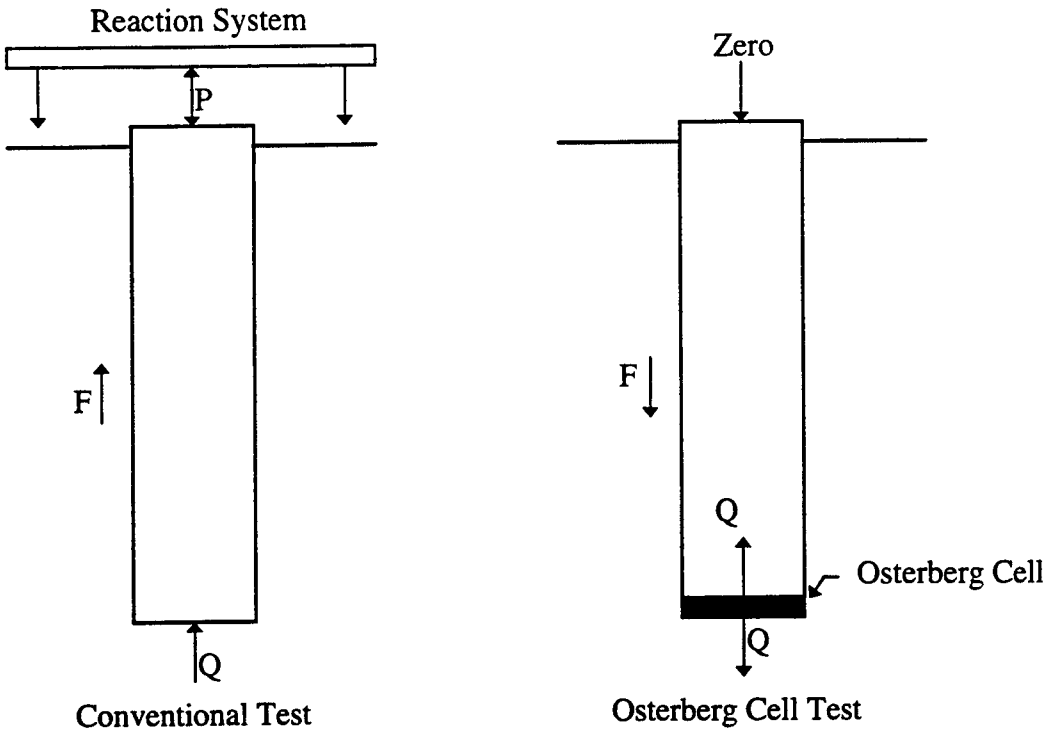

Figure 2.2 - Comparison Between Osterberg Cell and Conventional Load Tests

The Osterberg cell is pressurized using a compressed air driven pump with diluted automotive antifreeze as the hydraulic fluid. The cell is expanded without any need for a surface reaction system. The soil and/or rock surrounding the shaft or pile provides the reaction for the load test. As the cell is pressurized, the bottom of the cell moves downward, testing end bearing, while the top of the cell moves upward, testing side resistance. The cell is expanded until the expansion force is some desired multiple of the design loading, The O-cell reaches its maximum expansion, or the shaft fails in either end bearing or side resistance. The hydraulic loading can be held at a relatively constant load level allowing for the study of creep. The load may also be cycled to study the effects of

repetitive loading. At the completion of the test, the cell may be filled with grout to reestablish its integrity and permit the test shaft or pile to become a component of the structure (Schmertmann, 1993).

Full scale load testing using the Osterberg load cell has many advantages over the conventional load test. The cost of an Osterberg load test is typically one third to two thirds less than that of a conventional load test. The cost savings also tend to increase when the capacity requirements increase. The test energy of an Osterberg load test is placed deep into the ground increasing the safety over the surface reaction system of a conventional test. Due to eliminating the need for a surface reaction system, the Osterberg load test decreases the amount of time needed to prepare the test site and enables the test to be performed on battered piles and over-water shafts and piles. When the cell is placed at the bottom of a rock socket, the load is assured to load the shaft in side resistance and end bearing. The Osterberg cell allows for the separation of the load carrying components. The soil or rock axial capacity is automatically separated into end bearing and side resistance without the need for additional instrumentation. Finally, large capacities are easily obtained from the Osterberg cell test. Using a 34 inch diameter cell calibrated for a 3,000 ton load, the cell is pressurized applying load to the shaft in end bearing and upward side resistance simultaneously, which would be equivalent to a conventional top loading of 6,000 tons. This allows for the proof testing of large shafts and eliminates the need for the construction of special smaller shafts or piles normally needed due to the load limitations of conventional test methods (Schmertmann, 1993).

However, the Osterberg cell has some disadvantages over conventional load testing. The Osterberg load cell test must be planned before construction. The test cannot be performed on an existing pile or shaft. The pile or shaft fails in only one load carrying component, end bearing or side resistance. Movement during a test is also limited to the maximum expansion of the Osterberg load cell, usually six inches. The Osterberg cell is difficult or impossible to install on some types of piles, such as H-piles. Prestressed concrete piles need to have the cell installed at the time of casting. The equivalent top load deflection curve of the shaft or pile is a reconstructed curve, which is constructed from the upward and downward curves obtained directly from the test. The equivalent top load deflection curve is based on the assumption that the downward friction deflection in an Osterberg test matches the upward friction deflection in a conventional test. Engineers believe this to be a conservative assumption (Schmertmann, 1993).

Loadtest, Incorporated, headquartered in Gainesville, Florida, is the sole source for the patented Osterberg cell. Loadtest, Inc. was formed by geotechnical engineers for the purpose of furnishing equipment and engineering services associated with the Osterberg cell.

CHAPTER THREE

TEST METHODS AND PROCEDURES

3.1 Shaft Excavation

Hayes Drilling Inc. of Kansas City, MO, began shaft construction on December 9, 1996. Three shafts were excavated using a truck-mounted rotary drill. An 18 inch auger bit with carbide cutting teeth was used to excavate the overburden as well as the rock socket. Water was used as lubrication during the drilling process and to facilitate the removal of the rock cuttings. The base of the socket was cleaned by rapidly spinning the auger bit after the addition of water and then lifting out the rock cuttings. An attempt was made to use a core barrel to excavate the bedrock but the nature of the socket material and drilling equipment rendered this method impractical. Figure 3.1.1 illustrates the shaft layout.

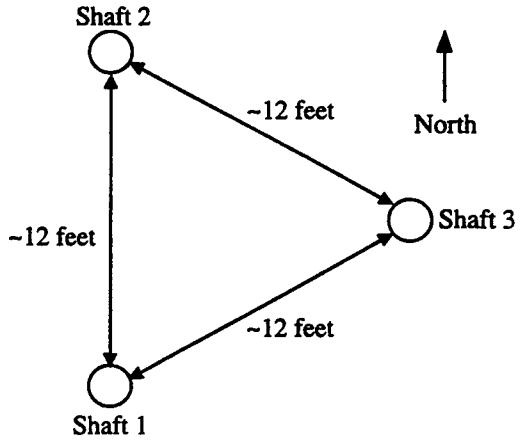

Figure 3.1 - Drilled Shaft Layout

3.2 Osterberg Cell Assembly and Placement

The Osterberg cells used in the base of the three shafts were 13 inches in diameter and approximately 12 ½ inches high. The cells had a maximum load producing capability of 450 tons in each direction (end bearing and upward shear). Osterberg cell number 6678-1 was placed in shaft 1, 6261-4 in shaft 2, and 6261-5 in shaft 3. The calibration records for each cell can be found in Appendix B.

The Osterberg cell was welded to a 20 foot frame constructed of 4 inch channel sections. This frame enabled the cell to be lowered into the shaft safely and also supported two hydraulic lines and four telltale rod casings. The hydraulic lines were 3/8 inches in diameter with a 5000 psi working pressure and a 20,000 psi burst pressure. The telltale rod casings consisted of ½ inch galvanized pipe. Two casings were attached to opposite sides of the base plate and the remaining two casings were attached to opposite sides of the top of the Osterberg cell. Figure 3.2 illustrates the Osterberg cell assembly.

After the completion of drilling, a small seating layer of concrete was placed by free fall into the base of the shaft. The Osterberg cell base plate was greased to ensure no concrete adhesion. The cell was then lowered into the shaft using the channel frame and seated onto the base layer of concrete. The remaining concrete was then placed by free fall into the shaft until the level of the concrete was approximately 2 feet below the ground surface. Three concrete test cylinders were made for each shaft so that the strength of the concrete could be measured. The concrete was allowed to cure for 6 days before the load test was performed.

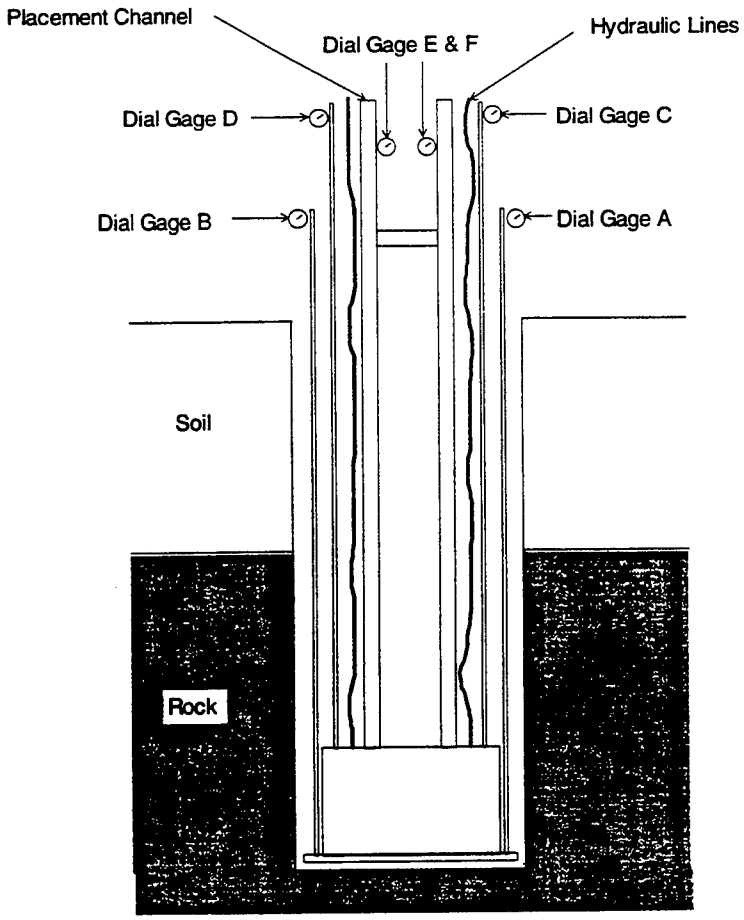

Figure 3.2 - Test Apparatus

3.3 Concrete Mix

The concrete mix was a Missouri DOT state B paving mix with entrained air. The predicted strength was 4000 psi. The maximum aggregate size was ½ inch. Calcium chloride was added to accelerate the rate of strength development of the material. Plastisizer was added to the mix at the test site to increase the slump. This was done to

aid in the even distribution of concrete in the shaft and to avoid air pockets that would decrease the strength of the shaft.

3.4 Load Test Procedure

A 4 inch channel reference beam was placed near the drilled shaft assembly. Six Ames digital dial gages with a 4 inch travel and a precession of 0.001 inches were attached to the reference beams by magnetic stands. The dial gages were designated A through F. Machined steel telltale rods were inserted into the telltale casings. Dial gages A and B measured the displacement of the base plate telltale rods and dial gages C and D measured the displacement of the top of cell telltale rods. Dial gages E and F were attached to the channel frame and measured the top of shaft displacement. The dial gages were connected to a laptop PC to collect the data.

A hydraulic pump driven by a regulated air compressor was used to pressurize the Osterberg cell. The hydraulic fluid was diluted automotive antifreeze. The Osterberg cell was pressurized in increments of approximately 500 psi. The pressure was held at each loading increment for a total of 4 minutes. The automated data collection system recorded movements at 30 second intervals. Along with the automated data collection system, data was recorded manually at 4 minute intervals with an average of 30 seconds required to adjust the cell pressure to the next load interval. The load increments were increased until side friction shear failure occurred.

CHAPTER FOUR

RESULTS AND DISCUSSION

4.1 Geology of Area

Boone County, Missouri, and more specifically the City of Columbia, lie in the southern end of the Dissected Till Plains Physiographic Province. The geology of the area is characterized by dissected Pleistocene age glacial drift that unconformably overlays Pennsylvanian aged limestones and shales which overlay Mississippian aged limestone (Lee, 1995).

The Pleistocene glacial drift can be further classified as Kansan and Nebraskan Glacial Till. This material varies greatly in its composition. The particles range in size from clay to coarse gravel and large boulders. The majority of the Kansan and Nebraskan till consists of a reddish yellow to brown heterogeneous mixture of clay, sand, and gravel (Unklesbay, 1952). The glacial till may contain small pockets or lenses of nearly clean sand (Lee, 1995). These soils are usually moderately to highly overconsolidated and exhibit high shear strengths and low compressibility characteristics.

Pennsylvanian rock deposits in this area are composed of mainly shale with interbedded limestone. These types of rock deposits occur erratically in the Columbia and Boone County area. The deposits tend to be thickest where they overlie valleys and depressions in the underling Mississipian surface (Unklesbay, 1952).

The Mississipian aged rock formations in this area are mostly of the Burlington Formation. The Burlington Formation is a fairly coarse-grained, massive, clastic limestone. The upper portion is commonly white to light gray or buff in color, and the lower portion is characteristically buff to reddish brown. The upper portion of the formation is also characterized by an abundance of chert (Lee, 1995). The limestone has been severely weathered to produce deep solution channels and a pinnacled surface. The Burlington Formation also exhibits high shear strength and low compressibility characteristics.

4.2 Site Investigation

The initial site investigation consisted of collecting eight previous subsurface investigations that were performed in the general vicinity of the three research shafts. These investigations were performed from 1988 to 1995 by Engineering Surveys and Services of Columbia, Missouri for the purpose of new construction.

The subsurface conditions of the area are highly variable. The overburden consisted of mostly glacial drift. This ranged in depth from zero to over 20 feet in some areas. This material consisted of sandy clay, sandy silty clay, gravelly clay and other variations of the aforementioned. Pennsylvanian shale exists in the area at depths ranging from zero to 36 feet. These materials are underlain by massive Mississippian limestone bedrock.

Burlington limestone bedrock was discovered in the area at depths ranging between 6 and 42 feet; with an average depth of 21 feet. The surface of the limestone was irregular and weathered in some areas. The weathered layer varied in thickness from a few inches to over 4 feet. Cores of this limestone revealed tan or light buff to bluish gray limestone. Beds of chert, inclusions of pyrite, and calcite-filled fractures were found within the limestone.

Boring logs of the Burington limestone include three unconfined compression tests and four rock quality designations. One boring shows a 6,336 psi rock strength at 5.5 to 6.7 feet, 10,718 psi at 7.4 to 8.9 feet, and 9,395 psi at 8.9 to 10 feet. Four borings included single rock quality designations (RQD) and percent recoveries. Individual borings yielded 90 percent recovery with a 78 RQD at 10 to 15 feet, 100 percent recovery with an 80 RQD at 15.5 to 20.5 feet, 100 percent recovery with a 100 RQD at 14 to 18 feet, and 100 percent recovery with an 85 RQD at 18 to 23 feet. Boring logs of these rock cores and other representative boring logs can be found in Appendix D.

The site investigation specific to the drilled shaft location consisted of observation of the shaft drilling process. The shaft and socket were constructed entirely using a rotary auger, leaving no core of limestone. The overburden was consistent with the glacial drift described earlier. It was predominantly clay with some silt, sand and gravel. No shale was found during the drilling process. However, a thin layer of weathered limestone was encountered on top of the limestone bedrock. The bedrock cuttings were light gray in color and seemed to be solid in nature.

After completion of the shafts, a feeler gage was used to scrape the sides of the socket in order to find seams of fractures. Small fractures were found in shafts 1 and 2 and no fractures were evident in shaft 3. No ground water was encountered in any of the shafts. The depth of the shafts are shown in the table 4.1.

Table 4.1 - Shaft Profiles

Shaft	1	2	3
Top of Rock	13.7'	13.2'	12.4'
Fracture Depth	17.5'	16'	NONE
Bottom of Shaft	18.4'	18.2'	17.5'

4.3 Presentation of Field Load Test Results

The dial gage readings from gages A through F and the pressure transducer readings were recorded manually at each change of load increment. The laptop PC recorded readings every 30 seconds. The PC-collected data as well as the data collected manually, are presented in Appendix C.

Various load movement curves were generated from the Osterberg cell load tests. The load movement curves for the downward movement of the bottom of the cell and the upward load movement curves for the top of the cell and the top of the shaft can all be obtained directly from the field data. The equivalent top load movement curve was constructed to simulate the downward loading of a conventional field load test. Creep movement curves were also constructed.

4.3.1 Downward End Bearing and Upward Side Resistance Load Movement Curves

The downward end bearing load movement curve was obtained directly from dial gages A and B, which were attached to the telltale rods extending to the base of the cell. The upward side resistance movement was obtained directly from dial gages C and D, which were attached to the telltale rods extending to the top of the Osterberg cell. The pressure corresponding to the above movements was obtained from the pressure transducer. The load was then calculated using the Osterberg cell calibration curves found in Appendix B. The side resistance load is the net load calculated by subtracting the weight of the shaft from the cell load. The loads for the downward end bearing movement are the total cell loads.

As mentioned previously, two telltale rods extended to opposite sides of the bottom of the cell and two telltale rods extended to opposite sides of the top of the cell. The average load movement curves were plotted for the downward end bearing movements and upward side resistance movements, as well as the load movement curves for each telltale rod.

Shaft 1 had a maximum downward movement of the bottom of the Osterberg cell of 0.708 inches with a maximum load of 396 tons. The maximum upward movement of the top of the Osterberg cell was 0.743 inches with a maximum net load of 394 tons. The net load used for upward shear is the total load minus the weight of the shaft. Shaft 2 was loaded twice due to equipment malfunctions. The maximum downward movement of the

bottom of the shaft in the first loading was 0.025 inches with a maximum load of 117 tons. The first loading maximum upward movement of the top of the Osterberg cell was 0.152 inches and had a maximum net load of 114 tons. The second loading maximum top of cell and bottom of cell movements were 0.754 inches and 2.03 inches, respectively with corresponding loads of 168 tons and 166 tons. Shaft 3 had a maximum downward cell movement and upward cell movement of 1.38 inches and 1.04 inches respectively with corresponding loads of 423 tons and 421 tons.

The loading of shafts 1 and 3 produced considerable tilting of the bottom Osterberg cell plate. This is evident by the difference in movement values of dial gages A and B. Average movements of dial gages A and B were calculated to estimate the movement of the center of the bottom Osterberg cell plate. Actual and average load movement curves for shafts 1, 2 and 3 are presented in figures 4.1 through 4.8.

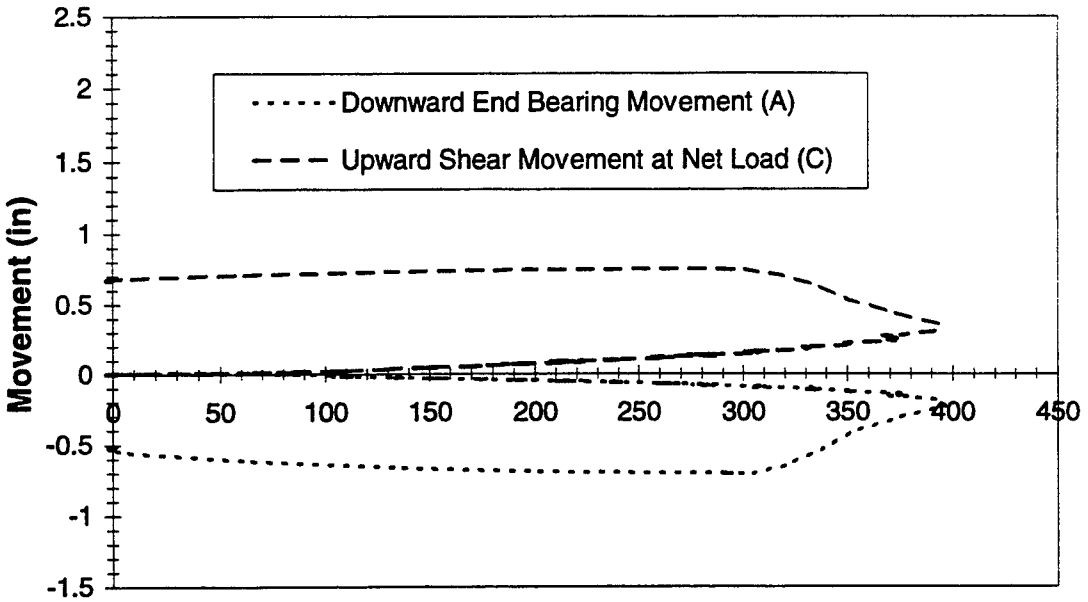

Figure 4.1a Osterberg Cell Load Movement Curve - Drilled Shaft #1

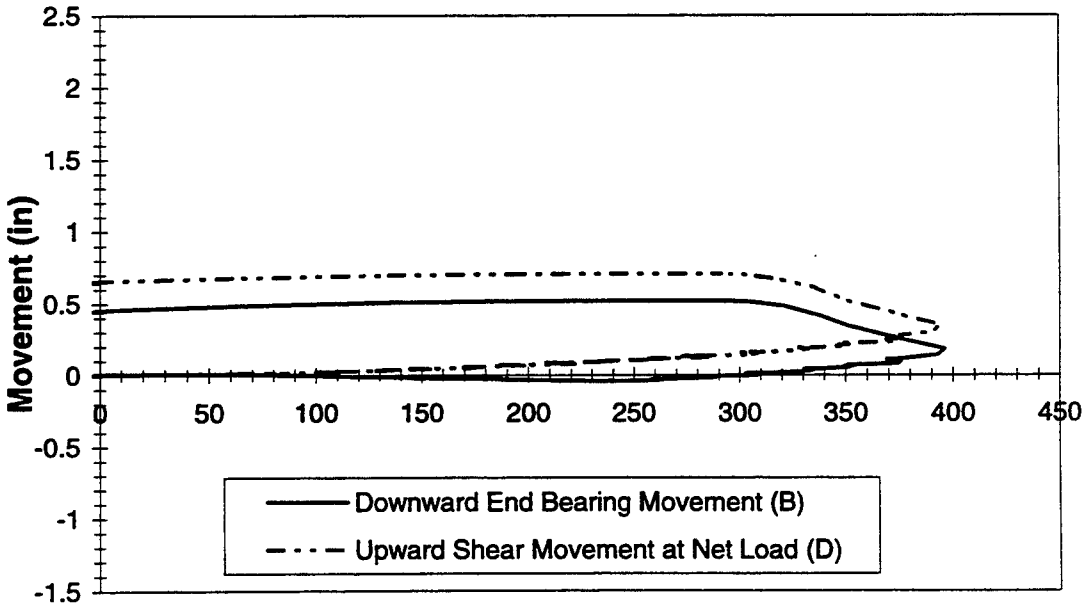

Figure 4.1b Osterberg Cell Load Movement Curve - Drilled Shaft #1

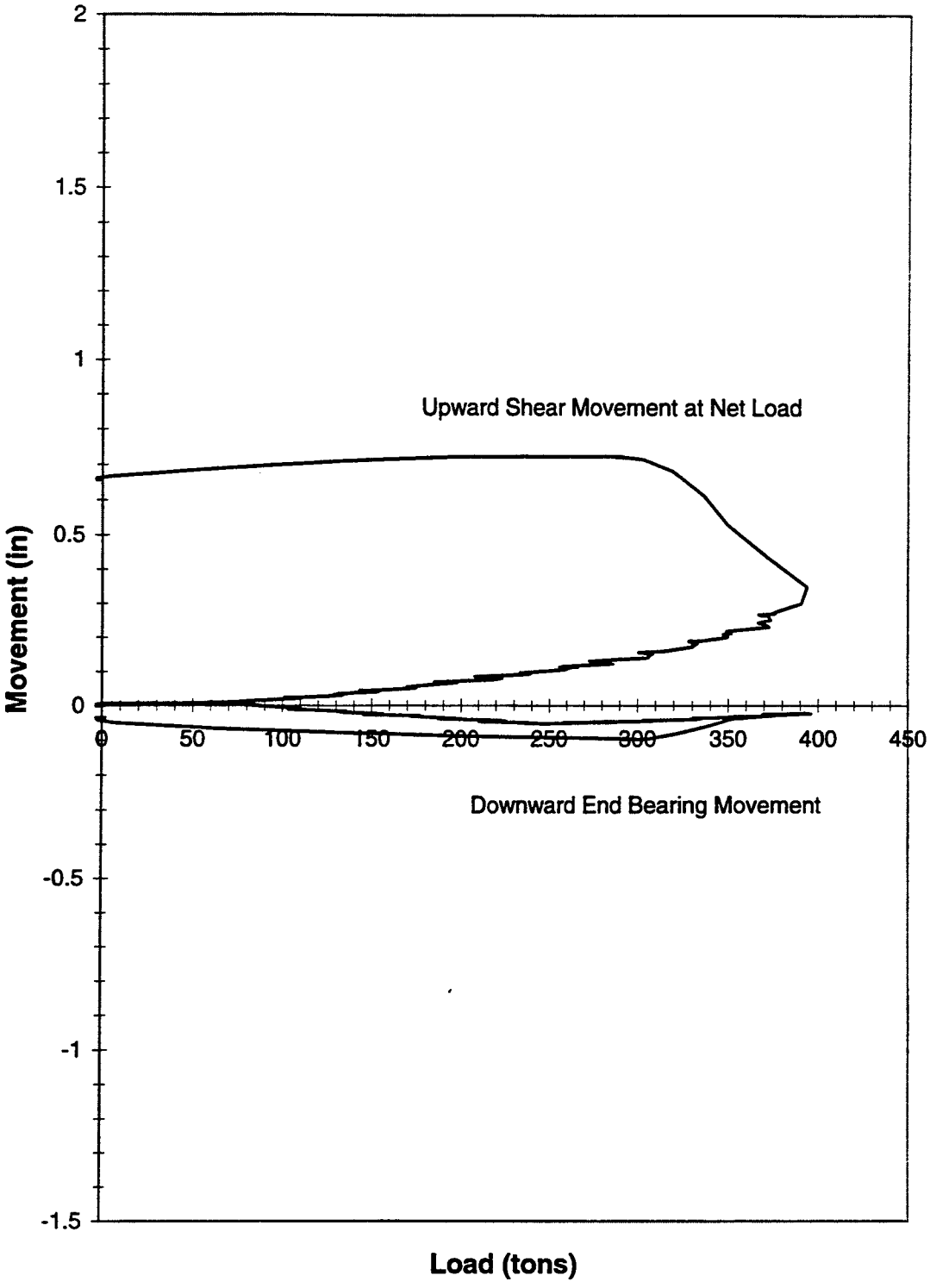

Figure 4.2 Osterberg Cell Average Load Movement Curve - Drilled Shaft #1

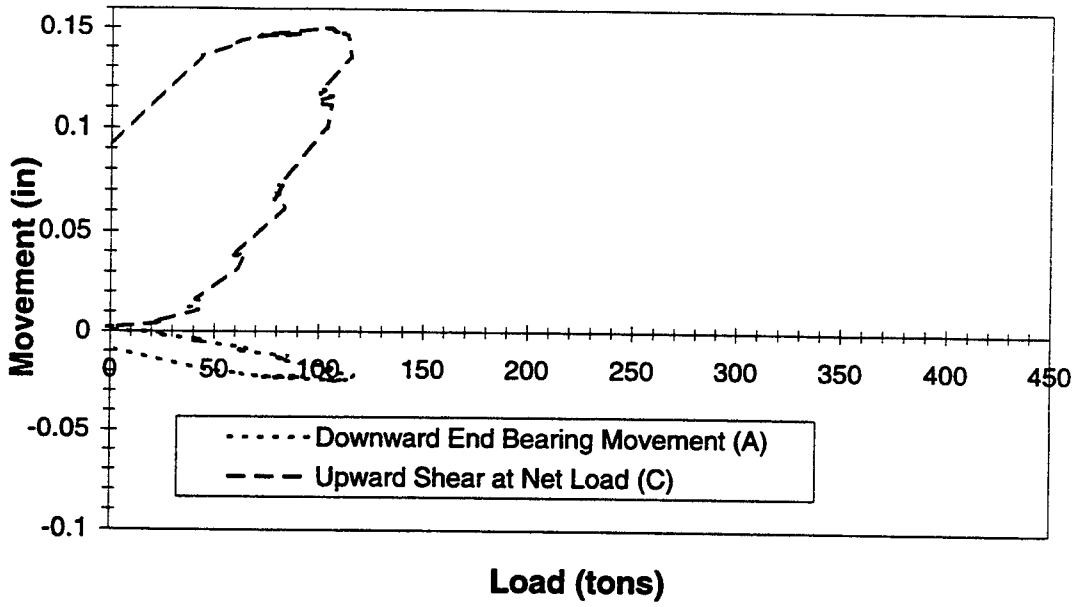

Figure 4.3a Osterberg Cell Load Movement Curve - Drilled Shaft #2 (1st Loading)

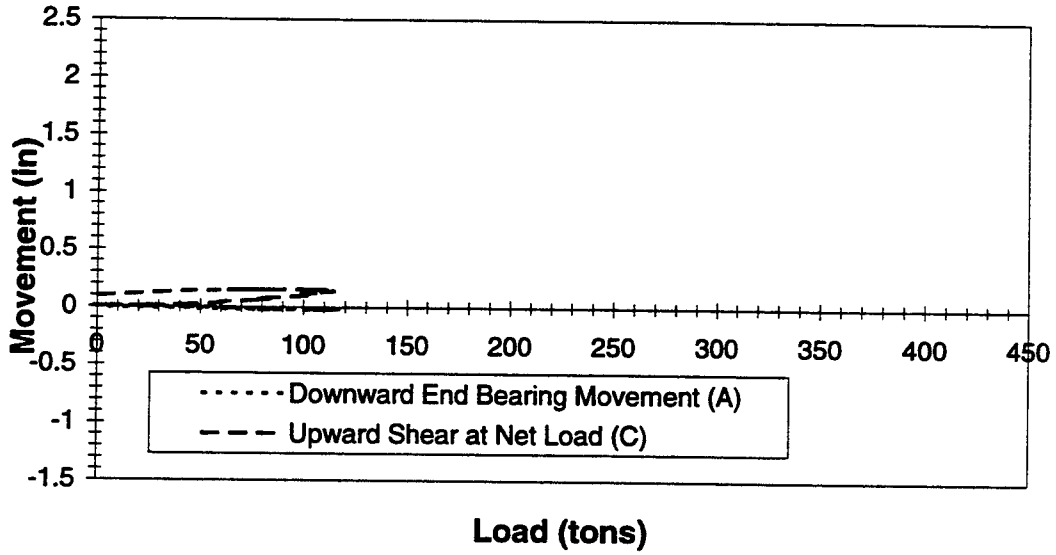

Figure 4.3b Osterberg Cell Load Movement Curve - Drilled Shaft #2 (1st Loading)

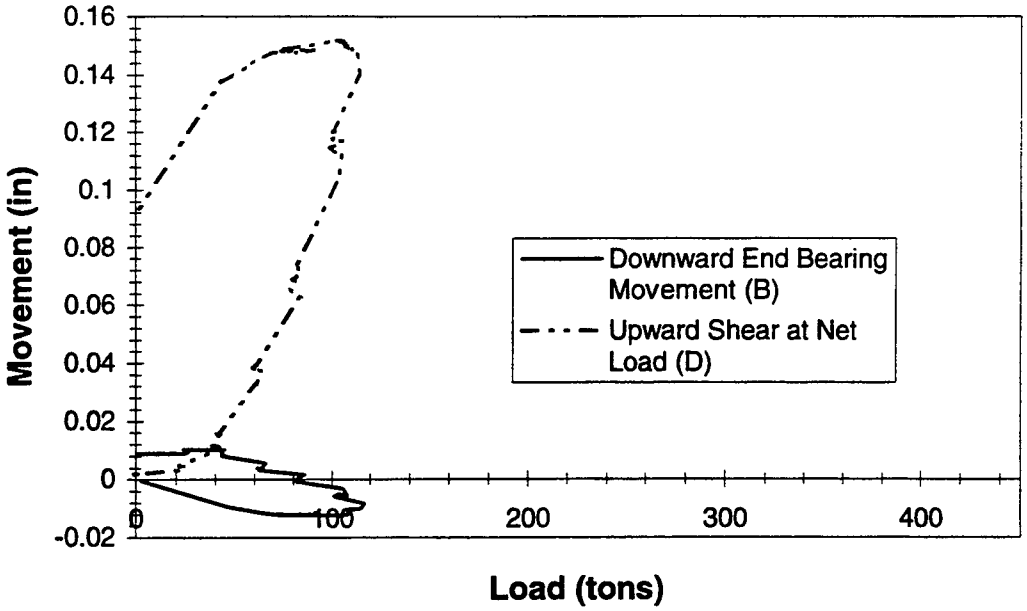

Figure 4.3c Osterberg Cell Load Movement Curve - Drilled Shaft #2 (1st Loading)

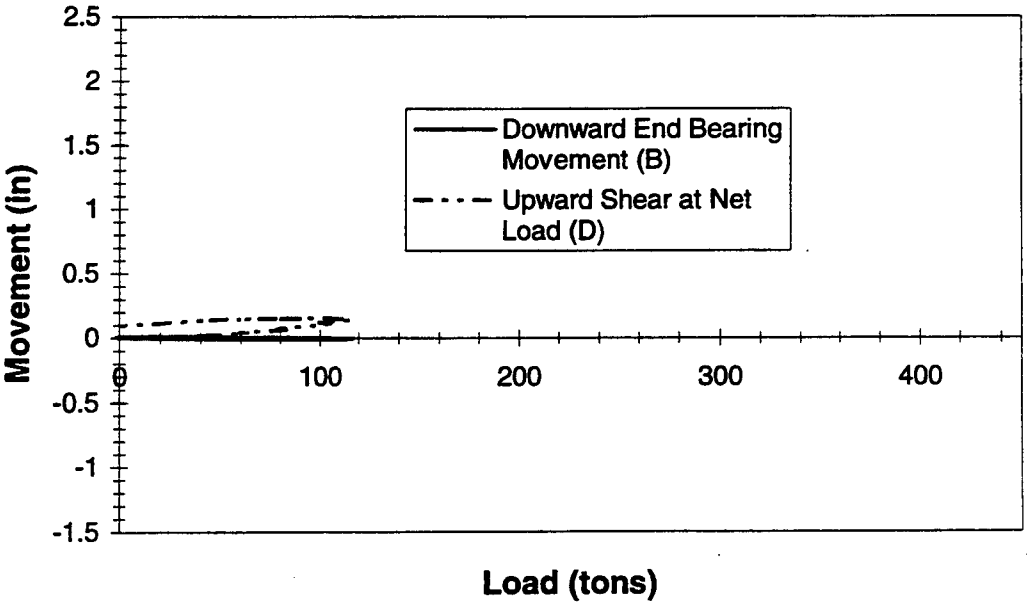

Figure 4.3d Osterberg Cell Load Movement Curve - Drilled Shaft #2 (1st Loading)

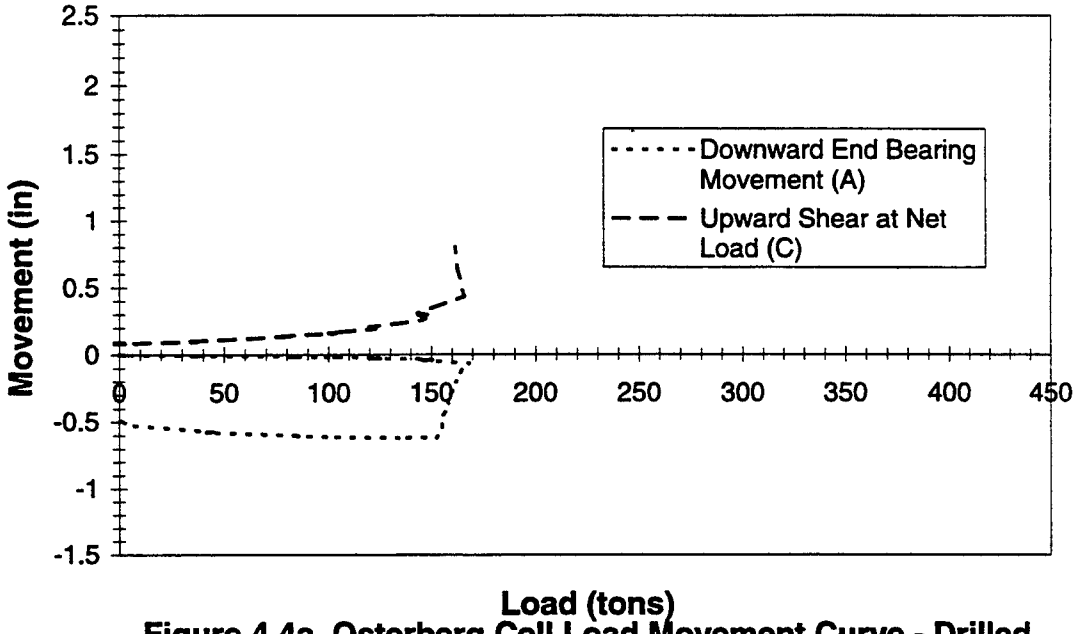

Figure 4.4a Osterberg Cell Load Movement Curve - Drilled Shaft #2 (2nd Loading)

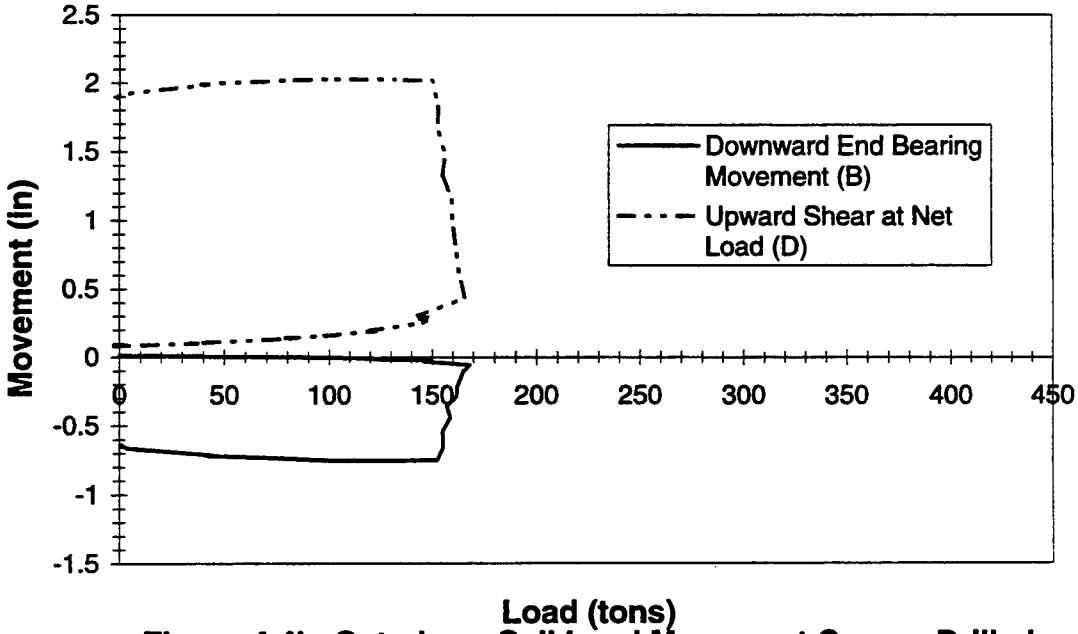

Figure 4.4b Osterberg Cell Load Movement Curve - Drilled Shaft #2 (2nd Loading)

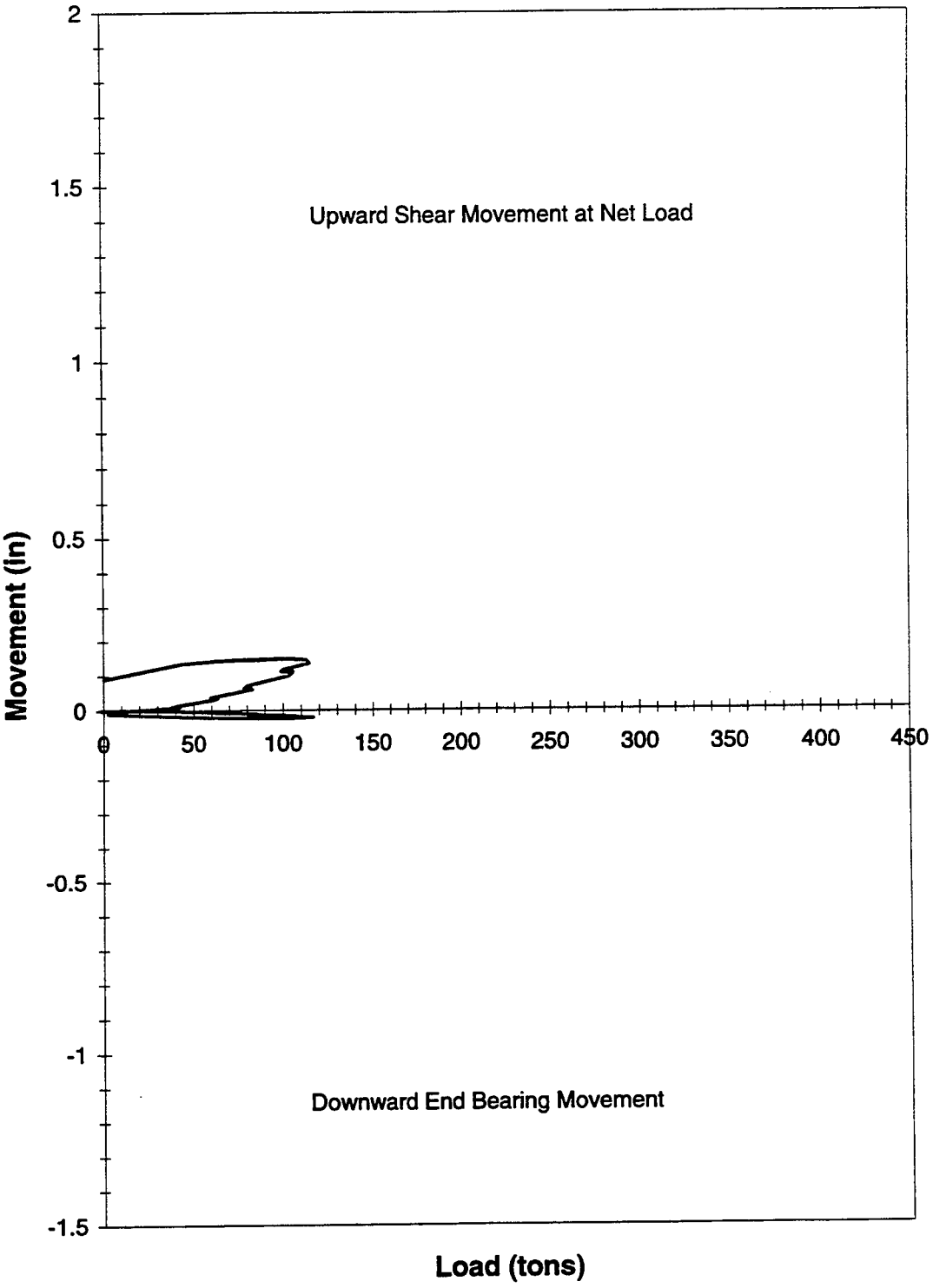

Figure 4.5 Osterberg Cell Average Load Movement Curve · Drilled Shaft #2 (1st Loading)

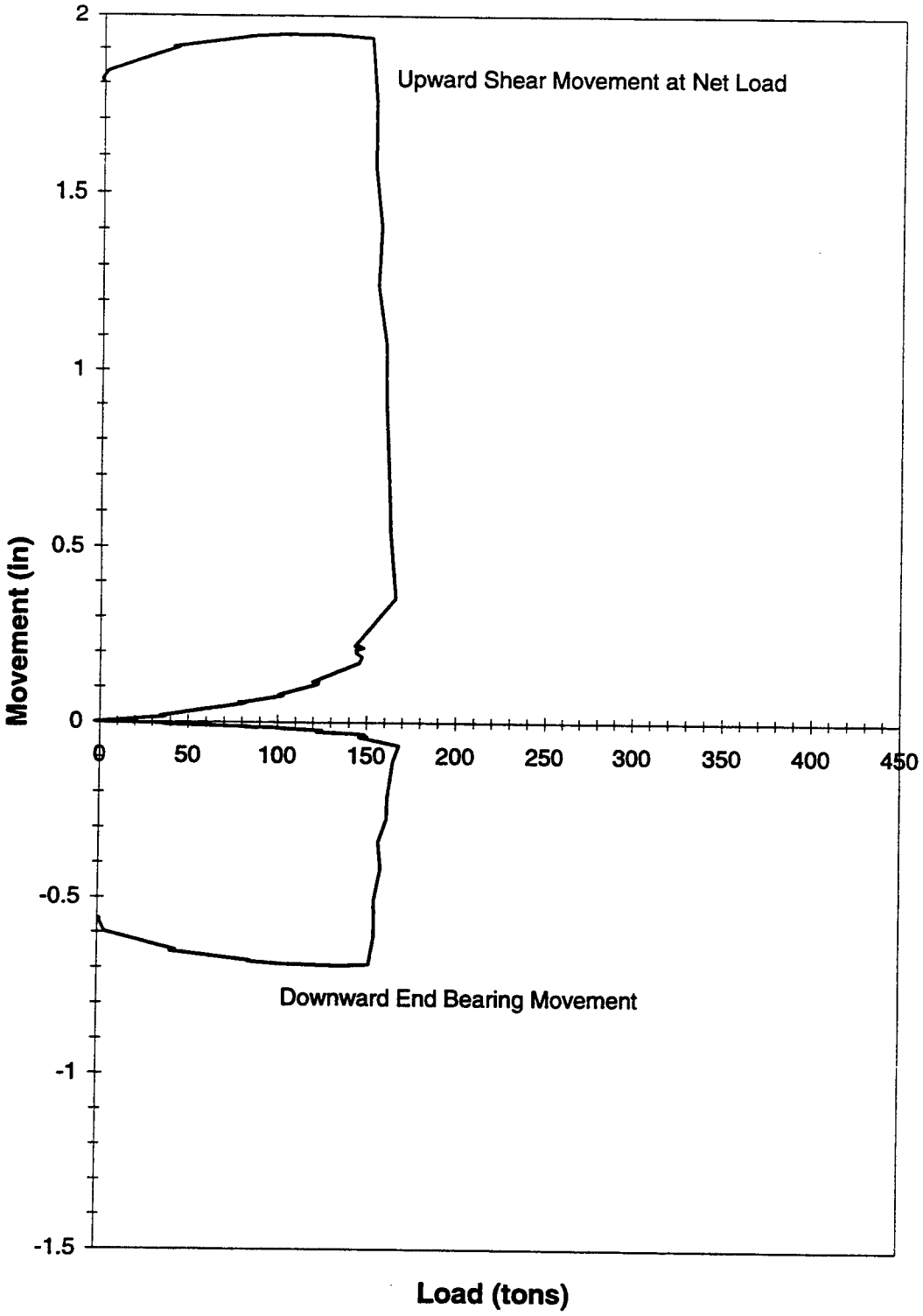

Figure 4.6 Osterberg Cell Average Load Movement Curve - Drilled Shaft #2 (2nd Loading)

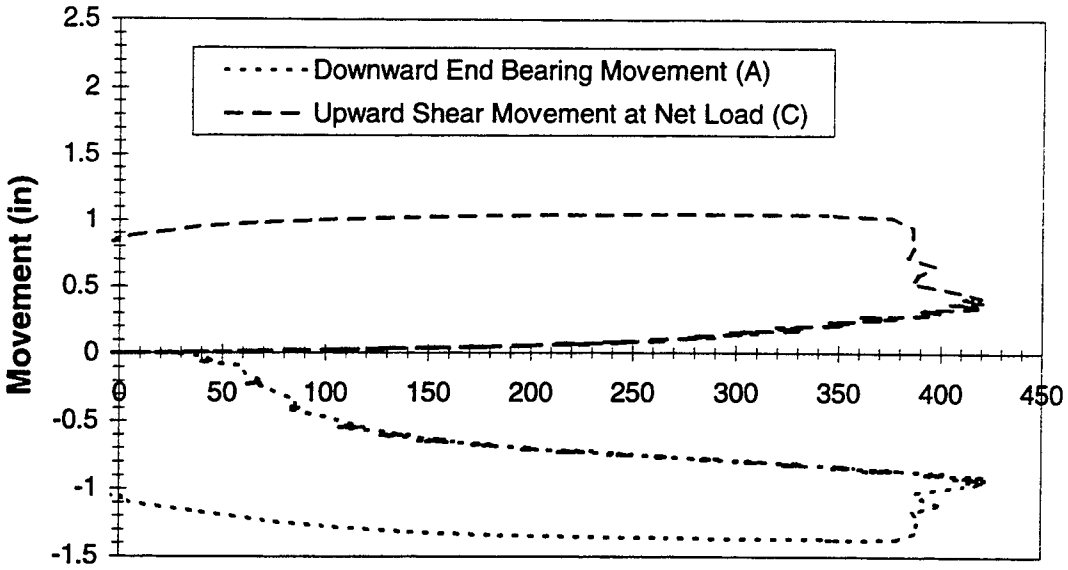

Figure 4.7a Osterberg Cell Load Movement Curve - Drilled Shaft #3

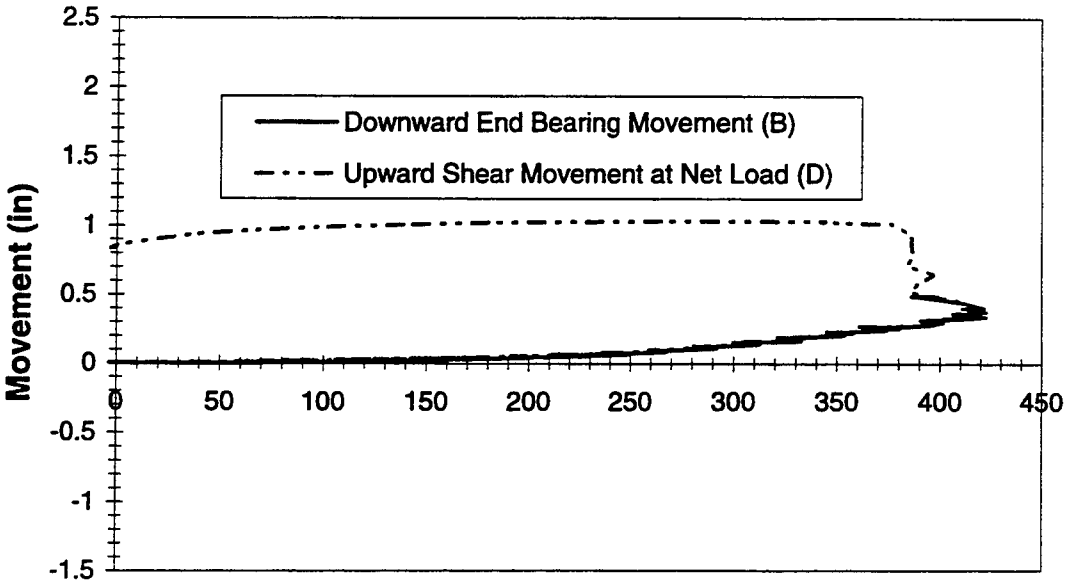

Figure 4.7b Osterberg Cell Load Movement Curve - Drilled Shaft #3

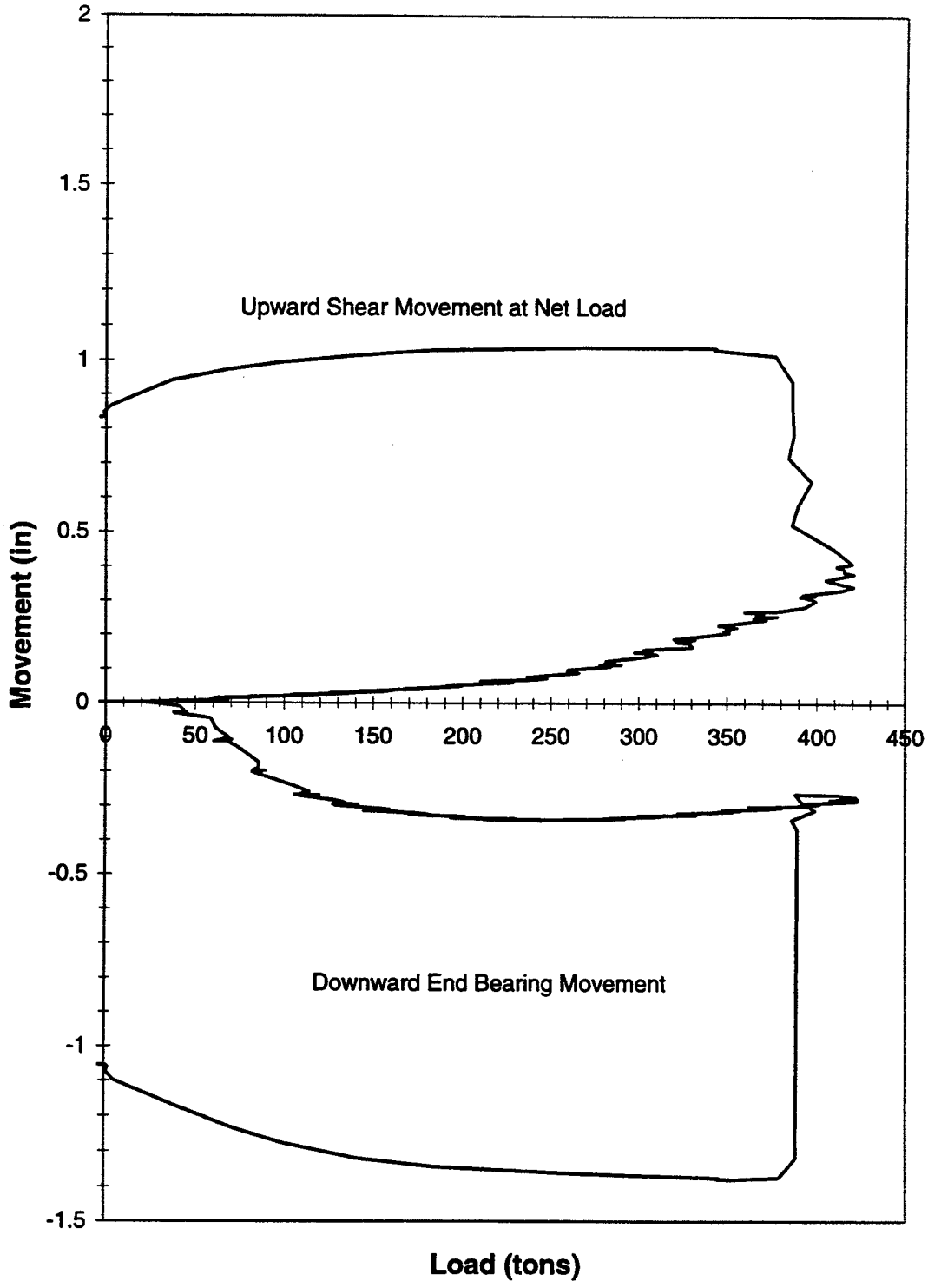

Figure 4.8 Osterberg Cell Average Load Movement Curve - Drilled Shaft #3

4.3.2 Reconstructed, Equivalent Top Load Movement Curve

The reconstructed, equivalent top load movement curve represents the load movement of the rock socketed drilled shaft as if the shaft was top loaded in the conventional field load test manner. This curve has been reconstructed using the following assumptions (Goodwin, 1993):

(a) The end bearing load movement in a conventionally loaded shaft is the same as the load movement curve developed by the bottom of the Osterberg cell.
(b) The upward side resistance movement curve for the Osterberg cell test is the same as the downward side resistance movement in a conventionally top loaded test.
(c) The compression of the shaft is considered negligible and the shaft is assumed rigid.

The above-mentioned assumptions were used to reconstruct the equivalent load movement curve. At a given top settlement, the corresponding side resistance and end bearing components were added to give the equivalent top load of a conventional test. This was done up to maximum movement of the upward or downward movement, whichever was of lesser magnitude.

The equivalent top load curve for shaft 1 was reconstructed to a settlement of 0.184 inches with a corresponding load of 724 tons. The top load curve for shaft 2 was reconstructed to a settlement of 0.605 inches and a corresponding load of 317 tons. This was done for the second loading of shaft 2. The top load curve for shaft 3 was

reconstructed to a settlement of 1.037 inches and a corresponding load of 733 tons. The reconstructed equivalent top load movement curves for shafts 1, 2, and 3 are presented in figures 4.9 through 4.12.

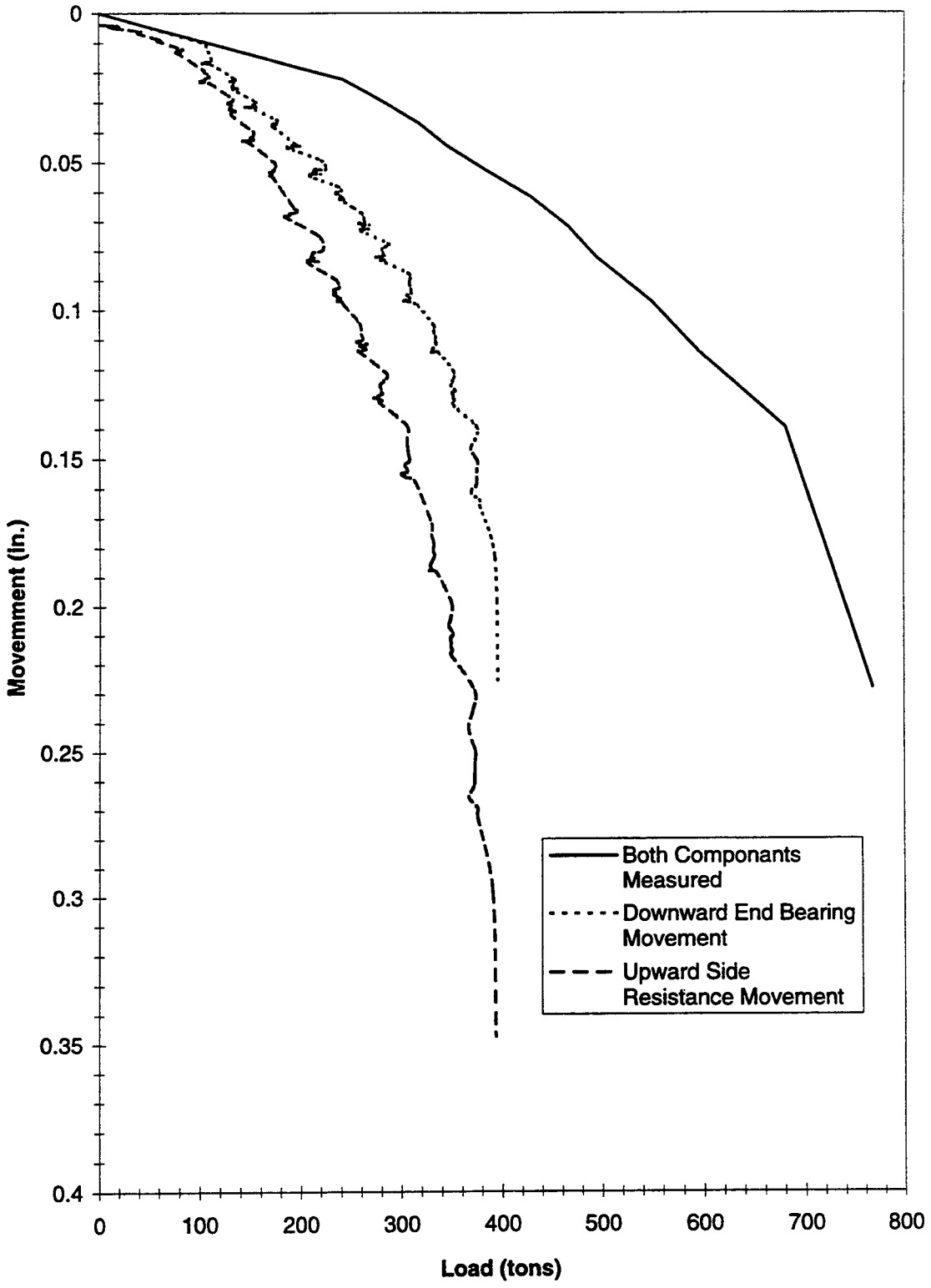

Figure 4.9 Equivalent Load Movement Curve - Drilled Shaft #1

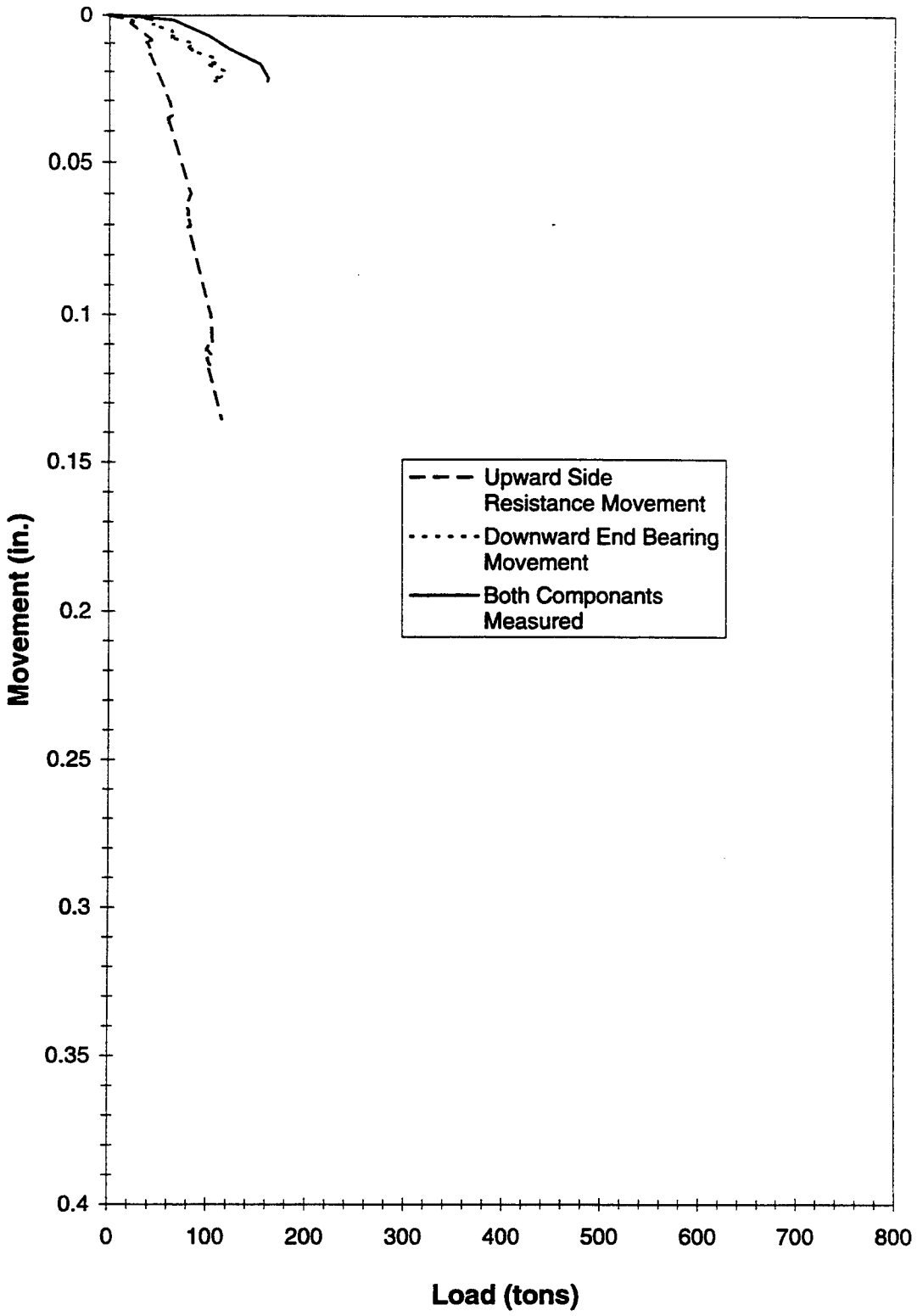

Figure 4.10 Equivalent Load Movement Curve - Drilled Shaft #2 (1st Loading)

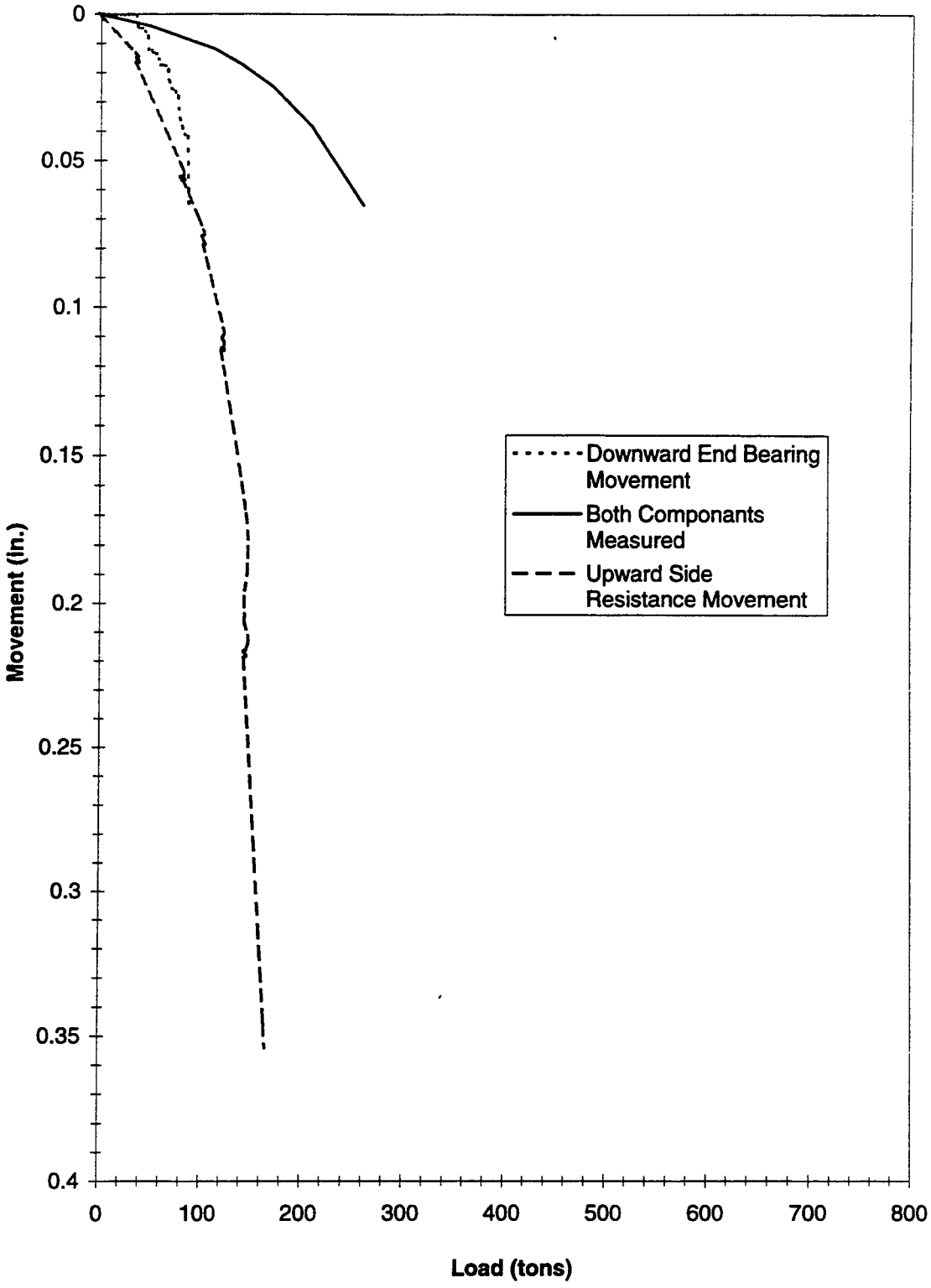

Figure 4.11 Equivalent Load Movement Curve - Drilled Shaft #2 (2nd Loading)

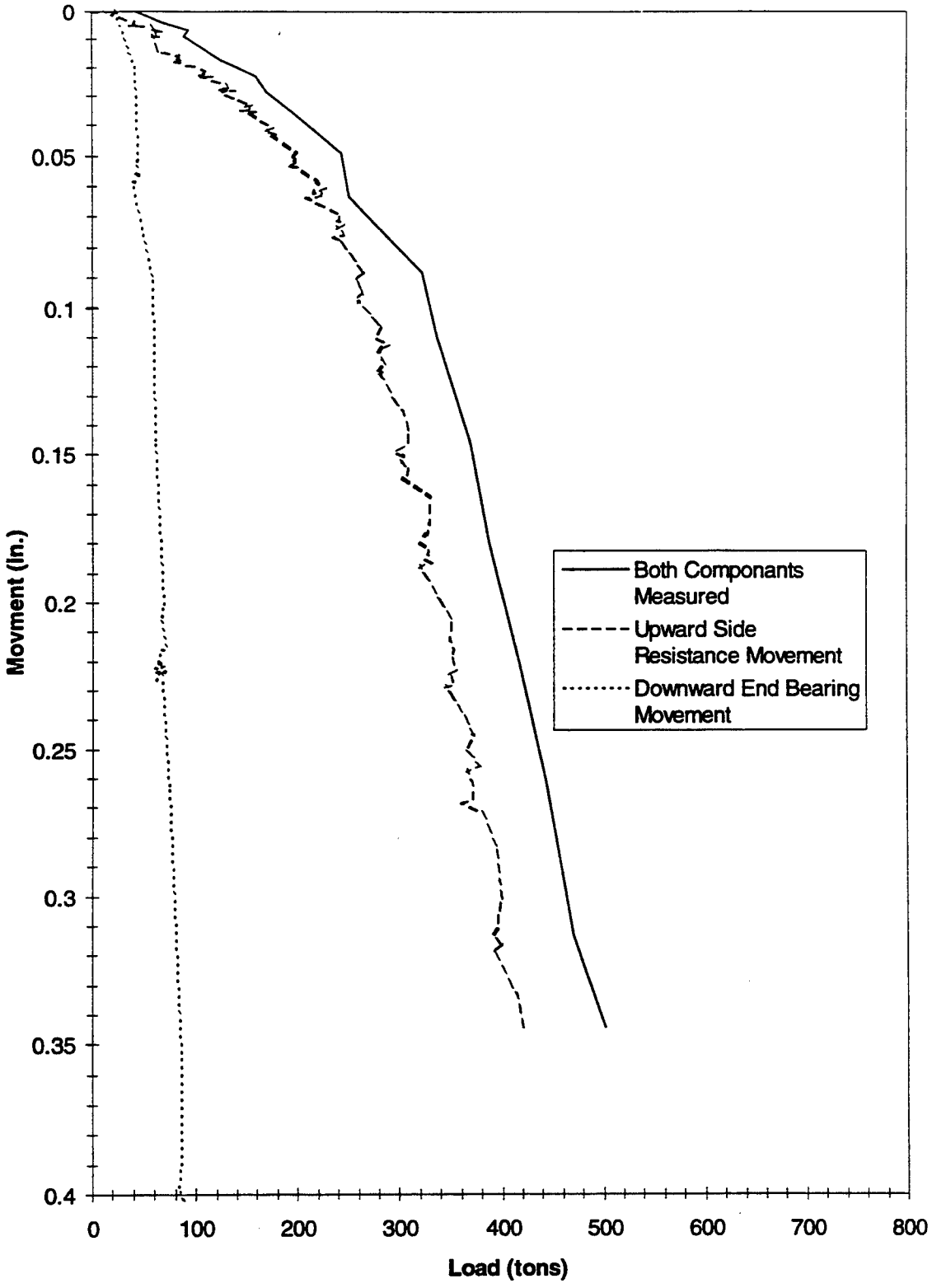

Figure 4.12a Equivalent Load Movement Curve - Drilled Shaft #3

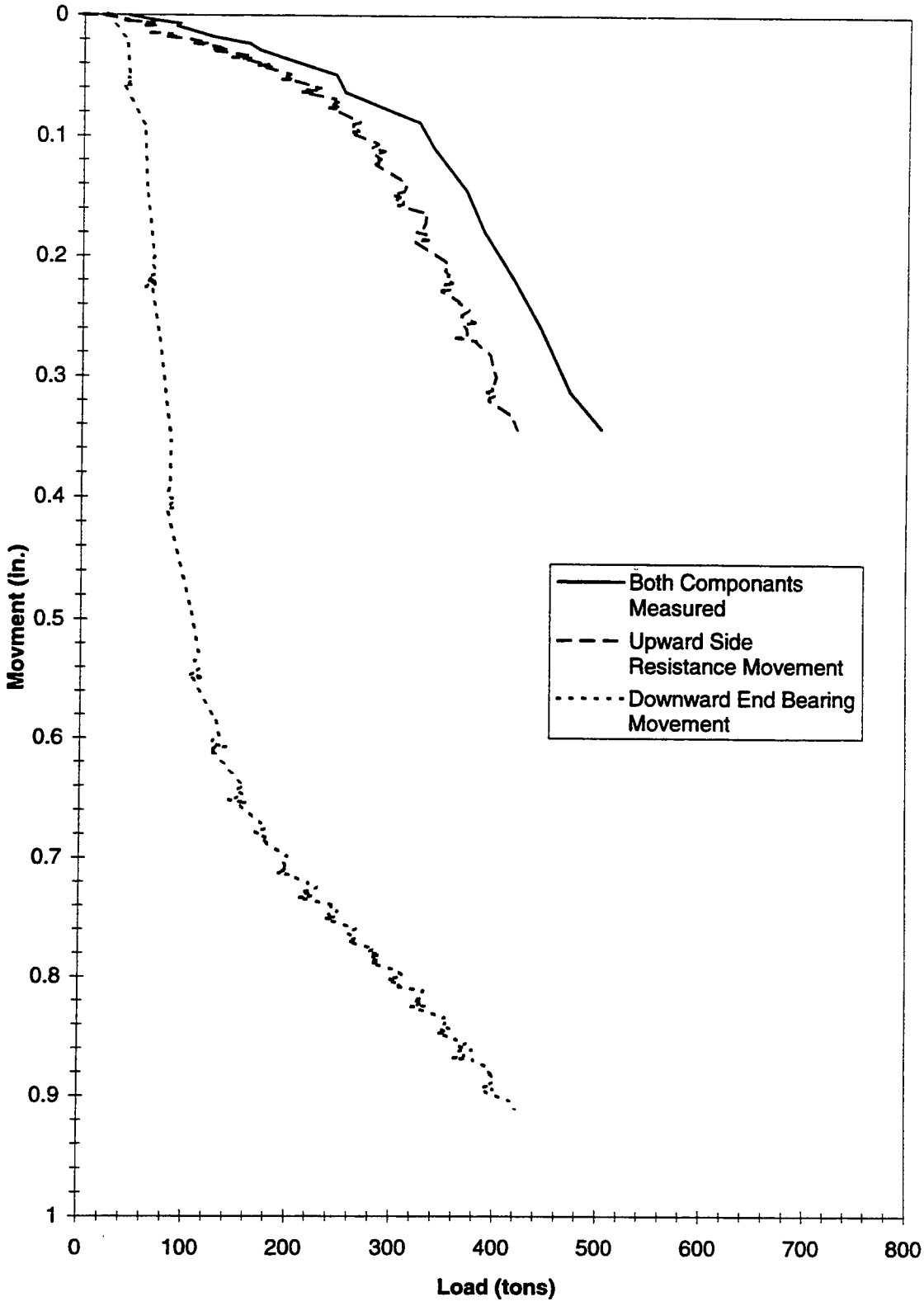

Figure 4.12b Equivalent Load Movement Curve - Drilled Shaft #3

4.3.3 Creep Limits

Dial gages E and F recorded the movements of the top of the shaft. This enabled the separation of creep measurements from the side resistance and end bearing movements. The movement over the 4 minute load increment was plotted against the magnitude of the load. This was done for the top of the shaft movement (dial gages E and F) and the bottom of the shaft movement (dial gages A and B). The creep was plotted as an average of dial gage readings for the bottom of shaft creep as well as the maximum creep readings. This was also done for the top of shaft creep movements.

There was no significant creep that occurred in the load testing of shaft 1, 2 and 3. This representation creep limit plots can be found in figures 4.13 through 4.18. Shaft 1 had a maximum bottom creep of about 0.012 inches at 350 tons and a top creep of about 0.001 at 370 tons. Shaft 2 had a maximum bottom creep of about 0.009 inches at 150 tons. Shaft 3 had a maximum bottom creep of about 0.16 inches at 50 tons and a top creep of about 0.009 at 50 tons. The creep limit curves have a significant amount of scatter. This scatter could have resulted in part from the inability to maintain a constant pressure of the Osterberg cell due to the limitations of the equipment.

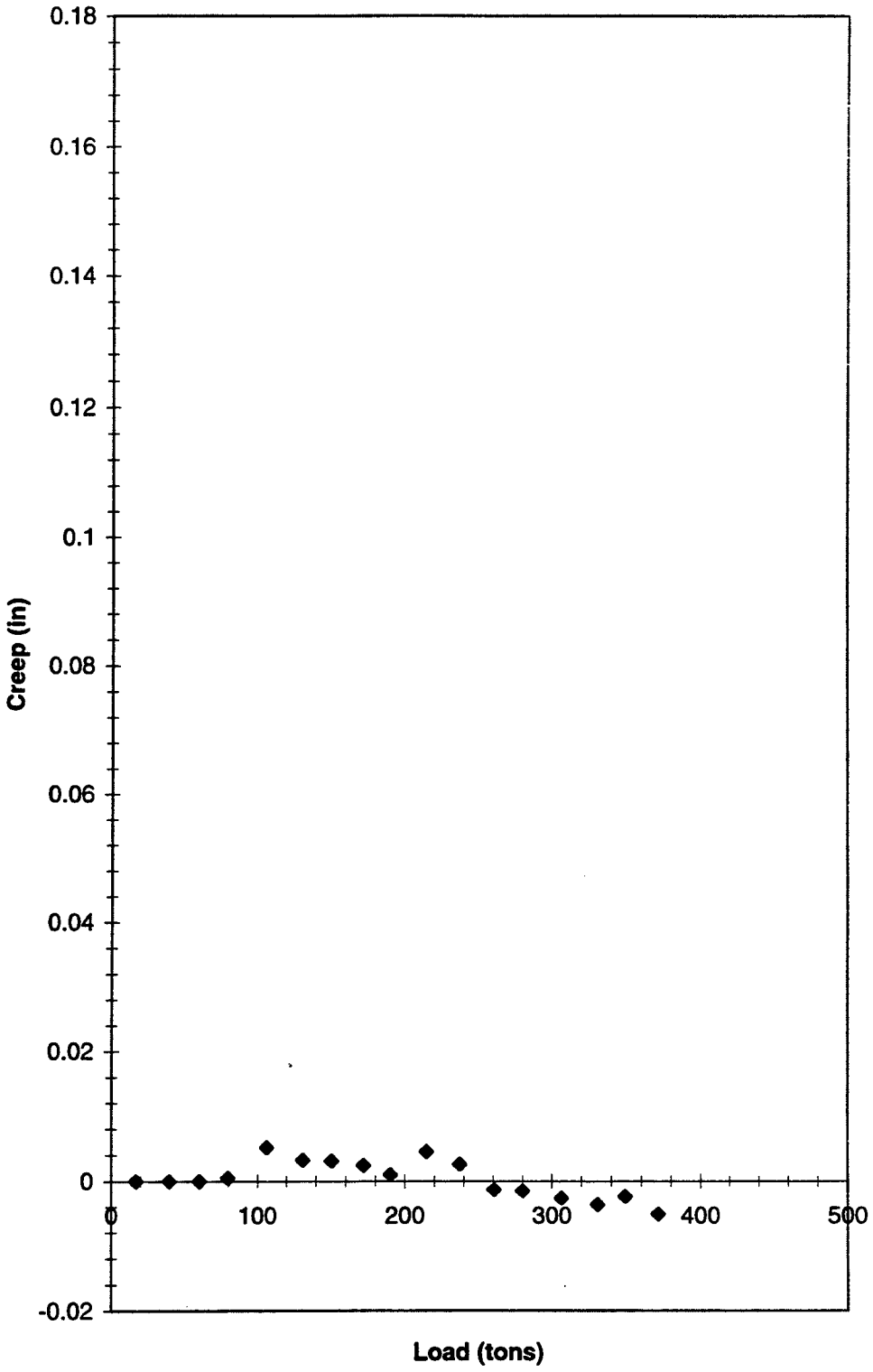

Figure 4.13 Average Bottom of Cell Creep Limit Curve - Drilled Shaft #1

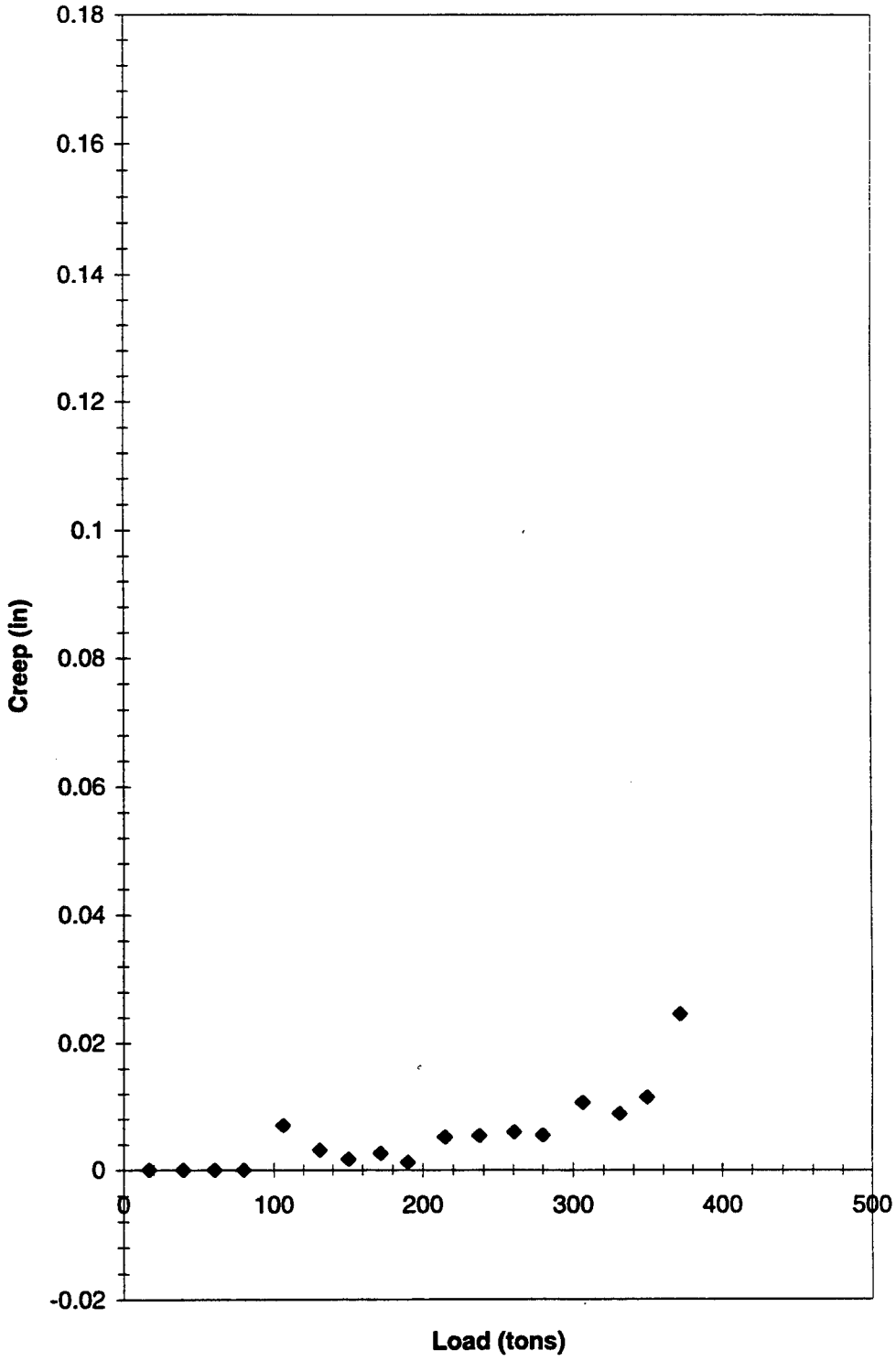

Figure 4.14 Maximum Bottom of Cell Creep Limit Curve - Drilled Shaft #1

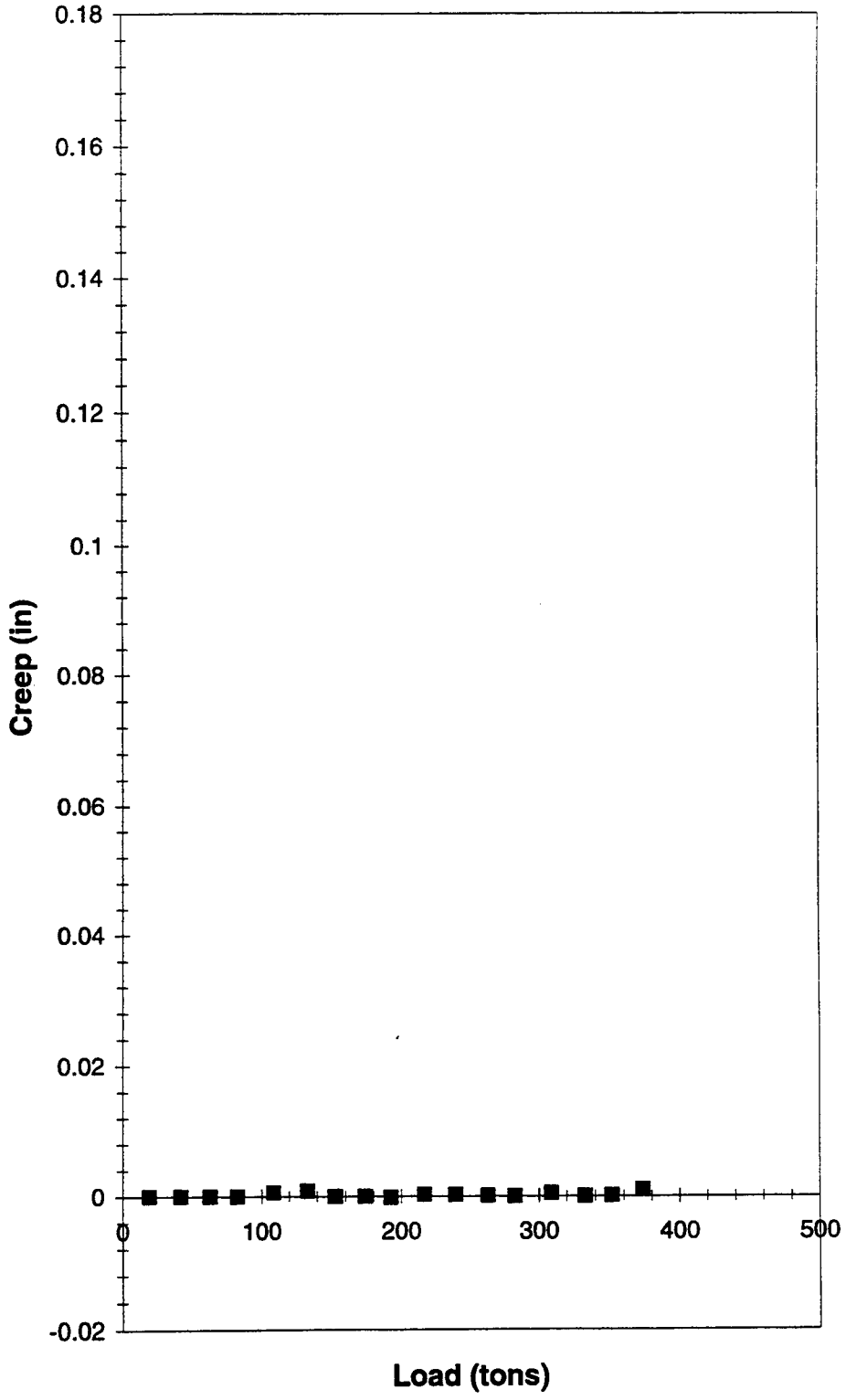

Figure 4.15 Average Top of Shaft Creep Limit Curve - Drilled Shaft #1

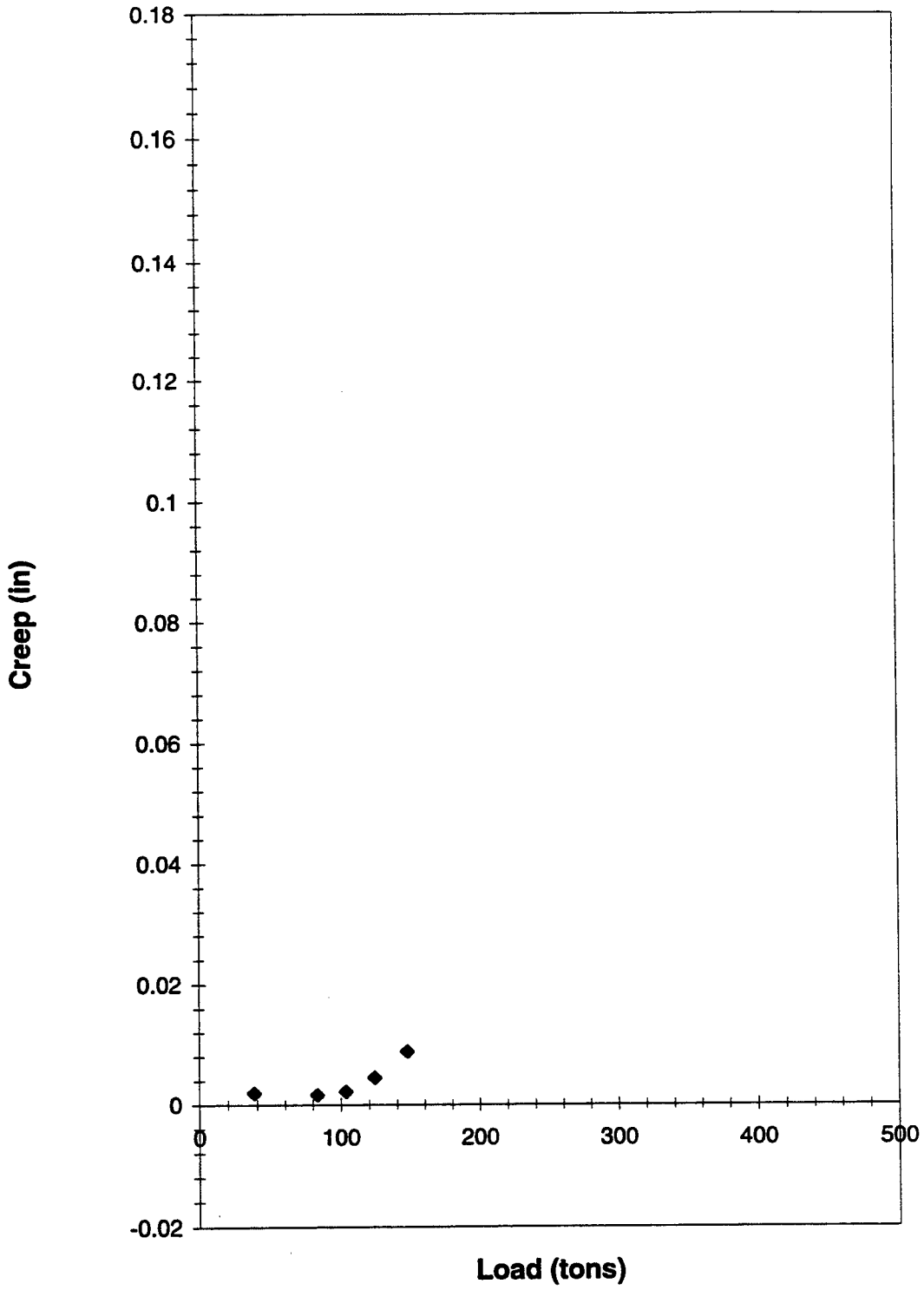

Figure 4.16 Average Bottom of Cell Creep Limit Curve - Drilled Shaft #2 (2nd Loading)

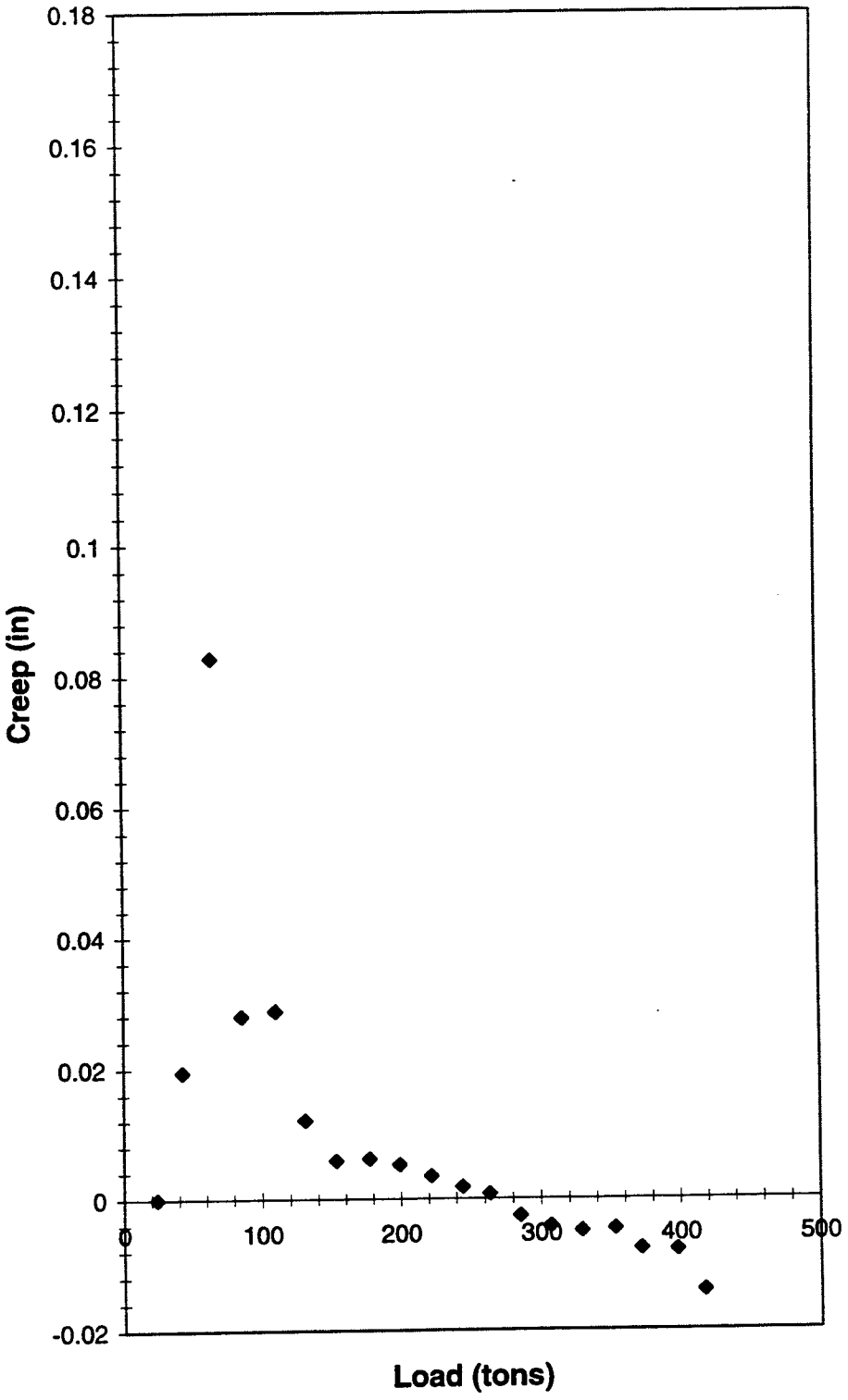

Figure 4.17 Average Bottom of Cell Creep Limit Curve - Drilled Shaft #3

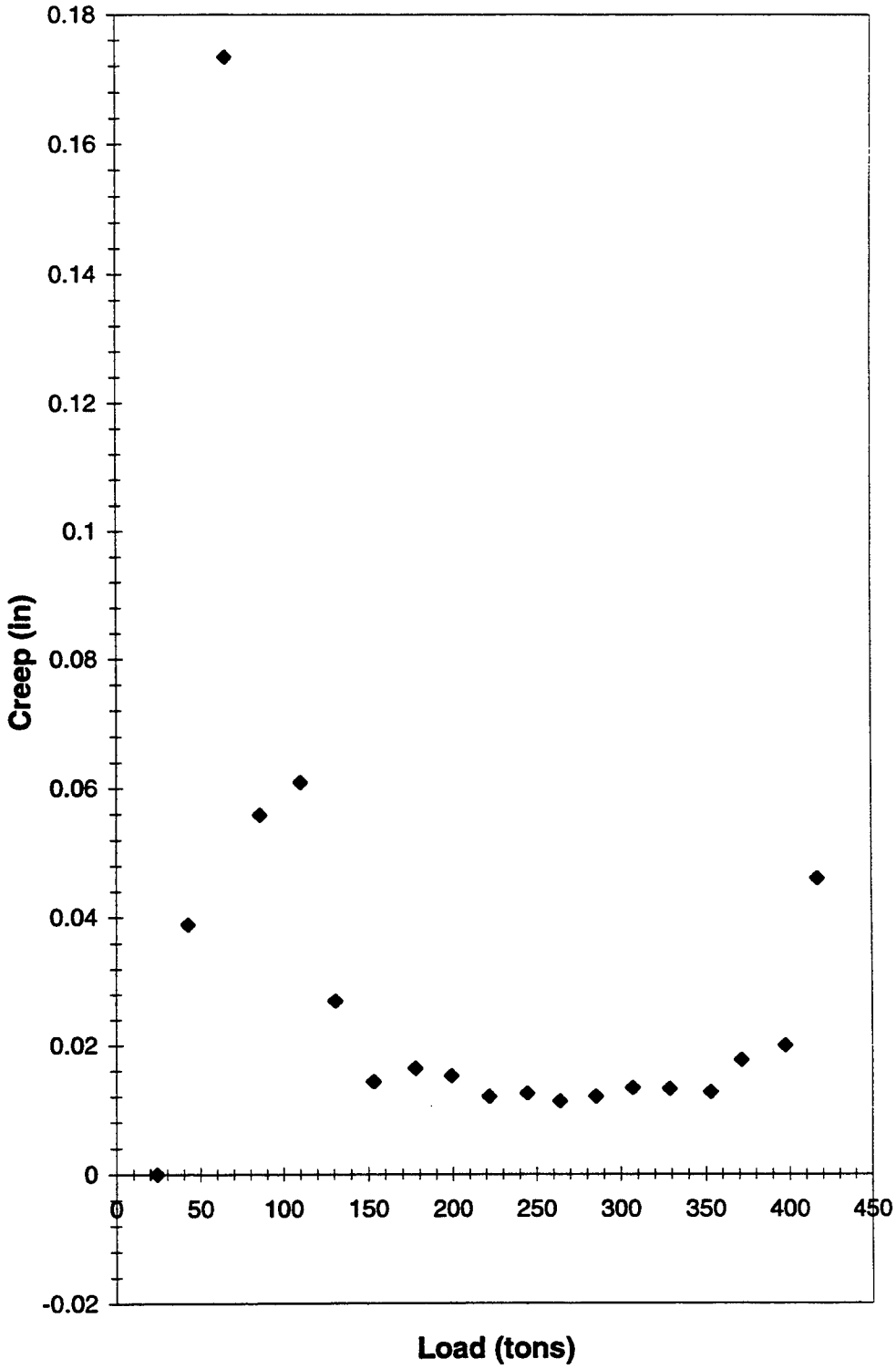

Figure 4.18 Maximum Bottom of Cell Creep Limit Curve Drilled Shaft #3

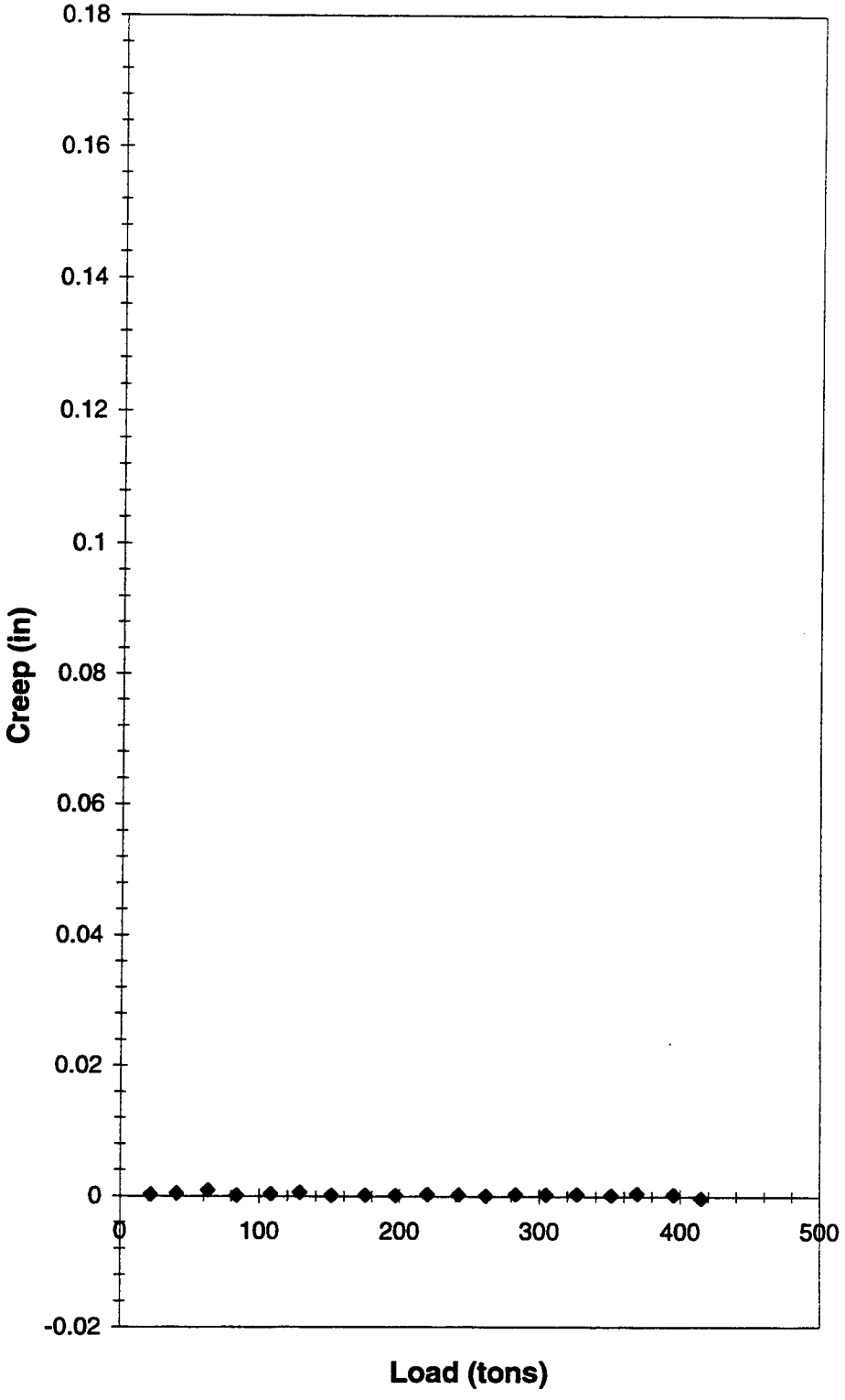

Figure 4.19 Average Top of Shaft Creep Limit Curve - Drilled Shaft #3

4.4 Comparison of Predicted Versus Actual Capacity

One of the motivations for the full scale load testing of rock socketed drilled shafts was that the predicted capacity of socketed shafts based on presumptive values of bearing capacity were believed to be overly conservative. The maximum side resistance of the three shafts was reached and therefore can be compared directly with predicted side resistance values. Due to the limitations of the bi-directional loading of the Osterberg cell the maximum capacity of end bearing was not reached. The predicted end bearing will be compared to the maximum end load of the test shafts with the knowledge that the end bearing capacity was not reached.

4.4.1 Comparison of Predicted Versus Actual Side Resistance

The predicted side capacity was calculated using Equations 3, 6, and 7 from section 2.1.3. Equations 4, 5, 8, 9, and 10 are for soft rock and cannot be used in comparison with the results from shafts 1, 2, and 3 which were socketed into hard limestone. The predicted side resistance capacities were calculated using a concrete strength of 5300 psi (381.6 tsf) rather than the unconfined compressive strength of the rock (8000 psi). The lower value of the unconfined compressive strength of the rock and the concrete strength should be used when calculating predicted side resistance capacity using the previously mentioned formulas. Side resistance failure will occur in the lower

strength material. Table 4.4.1 contains the direct comparison of maximum side resistance values from the field load test as well as the predicted side resistance values.

	Side Resistance
Shaft 1	24.5 tsf
Shaft 2	9.6 tsf
Shaft 3	23.8 tsf
Equation 3	16.32 tsf
Equation 6	13.09 tsf
Equation 7	12.31 tsf

Table 4.2 Actual and Predicted Side Resistance Values

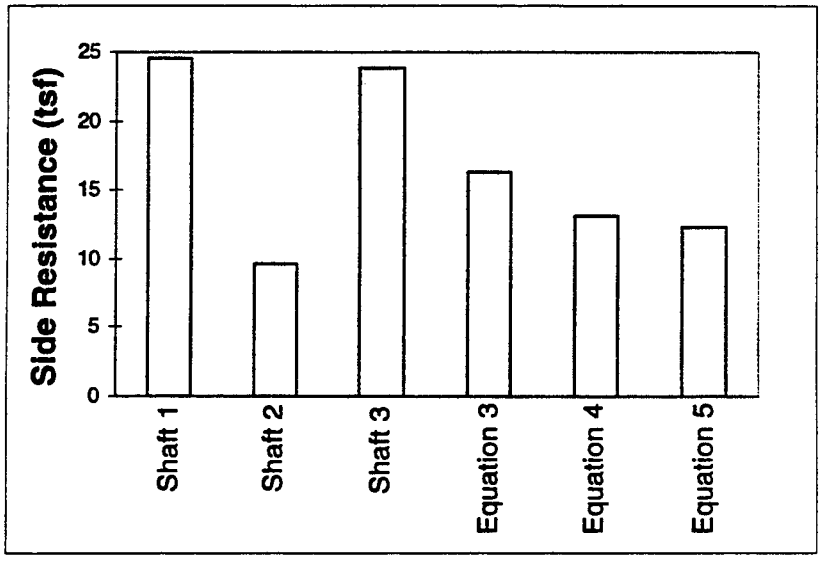

Figure 4.20 Comparison of Actual Versus Predicted Side Resistance Values

The predicted values of side resistance are significantly lower than the values of side resistance obtained from shafts 1 and 3. The side resistance value from shaft 2 could be falsely low due to a pump malfunction during testing and the subsequent reloading of the shaft. The actual side resistance of Shaft 1 is 50 percent higher than equation 3, 87 percent higher than equation 6, and 99 percent higher than equation 7. The actual side resistance of Shaft 3 is 46 percent higher than equation 3, 82 percent higher than equation 6 and 93 percent equation 7.

After the maximum side resistance was reached residual side resistance was observed. Shaft 1 reached maximum side resistance of 24.5 ton per square foot at about 0.36 inches of upward movement. The observed residual side resistance was an average of 21.7 tons per square foot, up to an upward movement of 0.7 inches. Shaft 2 reached its maximum side resistance of 9.6 ton per square foot at about 0.4 inches of upward movement. The observed residual side resistance was an average of 9.03 tons per square foot up to an upward movement of 2.0 inches. Shaft 3 reached its maximum side resistance of 23.8 ton per square foot at about 0.4 inches of upward movement. The observed residual side resistance was an average of 20.9 tons per square foot up to an upward movement of 1.0 inches.

The presence of this significant side resistance shows that even after the maximum side resistance is reached a significant portion of the load will still be carried in side resistance and never reach end bearing. This contradicts some of the current design procedures which specify the design of socketed drilled shafts to be designed using only

one of the load bearing mechanisms. The results of the load tests show that even after side resistance failure a large amount of side resistance will remain.

4.4.2 Comparison of Actual End Bearing Values Versus End Bearing Assumptions

Due to the limitations of the Osterberg cell it was not possible to reach the maximum end bearing capacity. Since the Osterberg load cell loads the shaft from the bottom, the applied load can only be as large as the load bearing mechanism with the lowest capacity. In the case of shafts 1, 2, and 3 it was side resistance. Table 4.3 presents the observed end bearing loads at the termination of testing.

	Observed End Bearing Load
Shaft 1	396 tons (224.1 tsf)
Shaft 2	168 tons (95.1 tsf)
Shaft 3	423 tons (239.4 tsf)

Table 4.3 Observed End Bearing Loads

The most common design method for estimating the ultimate end bearing capacity is to simply use the unconfined compressive strength of the rock. No compression tests were taken from the test shafts but tests from other site investigations in the immediate vicinity had an average unconfined compressive strength of about 8000 psi (576 tsf). This value is difficult to compare to the observed end bearing pressures due to the inability to load the shafts to reach their ultimate end bearing capacity.

Section 2.1.4 outlines some of the allowable end bearing pressure values provided by various building codes. Table 4.4 contains the allowable end bearing code values as they apply to shafts 1, 2, and 3. Available site investigations and foundation recommendations of construction near the test site also recommended an allowable end bearing pressure of 20 tsf.

Table 4.4 Allowable Presumptive End Bearing Values for Limestone Bedrock

	Allowable End Bearing Pressure
BOCA	100 tsf
National Building Code of Canada	10 tsf
Chicago Building Code	167 tsf
Unified Building Code	5.83 tsf

It is also relevant to note that the code values listed above allow for increased allowable pressures with proper site investigations.

The observed values of foundation pressures of the test shafts significantly exceed the suggested allowable values listed above. This is of particular interest since the ultimate end bearing was not obtained. This helps to validate the belief that building code values of end bearing are overly conservative.

4.5 Discussion

Many rock socketed drilled shafts that have sockets in strong rock such as limestone are designed to carry the entire load in end bearing. This is believed to be an overly conservative method of design. Side resistance will carry a significant portion of the load and in some cases, it may carry nearly all of the load with no load carried in end bearing.

The following example illustrates the conservatism of an end bearing designed shaft that is socketed into strong rock. Engineering recommendations for recent construction projects in the area of the test area recommend an allowable end bearing pressure of 40 kips per square foot. Given a total shaft load of 600 kips and an allowable end bearing pressure of 40 kips per square foot, the shaft would have a diameter of 54 inches. It is assumed that the shaft is socketed two feet into the rock. The observed average side resistance of shafts 1 and 3 was 335 pounds per square inch. Using this value and a rock concrete bond area of 12,791 square inches, the shaft would support 1363 kips in side resistance alone and none of the load would be carried in end bearing.

This example helps to show the conservative nature of design in end bearing only. It is also believed that it is overly conservative to disregard side resistance completely after the initial failure of the side resistance mechanism. The data from Shaft 1, 2, and 3 suggest that there is significant side resistance capacity even at higher deflections.

CHAPTER FIVE

SUMMARY OF CONCLUSIONS

The full scale load tests of three rock socketed drilled shafts using the Osterberg load cell illustrated the extreme conservative nature of current rock socketed drilled shaft design. Based on the results of this study the following conclusions can be drawn:

1. *The observed values of side resistance significantly exceed the values obtained through current methods of side resistance prediction.* Shafts 1 and 3 developed a side resistance of about 24 tons per square foot. This is approximately 50 percent higher than the nearest value calculated using current methods of side resistance prediction.
2. *The observed values of end bearing exceed those suggested by building codes.* The values of end bearing obtained during testing were less than ultimate capacity. Due to equipment limitations the shafts were unable to be failed in end bearing. Regional practice has been to use an assumed value end bearing pressure of approximately 20 tons per square foot. The observed values for end bearing pressure in shafts 1 and 2 were over 10 times greater than the value cited above.
3. *Residual side resistance capacity exists when large movements have occurred and the ultimate side resistance has been exceeded.* The residual side resistance observed in test shafts 1 and 3 was about 20 tons per square foot. The residual side resistance is

commonly ignored in the design of socketed drilled shafts. Even when relatively large movements occur, the test data implies that a large portion of the load will be carried by residual side resistance.

4. *Shafts in strong rock that are designed using end bearing as the only load bearing mechanism appear to be overly conservative.* Test data show that side resistance will carry a large portion of the load and in some cases, the entire load.

The current regional design of rock socketed drilled shafts would be to use end bearing as the only load carrying mechanism with an allowable end bearing pressure of 20 tons per square foot. This implies that the test shafts would be allowed to carry a load of 36 tons. The equivalent top load movement curves for shafts 1 and 3 found in figures 9 and 12 indicate a maximum load of about 750 tons for shaft 1 and 500 tons for shaft 3. The maximum equivalent top loads are 20 and 14 times the current allowable load for socket shafts of the same size. The equivalent top loads are even less than capacity due to the inability of the equipment to fail test shafts in end bearing. This comparison shows the grossly conservative nature of the current design of rock socketed drilled shafts. Although complete site investigations are needed to accurately predict the performance of socketed shafts, the cost savings due to smaller and/or fewer rock socketed drilled shafts will, in most circumstances, surpass the cost incurred by the complete site investigation. In conclusion, the revision of current rock socketed drilled shaft design procedures to produce a less conservative but equally safe socketed shaft could lead to substantial construction cost savings.

REFERENCES

Baker, C. N., & Kahn, F. (1971). Caisson construction problems and correction in Chicago. ASCE, Journal of Soil Mechanics and Foundation Division, 97, 417-440.

Building Officials & Code Administrators International, Inc. (1980). The BOCA Basic Building Code (8th ed.) (pp. 209-227). Homewood, IL: Author.

Carter, J. P., & Kulhawy, F. H. (1988). Analysis and design of drilled shaft foundations socketed into rock. EPRI Report El-5918. Palo Alto, CA: Electric Power Research Institute.

Donald, I. B., Chiu, H. K., & Sloan, S. W. (1980). Theoretical analysis of rock socketed piles. In P. J. N. Pells (Ed.), Proceedings of the International Conference on Structural Foundations on Rock (pp. 303-316), Sydney, Australia. Rotterdam, Netherlands: A. A. Balkema.

Engineering Surveys and Services. (Unpublished manuscript). Subsurface investigation, soil analysis and foundation design recommendations for University of Missouri Veterinary Medicine Building renovation and replacement, Columbia, Missouri. Report prepared for the University of Missouri General Services, Columbia, Missouri.

Freeman, C. F., Klajnerman, D., & Prasad, G. D. (1972). Design of deep socketed caissons into shale bedrock. Canadian Geotechnical Journal, 9, 105-114.

Glos, G. H., & Briggs, O. H. (1983). Rock sockets in soft rock. Journal of the Geotechnical Engineering Division, ASCE, 109(4), 525-535.

Goodwin, J. W. (Unpublished manuscript). Bi-directional load testing of shafts to 6000 tons. Presented at the 1993 ASCE Annual Convention, Dallas, TX.

Gupton, C., & Logan, T. (1984). Design guidelines for drilled shafts in weak rocks of south Florida. Proceedings of the South Florida Annual ASCE Meeting. ASCE.

Horvath, R. G., & Kenney, T. C. (1979). Shaft resistance of rock-socketed drilled piers. Proceedings of the Symposium on Deep Foundation. ASCE.

International Conference of Building Officials (1997). Uniform Building Code (Vol. 1), (pp. 169-176). Whittier, CA: Author.

Jackson, W. T., Perez, J. Y., & Lacroix, Y. (1974). Foundation, construction and performance for a 34-storey building in St. Louis, Geotechnique, 24, 63-90.

Ladanyi, B. (1977). Friction and end bearing tests on bedrock for high capacity socket design: Discussion. Canadian Geotechnical Journal, 14, 153-155.

Ladanyi, B., & Domingue, D. (1980). An analysis of bond strength for rock socketed piers. In P. J. N. Pells (Ed.), Proceedings of the International Conference on Structural Foundations on Rock (pp. 363-373), Sydney, Australia. Rotterdam, Netherlands: A. A. Balkema.

McVay, M. C., Townsend, F. C., & Williams, R. C. (1992). Design of socketed drilled shafts in limestone. Journal of Geotechnical Engineering, 118(10), 1626-1637.

Osterberg, J. O., & Pepper, S. F. (1984). A new simplified method for load testing drilled shafts. Foundation Drilling, Association of Drilled Shaft Contractors, 9-11.

Pells, P. J. N., Rowe, R. K., & Turner, R. M. (1980). An experimental investigation into side shear for socketed piles in sandstone. In P. J. N. Pells (Ed.), Proceedings of the International Conference on Structural Foundations on Rock (pp. 291-302), Sydney, Australia. Rotterdam, Netherlands: A. A. Balkema.

Reese, L. C., & O'Neill, M. W. (1987). Drilled shafts: construction procedures and design methods. Design Manual. McLean, VA: U.S. Department of Transportation, Federal Highway Administration.

Reynolds, R. T., & Kaderabek, T. J. (1980). Miami limestone foundation design and construction. ASCE. New York, NY: ASCE.

Rosenberg, P., & Journeaux, N. L. (1976). Friction and end bearing tests on bedrock for high capacity socket design. Canadian Geotechnical Journal, 13, 324-333.

Rowe, R. K., & Armitage, H. H. (1987). Theoretical solutions for axial deformation of drilled shafts in rock. Canadian Geotechnical Journal, 24, 114-125.

Rowe, R. K., Booker, J. R., & Balaam, N. (1978). Application of the initial stress method to soil-structure interaction. International Journal of Numerical Methods in Engineering, 12(5), 873-880.

Rowe, R. K., & Pells, P. J. N. (1980). A theoretical study of pile-rock socket behavior. In P. J. N. Pells (Ed.), Proceedings of the International Conference on Structural Foundations on Rock (pp. 253-264), Sydney, Australia. Rotterdam, Netherlands: A. A. Balkema.

Seychuck, J. L. (1970). Load tests on bedrock. Canadian Geotechnical Journal, 7, 464-470.

Schmertmann, J. H. (Unpublished manuscript). The bottom-up, Osterberg cell method for static testing of shafts and piles. Thirteenth Central PA Geotechnical Seminar, Hershey, PA, 12-14 Apr, 1993.

Thorne, C. P. (1980). The capacity of piers drilled in rock. In P. J. N. Pells (Ed.), Proceedings of the International Conference on Structural Foundations on Rock (pp. 223-233), Sydney, Australia. Rotterdam, Netherlands: A. A. Balkema.

Unklesbay, A. G. (1952). Geology of Boone County Missouri (Vol. 33). Jefferson City, MO: State of Missouri.

Williams, A. F., Johnston, I. W., & Donald, I. B. (1980). The design of socketed piles in weak rock. In P. J. N. Pells (Ed.), Proceedings of the International Conference on Structural Foundations on Rock (pp. 327-347), Sydney, Australia. Rotterdam, Netherlands: A. A. Balkema.

Wyllie, D. C. (1992). Foundations on Rock. New York: Chapman & Hall.

APPENDIX A

This appendix is a review of the some of the current design procedures available for rock socketed drilled shafts. This report entitled *Design of Rock Socketed Drilled Shafts* was completed July, 1996 by Chad Kiehne in partial fulfillment of Civil Engineering 350 - Honors Research at the University of Missouri-Columbia with Dr. Brett Gunnink as the Honors Research advisor.

LIST OF TABLES

Table		Page
1	Rock Quality and Deformability Correlation	107
2	Percentage of Load in End Bearing	107
3	Factors for Embedment Ratio	107

LIST OF FIGURES

FIGURE		Page
1	Design Charts for a Complete Socketed Pier	95
2	Design Charts for a Complete Socketed Pier	96
3	Design Charts for a Complete Socketed Pier	97
4	Elastic Settlement Influence Factors for a Complete Socket	98
5	Reduction Factors for a Recessed Socket	99
6	Settlement Influence Factor as a Function of Embedment Ratio and Modular Ratio	100
7	Engineering Classification of Intact Rock	101
8	Modulus Reduction as a function of RQD	102
9	Reduction Factors for a Recessed Socket	103
10a	Reduction Factors for Calculation of Average Settlement of End Bearing Sockets	104
10b	Elastic Settlement Influence Factors for Side-Wall Resistance Socketed Piers	104
11	Data on Load Transfer of Socketed Piers	105
12	Influence Factors and End Bearing Ratios for Complete Socketed Piers	106

TABLE OF CONTENTS

LIST OF TABLES....66

LIST OF FIGURES....67

CHAPTER ONE INTRODUCTION....69

CHAPTER TWO INVESTAGATIONS FOR SOCKETED DRILLED SHAFTS..71

CHAPTER THREE LOAD CAPACITY OF SOCKETED DRILLED SHAFTS IN COMPRESSION....73

CHAPTER FOUR DESIGN OF ROCK SOCKETED DRILLED SHAFT....75

CHAPTER FIVE CONCLUSION....93

FIGURES AND TABLES....94

REFERENCES....108

DESIGN OF ROCK SOCKETED DRILLED SHAFTS

CHAPTER ONE
INTRODUCTION

Drilled shafts are constructed by drilling a cylindrical hole to the required depth, placing a rebar cage in the hole and subsequently filling it with concrete. Drilled shafts are also often referred to as drilled piers, drilled caissons and bored piles (Bowles, 1996). The focus of this paper will be rock socketed drilled shafts, which are set into rock several shaft diameters deep. Rock socketed drilled shafts are used when rock is overlain by weak material and when large service loads are applied.

Drilled shafts have some distinct advantages over other types of deep foundations. First, the cost of mobilization and demobilization of drilling equipment is much less than that of a pile driver. Mobilization can be a significant portion of the total cost, especially on smaller projects. Secondly, the construction methods for drilled shafts cause less noise and vibration than pile drivers, which can be important when working in close vicinity to existing structures. Also, the soil excavated during construction may be examined and compared with anticipated soil conditions. Compensation, such as increased diameter or length, for unexpected soil conditions can be easily made. In addition, drilled shafts can penetrate rocky soils and bedrock when needed. Finally, one large shaft can support a column, which eliminates the need for a pile cap (Coduto, 1994).

Along with the advantages of this type of foundation construction, there are disadvantages. Error in construction is possible. Caving soil can reduce the shaft diameter in localized areas and cause the shaft to be unable to support the design load, however, these errors and defects are not usually visible. Another disadvantage is that drilled shafts do not produce the lateral stress that is produced in piles. This is due to the removal of soil instead of the displacement caused by pile driving, which increases the lateral pressures. Due to budget constraints, the expensive full scale load tests normally required to determine axial load capacity are not performed. Instead, empirical methods based on soil properties are used to predict axial load capacity, which often leave many drilled shafts overdesigned due to the uncertainty of soil conditions (Coduto, 1994).

CHAPTER TWO

INVESTIGATIONS FOR SOCKETED DRILLED SHAFTS

The initial site investigation is an important part of rock socketed drilled shaft design and construction. A thorough site investigation will reduce uncertainty and allow for less conservative designs while maintaining safety. Knowledge of subsurface conditions such as soil type, depth and the condition of the rock are useful in almost all design situations. Construction costs for rock sockets are significant and the cost of a thorough subsurface investigation can lead to smaller socket lengths and diameters which could result in a lower overall project cost.

The identification of geological features is also important because the location and variation of the rock surface can help determine the length of the shaft. Areas that have weak rock, shattered rock or clay seams should be located and the spacing and thicknesses of the joints in the rock should be recorded. In areas of karstic formations it is not uncommon to have solution cavities embedded in otherwise sound rock. Exploratory drill holes must extend well below the envisioned foundation depth to ensure that there are no cavities in the end bearing zone. During the investigation process, the location of any groundwater should also be noted (Reese and O'Neill, 1988).

Information must be gathered on the compressive strength of the rock in order to determine the allowable bearing pressure and shear strength. Compressive strength can be measured in the laboratory using an unconfined compression test on rock cores. The modulus of the rock is also needed to determine the settlement characteristics. The rock

modulus used in design is the rock mass modulus and needs to be estimated in the field. If the rock is fractured in many directions a "reduced modulus" or mass modulus must be used to represent the rock modulus, which could be considerably less than the laboratory value obtained from a solid core sample. In situ tests such as the pressuremeter test are useful in determining design values of the rock mass modulus (Wyllie, 1992). The Rock Quality Designation (RQD) is also helpful in determining the rock behavior. In determining rock characteristics, experienced drilling personel are also helpful. An experienced driller will be able to help predict rock characteristics by observing rock cuttings and drill progress.

CHAPTER THREE

LOAD CAPACITY OF SOCKETED DRILLED SHAFTS IN COMPRESSION

There are three mechanisms in which axial compressive loads are carried by rock socketed drilled shafts. The load can be carried by side wall shear exclusively, end bearing exclusively, or a combination of end bearing and side shear. The mechanism chosen for the design depends on the subsurface conditions at the site of construction. A socketed shaft can be designed to carry a load entirely in side shear if the socket bottom cannot be cleaned or if the designer is uncertain of the condition of the bottom. Alternatively, if a relatively strong stratum of rock underlies a weak overburden material it is possible to carry all of the applied load in end bearing. In the case of socket drilled into sound rock, it is assumed that a combination of side shear and end bearing is used to sustain service loads (Wyllie, 1992).

The magnitude of the support developed by end bearing and side wall shear depends on several factors: the moduli of the socket material and that to the pier material. The magnitude of loading as compared to the shear strength of the socket material. If the loading exceeds the shear strength of the socket material, the socket will fail in side shear, making end bearing the prominent load carrying mechanism. The method of construction also dictates how the applied load is dispersed. For example, if water is used to drill through shale, soft, remolded cuttings can remain on the sides of the socket. This will reduce the friction and thus reduce the side shear capacity. The extent to which the bottom was cleaned will also affect the end bearing capacity (Wyllie, 1992).

There are several factors that dictate the total load carrying capacity of a socketed drilled shaft. First, the geometry of the socket, specifically the length to diameter ratio has significant effects on the capacity of a shaft. As the ratio increases from zero, the amount of load carried in end bearing decreases as progressively more load is carried in side shear. Second, the ratio of the rock modulus to the concrete modulus has an affect on the capacity of a shaft. The shear stress developed in a system is partially dependent on the normal stress developed. The magnitude of the normal stress is directly dependent on the modulus of the rock: as the modulus of the rock increases the normal stress increases. This results in more of the load being carried by side shear in the upper part of the shaft. Third, end bearing and side shear depend on rock strength. The higher the strength, the greater the end bearing capacity. The side shear capacity increases with the increase in rock strength until the rock strength reaches that of the concrete (Wyllie, 1992).

CHAPTER FOUR

DESIGN OF ROCK SOCKETED DRILLED SHAFTS

Currently, there are several methods available for the design of rock socketed drilled shafts published in text books and journals. Many of the methods use similar procedures; some methods are distinctly different in their rock property and bearing capacity values. Most methods take a semi-empirical approach to design but some theoretical studies have been published. The wide range of rock properties have led to somewhat different approaches in empirical design methods. Several of the different methods are explained in the following paragraphs.

Rowe and Armitage Method

Rowe and Armitage (1986) present the following design procedure for a non-recessed complete socket with no excessive soil-filled or weathered seams along the walls of the socket. A shaft is non-recessed if the entire shaft length is contributing to the side wall resistance.

Step 1

Determine the following parameters:

1. Allowable design settlement, ρ_d
2. Socket diameter, D
3. Applied axial load (factored), Q_t

4. Modulus of pier (factored), E_p

5. Unconfined compressive strength of the rock, σ_c

Step 2

Calculate expected values of side shear resistance and rock modulus:

$$\tau = 0.45\sqrt{\sigma_c} \quad \text{for regular clean sockets} \qquad (1)$$

$$\tau = 0.6\sqrt{\sigma_c} \quad \text{for clean rough sockets} \qquad (2)$$

$$E_r = 215\sqrt{\sigma_c}\text{, rock modulus} \qquad (3)$$

$$\tau_d = 0.7\tau\text{, design side shear} \qquad (4)$$

Values from 0.5 to 0.7 are commonly used to obtain design values for side shear and rock mass modulus. These values depend on the reliability of the data; if more accurate values of side shear resistance and rock modulus are available from field testing these values should be used.

Step 3

Calculate modulus ratios E_p/E_d and E_b/E_r

E_p = modulus of the pier

E_d = rock mass modulus, $E_d = 0.7E_r$

E_b = modulus of the socket base

Step 4

Calculate the dimensionless socket length required if all load would be carried in side shear:

$$(L/D)_{max} = Q_t/(\pi D^2 \tau_d) \qquad (5)$$

L = Length of socket

D = diameter of socket

Q_t = load at top of shaft

Q_b = load transferred to the base of the shaft.

τ_d = expected side shear

Calculate the design settlement influence factor, I_d:

$$I_d = \rho_d E_d D/Q_t \qquad (6)$$

Estimate S, the percentage of weak compressible seams expected along the shaft of the socket. S = sum of the seam thickness/expected socket length.

Step 5

(a) Choose the appropriate design chart for $E_p/E_r = E_p/E_d$ and E_b/E_r (see figures 1, 2, and 3). On the design chart, draw the "factored design line," which is a straight line between the coordinates L/D = 0, Q_b/Q_t = 100% and L/D = L_{max}/D, Q_b/Q_t = 0.

(b) Locate the intersection between the "factored design line" and the curve corresponding to the "design" settlement influence factor, I_d. Then from the intersection point draw a vertical line to the L/D axis and determine the design length to diameter

ratio, $(L/D)_d$ and calculate the corresponding socket length. Draw a horizontal line to the Q_b/Q_t axis and read off the design ratio for load carried to the base $(Q_b/Q_t)_d$. If an intersection can be found, then the pier of length L_d will satisfy the design settlement. The stress on the base rock must also be checked to ensure that there is an adequate factor of safety against over stressing the rock and causing excessive settlement.

(c) If no intersection point can be established on this design chart, it is necessary to check whether the pier can be designed for the given conditions. Select the appropriate graph for E_b/E_r from Figure 4 and draw a horizontal line for $I = I_d$. Find the intersection of this line with the curve for the appropriate value of $E_p/E_r = E_p/E_d$. If there is an intersection point on this curve the pier can be designed elastically. The required $(L/D)_d$ can be obtained from the intersection of the I value on the curve. The portion of the load transferred to the base of the shaft can then be found by the same method using Figure 4. If there is no intersection point, go back to Step 1 and increase the settlement or diameter. If a situation requires a E_p/E_r that lies between two design charts interpolation should be used to determine the design values.

Step 6

Check the end-bearing pressure:

$$q_t = Q_t/(\pi D^2/4) \qquad (7)$$

q_t = stress at top of pier

$$q_{ba} = \sigma_c \qquad (8)$$

q_{ba} = allowable stress at bottom of pier

$$q_b = (Q_b/Q_t)_d q_t \quad (9)$$

q_b = stress at the bottom of the pier

$q_b \leq q_{ba}$

The above calculations ensure that the rock beneath the shaft behaves elastically. The following procedure will provide a check of the ultimate capacity of the rock.

$$q_{bm} = 2.5\sigma_c \quad (10)$$

q_{bm} = maximum base pressure

$$q_{bu} = qt - 4(L/D)(0.7\tau) \quad (11)$$

q_{bu} = ultimate base pressure

$q_{bm} \leq q_{bu}$

The above procedure does not take into consideration weathered seams or areas of weak rock. If the area of concern is localized to a small area it is possible to neglect this portion of the rock and extend the pier below this area. Thus, the length of the pier increases. If the area containing weak rock is a significant portion of the shaft length, a different approach is needed.

If this is the case, estimate the proportion of the seams τ_d*, the total length of the shaft, S, the modulus of the seams, E_s, and the pier seam interface strength, τ_s. Calculate the modified side shear resistance.

$$\tau_d^* = 0.7(S\tau_s + (1-S)\,\tau) \quad (12)$$

Calculate the modified maximum pier geometry.

$$(L/D)^* = Qt/\pi D\tau_d^* \quad (13)$$

Calculate a modified modulus.

$$E_d^* = (1-S+SE_s/E_r)Ed \quad (14)$$

Calculate a new estimate of I_d^*.

$$I_d^* = \rho d E_d^* D/Q_t \quad (15)$$

Repeat steps 5 and 6 as previously described.

If the upper portion of the shaft has no side resistance contribution, it is considered recessed and should be designed following steps 1-6, This will be a conservative design but it can be adjusted. Determine the recessment length, L_e, the modulus of the rock adjacent to the recessed length, E_t and the ratios L_e/D, and E_t/E_r. Having determined an initial estimate $(L/D)_d$. determine the settlement reduction factor, RF, from figure 5. Adjust the design value of I_d.

$$I_d^* = I_d/RF \quad (16)$$

Repeat step 5 using the revised I_d^*. The adjusted value $(L/D)_d^*$ should be used to compute the new value of RF. The new value of RF is then compared to the previous RF. Iterations of step 5 may be needed to obtain an accurate value using the new value of I_d^* calculated with the most recent value of RF.

Federal Highway Administration Method

Reese and O'Neill (1988) present the following procedure, originally developed by Kulhaway (1983) in the Federal Highway Administration publication on Drilled Shafts. The basic steps are as follows:

1. Obtain the required penetration of the drilled shaft into the rock for the given axial load by using an appropriate value of side resistance.

2. Compute the settlement of the drilled shaft at the top of the rock by adding the elastic shortening to the settlement required to develop end bearing, assuming that the full load is taken by the base of the drilled shaft. The stiffness of the rock mass is needed for this computation.

3. If the computed settlement is less than approximately 0.4 inches, the side resistance will dominate and little load can be expected to reach the base of the foundation.

4. If the computed settlement is more than approximately 0.4 inches, the bond in the socket may be broken and the tip resistance will be important.

Although Kulhaway (1983) presents curves that will give the approximate distribution of the load for steps 3 and 4, the Federal Highway Administration (FHWA) conservatively recommends assuming that the load is carried entirely in side resistance or entirely by end bearing, depending on whether or not the computed settlement is more or less than 0.4 inch.

The maximum load transfer in side resistance will occur at the top of the shaft where the relative settlement is the greatest. As the rock reaches failure at the top portion of the shaft, the stress is transferred downward resulting in a progressive failure. This lends support to the FHWA recommendation that only one load carrying mechanism be considered in design. The settlement for a load carried in side resistance only can be very small when compared to that of a load carried in end bearing only. Therefore the

settlement in end bearing must be checked carefully to ensure it does not exceed serviceability limits.

The following recommendations are made by Reese and O'Neill (1988) in order to implement the above general procedure for design:

1. Horvath and Kenney (1979) obtained a "best fit curve" for the side resistance after an extensive study of the side resistance of rock-socketed drilled shafts, with no attempt to roughen the walls.

$$f_s = 2.5\,(q_u)^{0.5} \qquad (17)$$

f_s = ultimate side resistance, psi

q_u = uniaxial compressive strength of the rock or concrete, whichever is less, psi

Carter and Kulhaway (1987) recommend the following equation for weak rock:

$$f_s = 0.15 q_u \qquad (18)$$

The FHWA proposed the Carter and Kulhaway equation be used for computing the ultimate side resistance for rock with a uniaxial compressive strength up to 280 psi and the Horvath and Kenney equation be used for rock with values of larger compressive strength.

2. The shortening of the shaft may be found by the following equation:

$$\rho_c = \frac{Q_{st}L}{AE_c} \qquad (18)$$

ρ_c = the shortening of the shaft

L = the penetration of the socket

Q_{st} = the load at the top of the socket

A = the cross-sectional area of the socket

E_c = the equivalent modulus of the concrete in the socket,

considering the stiffening effects of any reinforcing steel.

3. The settlement of the base is calculated using the following equation which assumes that the rock will behave elastically:

$$w = \frac{Q_{st} I_\rho}{B_b E_m} \qquad (19)$$

w = settlement of the base of the drilled shaft

I_ρ = influence coefficient

B_b = diameter of drilled shaft

E_m = modulus of the in situ rock, taking the joints and their spacing into account

4. The value of I_ρ can be found by using the figure 6 (Donald, 1980). The symbol E_C in the figure refers to the modulus of the concrete in the drilled shaft.

5. The modulus of the intact rock sample is found by unconfined compression test or by selecting a value from figure 7. The value of the modulus of the in situ rock can be found by test or an approximation can be made by modifying the intact modulus by the use of the RQD and figure 8.

6. The bearing capacity of the rock can be computed by a method proposed by the Canadian Geological Society (1978).

$$q_b = K_{sp} q_u \qquad (20)$$

$$K_{sp} = \frac{9+\frac{3c_s}{B_b}}{10(1+\frac{300\delta}{c_s})^{0.5}} \qquad (21)$$

q_b = ultimate bearing pressure

K_{sp} = empirical coefficient that depends on the spacing of discontinuities and includes a factor of safety of 3

q_u = average unconfined compressive strength of rock cores

c_s = spacing of discontinuities

δ = thickness of individual discontinuity

B_b = diameter of socket

The equation for K_{sp} is valid for rock masses with spacings of discontinuities greater than 12 inches, thicknesses of discontinuities less than 0.2 inches (1 inch if filled with soil of rock debris), and for a foundation with a width greater than 12 inches. For sedimentary or foliated rocks, the strata must be nearly level.

Wyllie Method

Wyllie (1992) presents the following design procedure where side wall shear resistance is simplified by assuming that the shear stress is uniformly distributed down the walls of the socket. The allowable load capacity in side shear is given by:

$$Q = \tau_a \pi B L \qquad (22)$$

Q = total applied load

τ_a = allowable side wall shear stress

B = diameter of the socket

L = length of the socket

A correlation between observed side wall shear stress and the strength of the rock in the socket has been developed by Williams and Pells, 1981. The following equations have been developed using these observations.

$$\tau_a = 0.25 \sqrt{\sigma_{u(r)}} \qquad (23)$$

$\sigma_{u(r)}$ = unconfined compressive rock strength

Equation 23 is for clean sockets with side wall undulations between 1 mm and 10 mm and less than 10 mm wide.

$$\tau_a = 0.3 \sqrt{\sigma_{u(r)}} \qquad (24)$$

Equation 24 is for clean sockets with side wall undulations greater than 10 mm deep and 10 mm wide.

The two above equations include a factor of safety of about 2 with respect to the ultimate side resistance. They will also result in a pier behaving elastically with little risk of excessive settlement. If the rock is closely fractured with a low deformation modulus, the values of τ_a should be reduced due to lower confining pressures around the socket.

The allowable load capacity of a socketed pier in end bearing is given by:

$$Q_a = \sigma_{u(r)} \pi B^2/4 \qquad (25)$$

$\sigma_{u(r)}$ = uniaxial compressive strength of the rock at the base of the pier

B = diameter at the base of the pier

The above equation assumes that the base of the socket is at least one diameter below the ground surface, the rock is intact or tightly jointed at this depth and there are no cavities or voids below the base of the pier.

Settlement is dependent on the socket conditions, which include the geology of the site, construction methods and the load transfer mechanism. The following methods describe the process for calculating settlement for shafts loaded in end bearing only, side shear only, and a combination of the two.

The settlement for a side-wall shear supported recessed pier is given by:

$$\delta = RF\frac{QI}{BE_{m(s)}} \qquad (26)$$

Q = applied load

B = diameter of the socket

RF = reduction factor for a recessed socket (figure 9)

I = settlement influence factor (figure 10)

$E_{m(s)}$ = modulus of deformation of the rock

The influence factor can be obtained from figure 10 by determining the intersection of the socket length to diameter ratio (L/B) and the curve corresponding to the concrete modulus to shaft modulus ($E_c/E_{m(s)}$). The reduction factor is for a pier that is cased around the upper section, or extends through a layer of weathered rock where little or no side shear is developed. Rowe and Armitage, 1987 have developed a correlation between rock mass modulus and the compressive strength of the rock, incorporating a factor of safety of about 2.

$$E_{m(s)} = 110\sqrt{\sigma_{u(r)}} \tag{27}$$

The settlement for an end loaded pier in which no side wall shear is developed is given by:

$$\delta = \frac{4Q}{\pi B^2}\left[\frac{D}{E_c} + \frac{RF'C_d B\left(1-\nu^2\right)}{E_{m(b)}}\right] \tag{28}$$

E_c = concrete modulus

RF' = reduction factor for end bearing socket (figure 10)

D = depth of pier

C_d = shape and rigidity factor

(0.85 for flexible footing, 0.75 for rigid footing)

$E_{m(b)}$ = deformation modulus of the rock mass in the pier base

ν = rock mass Poisson's ratio

If the ratio of the pier modulus to the rock modulus is greater than 50 it can be considered a rigid footing; if it is less than 50 it can be considered a flexible footing. The reduction factor depends on the ratio of depth of embedment to the diameter of the pier and can be found in Figure 10.

The settlement of a pier supported by both end bearing and side shear is given by equation 26. The influence factors will differ and be less than that of a side shear only pier and are given in Figure 4. Three different sets of graphs are given according to the base modulus to shaft modulus ($E_{m(b)}/E_{m(s)}$). The figure also includes a ratio (Q_b/Q) to determine the percentage of load carried in end bearing.

A design procedure for a pile supported in side shear and end-bearing is to calculate the influence factor from an allowable settlement. Then using Figure 11, determine the required socket length. If there is no intersection between the horizontal line drawn from the I axis and the modulus curve, then a design value for the influence factor cannot be achieved. If the influence factor is too low and an intersection cannot be found, it is necessary to increase the allowable settlement or decrease the design load by increasing the number of piers or increase the size of the piers. If the influence factor is too high to create an intersection, the allowable settlement is too high and slip will occur along the shaft moving the shear from the elastic region to the plastic region. Thus, the allowable settlement must be decreased.

Merritt Method

Merritt (1983) presents the following design method. Analysis of bearing values q_u of rock indicates that they should not be significantly less than the uniaxial compression strength UC, possibly excluding weak sedimentary rock such as compacted shales and siltstones. With a factor of safety of three, the maximum allowable bearing value can be taken as:

$$q_a \leq 0.3UC$$

Concrete-rock bond stresses f_r have been established from a limited number of load tests. For rock with a RQD greater than 50%, f_r can be estimated as $0.05f'_c$ or 0.05UC, whichever is smaller. Values of f_r are not to exceed 250 psi. The value of rock mass modulus, E_r is related to RQD and can be approximated in table 1.

Design of rock sockets is conventionally based on

$$Q_d = \pi d_s L_s f_r + \pi d_s^2 q_a/4 \quad (29)$$

Q_d = allowable design load on socket

d_s = socket diameter

L_s = socket length

f_r = allowable concrete-rock bond stress

q_a = allowable bearing pressure on rock

The following steps present a simplified approach to rock socket pier design.

1. Proportion the rock socket for design load Q_d with equation (29) on the assumption that the end bearing stress, q_u is less than the allowable bearing pressure, q_a (say $q_a/4$, which is equal assuming the base load is $Q_b = (\pi/4)d_s^2 q_a/4$).

2. Calculate the base load $Q_b = RQ_d$, where R is the percent of base-load transmitted to the rock socket interpreted from table 2.

3. If RQ_d does not equal the assumed Q_b, repeat the procedure with a new q_a value until an approximate convergence is achieved and $q \leq q_a$.

Ladanyi Method

Goodman (1989) recommends the method proposed by Ladanyi (1977). This method provides for full bond strength developed over a socket length sufficient to reduce the end bearing pressures to acceptable values. The following iterative scheme will

achieve this result once the allowable bearing pressure and allowable shear stresses have been established.

Given the vertical load F_{total} on the top of the pier:

1. Assume a value for the allowable bond stress τ_{allow} on the wall of the rock socket.

$$\tau_{allow} \leq \tau_{bond}$$

$$\tau_{bond} = q_u/20 \text{ (hard rock)} \qquad (30)$$

q_u = unconfined compressive strength

$$\tau_{bond} = \alpha S_u \text{ (soft rock)} \qquad (31)$$

$\alpha = 0.3 - 0.9$

S_u = undrained shear strength

2. Select a radius a. This may be dictated by the allowable load in the concrete

3. Neglect end bearing and calculate the maximum length l_{max} of the rock socket:

$$l_{max} = \frac{F_{total}}{2\pi a \tau_{allow}} \qquad (32)$$

4. Choose a value l_1 less than l_{max} and using the ratio, l_1/a determine p_{end}/p_{total} from figure 12. The curves are drawn for values of E_r/E_c . Alternatively, corresponding to a lower value of bond stress, choose a value for μ, coefficient of side friction and calculate $p_{end}/p_{total} = \sigma/p_{total}$ from equation 33 (using $y = l_1$):

$$\sigma = p_{total} e^{-\{(2vc\mu / (1-vc+(1+vr)Ec/Er)(y/a)\}} \qquad (33)$$

a = diameter of socket

E_c = modulus of the concrete

E_r = modulus of the rock

y = depth of socket, l

μ = coefficient of side friction

ν_c = Poison's ratio of the concrete

ν_r = Poison's ratio of the rock

5. Calculate the load carried in end bearing.

$$p_{end} = (F_{total}/\pi a^2)(p_{end}/p_{total}) \quad (34)$$

6. Compare p_{end} to the allowable bearing pressure, nq_{allow}. Where q_{allow} is determined from local site conditions and n (embedment factor)is determined from the material at depth l_1, with a relative embedment ratio l_1/a (see table 3).

7. Calculate allowable bond strength.

$$\tau = (1- p_{end}/p_{total})\ (F_{total}/2\pi a l_1) \quad (35)$$

8. Compare τ with τ_{allow}.

9. Repeat with l_2 and a until $\tau = \tau_{allow}$ and $p_{end} \leq q_{allow}$

The settlement of the pier can be calculated from three components, the settlement of the base, the shortening of the pier itself, and the correction accounting for transference of the load through adhesion to the sides (which can be ignored when the socket length is small compared to that of the shaft in soil).

$$\omega = \omega_{base} + \omega_p - \Delta\omega \quad (36)$$

ω_{base} = settlement at the base

ω_p = shortening of the pile itself

$\Delta\omega$ = correction accounting for the load carried by side adhesion

$$\omega_p = p_{total}(l_0+l)/E_c \quad (37)$$

(l_0+l) = total length of shaft

l = length of socket

$$\omega_{base} = (\pi/2)\, p_{end}(1-\nu_r^2)a/\, E_r n \quad (38)$$

n = factor for embedment ratio (see table 3)

CHAPTER FIVE

CONCLUSIONS

The previous design methods were produced in a semi-empirical fashion. These uncertainties usually lead to a foundation that is overdesigned. Accuracy tests at Northwestern University allowed 20 people to analyze a foundation design. The 20 people were given extensive site information for two shafts, one that was cased and one that was drilled using bentonite slurry. Each person then submitted their interpretation of the capacity of the drilled shaft. The foundations were then subjected to full scale load tests (Coduto, 1994). All but one underpredicted the bearing capacity of the rock socketed drilled shaft and the average capacity was about half of the actual capacity. This example illustrates how most shafts are overdesigned. One way to improve this inaccuracy in the prediction of the capacity of rock socketed drilled shaft is by the full scale load testing of drilled shafts. The increased amount of data will continue to improve the accuracy of empirical formulas.

FIGURES AND TABLES

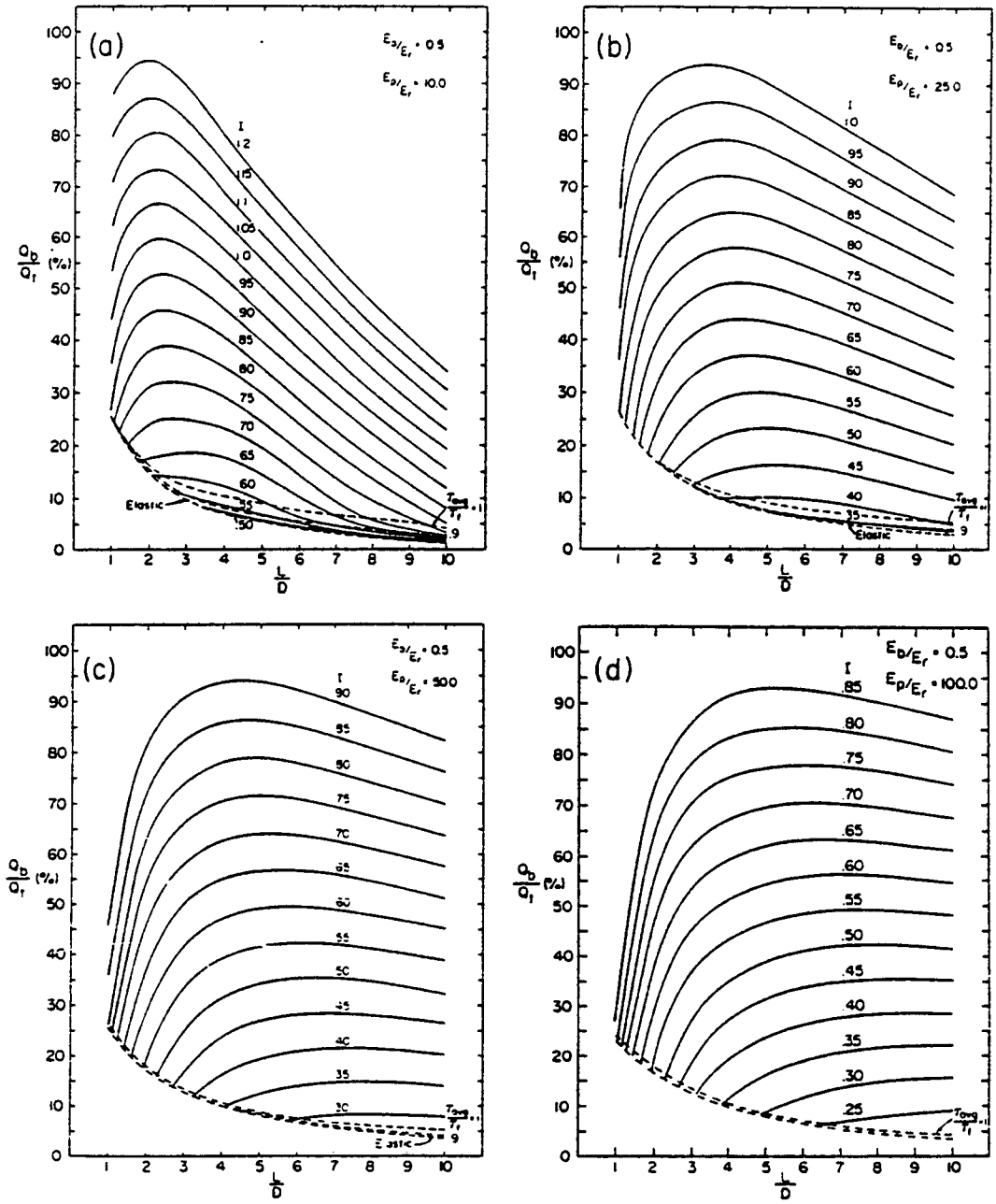

Figure 1 - Design Charts for a Complete Socketed Pier (Rowe and Armitage, 1987)

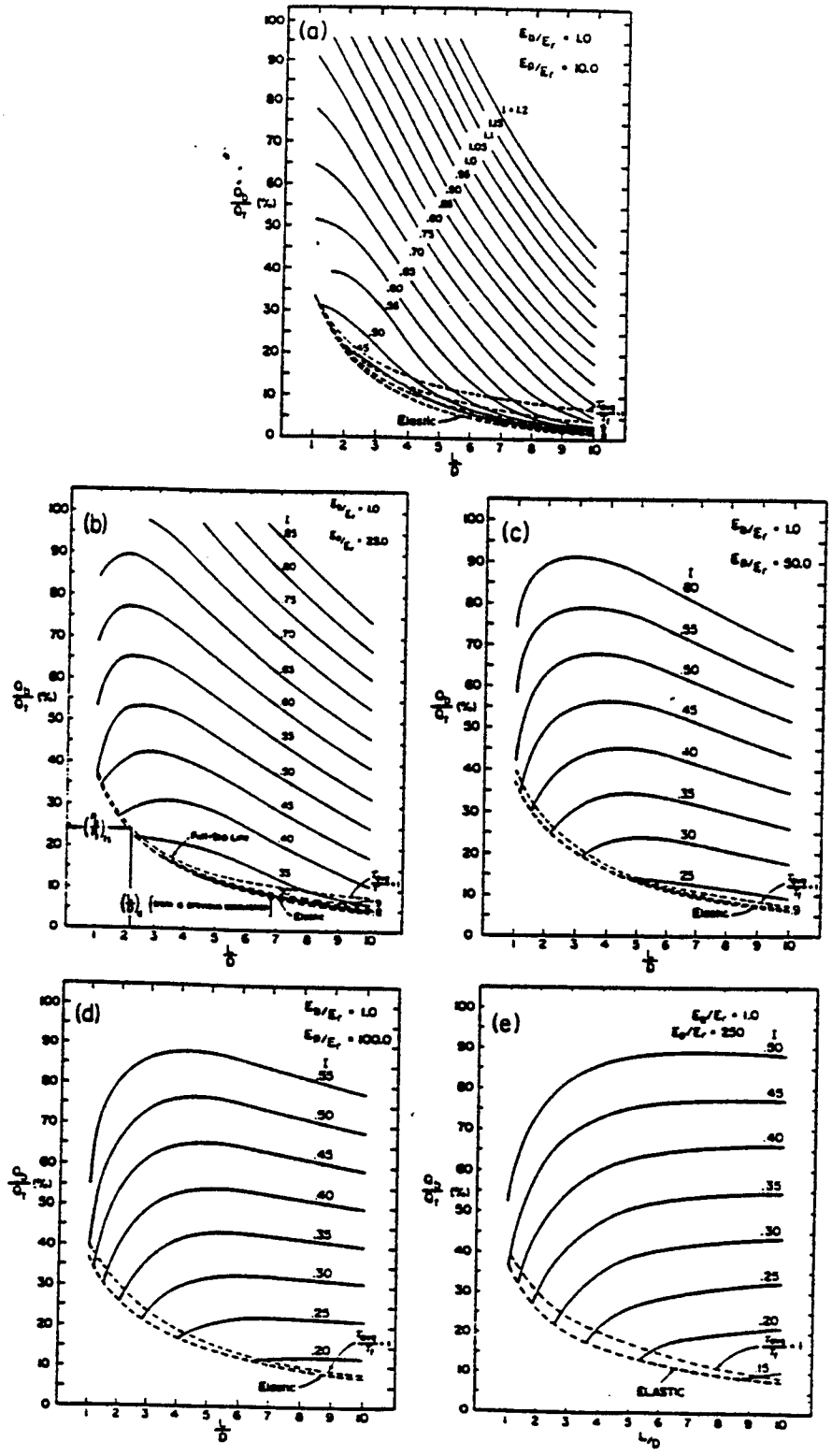

Figure 2 - Design Charts for a Complete Socketed Pier (Rowe and Armitage, 1987)

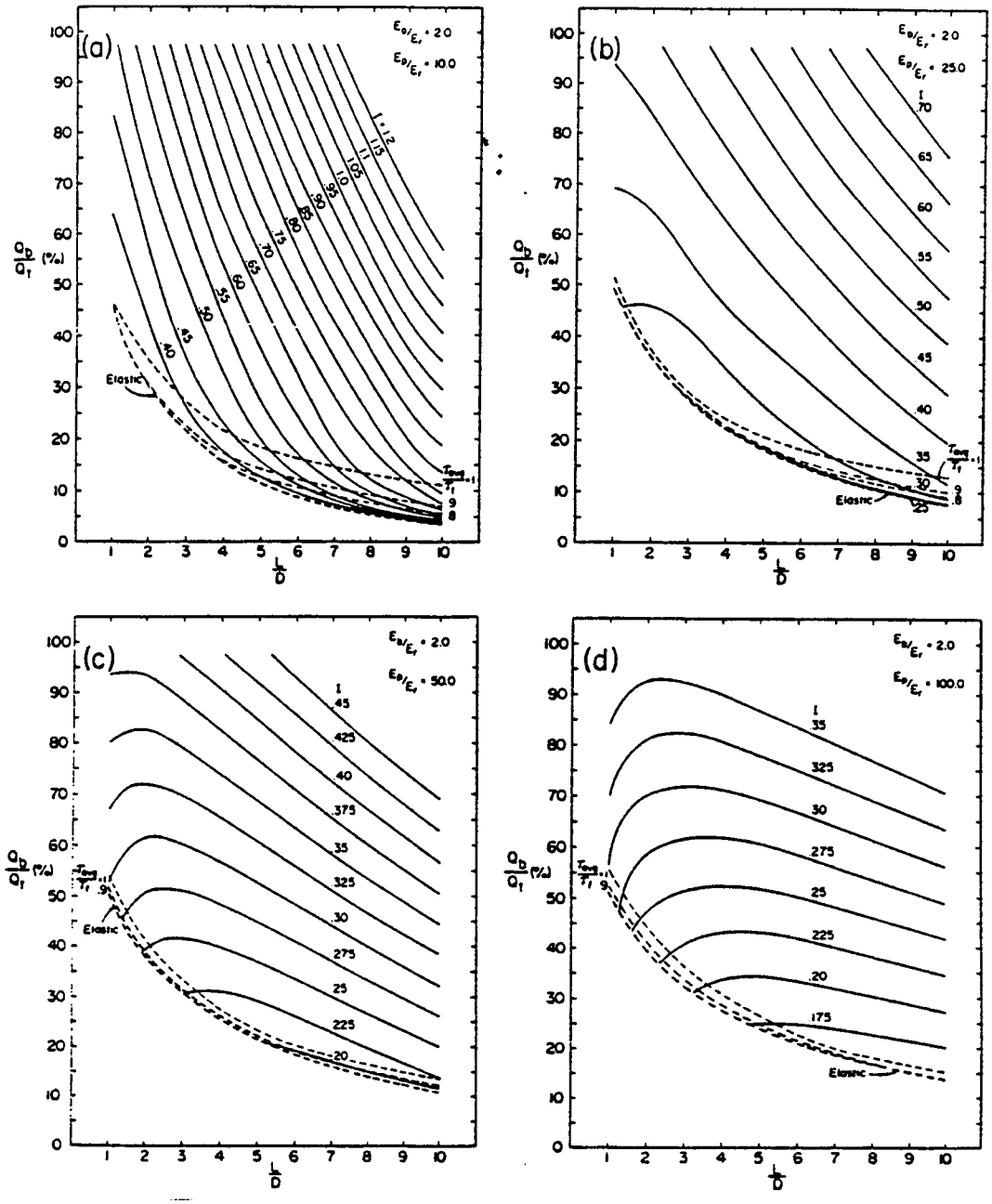

Figure 3 - Design Charts for a Complete Socketed Pier (Rowe and Armitage, 1987)

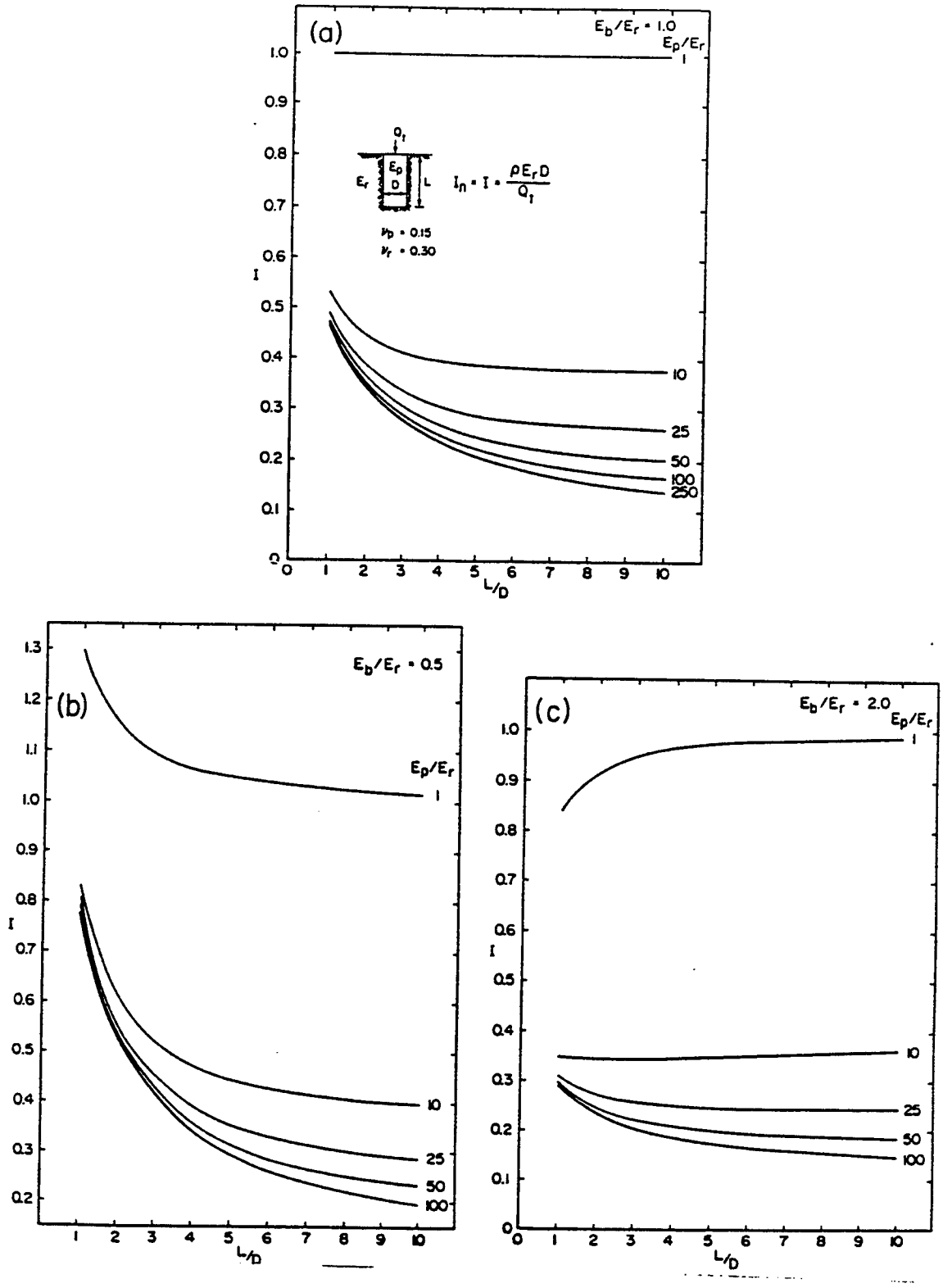

Figure 4 - Elastic Settlement Influence Factors for a Complete Socket (Rowe and Armitage, 1987)

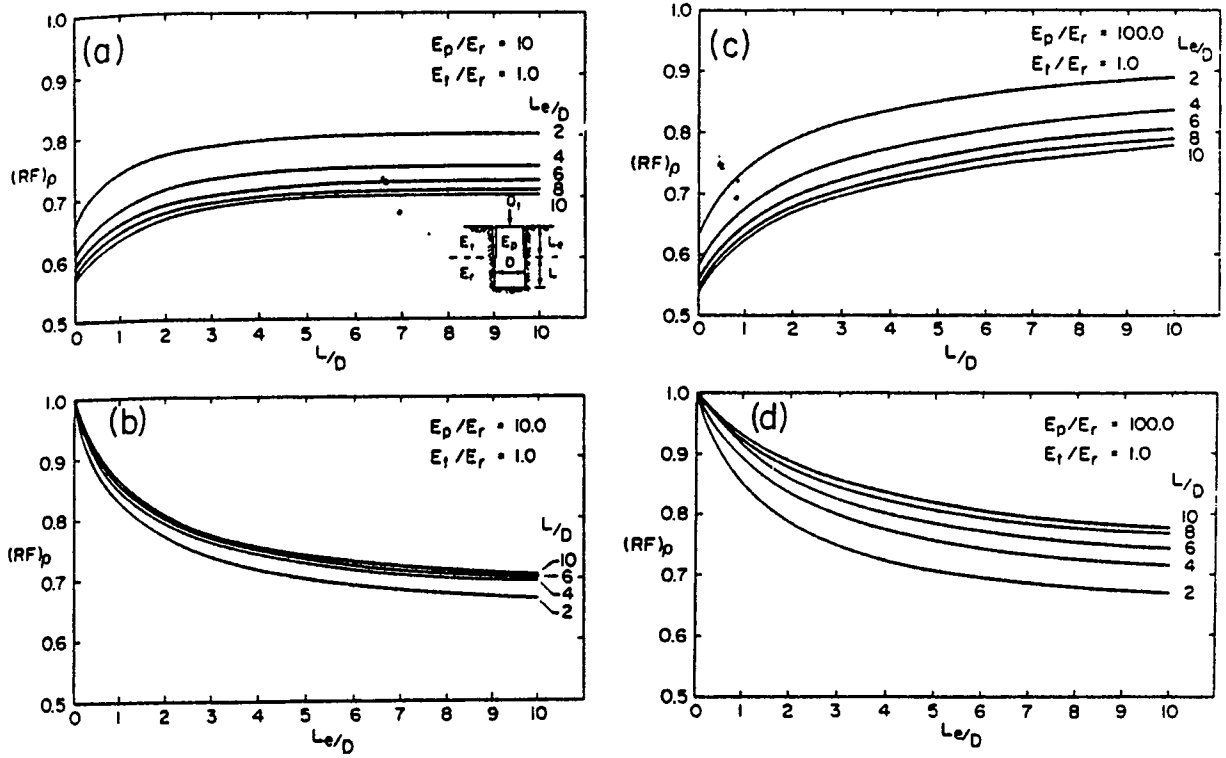

Figure 5 - Reduction Factors for a Recessed Socket (Rowe and Armitage, 1987)

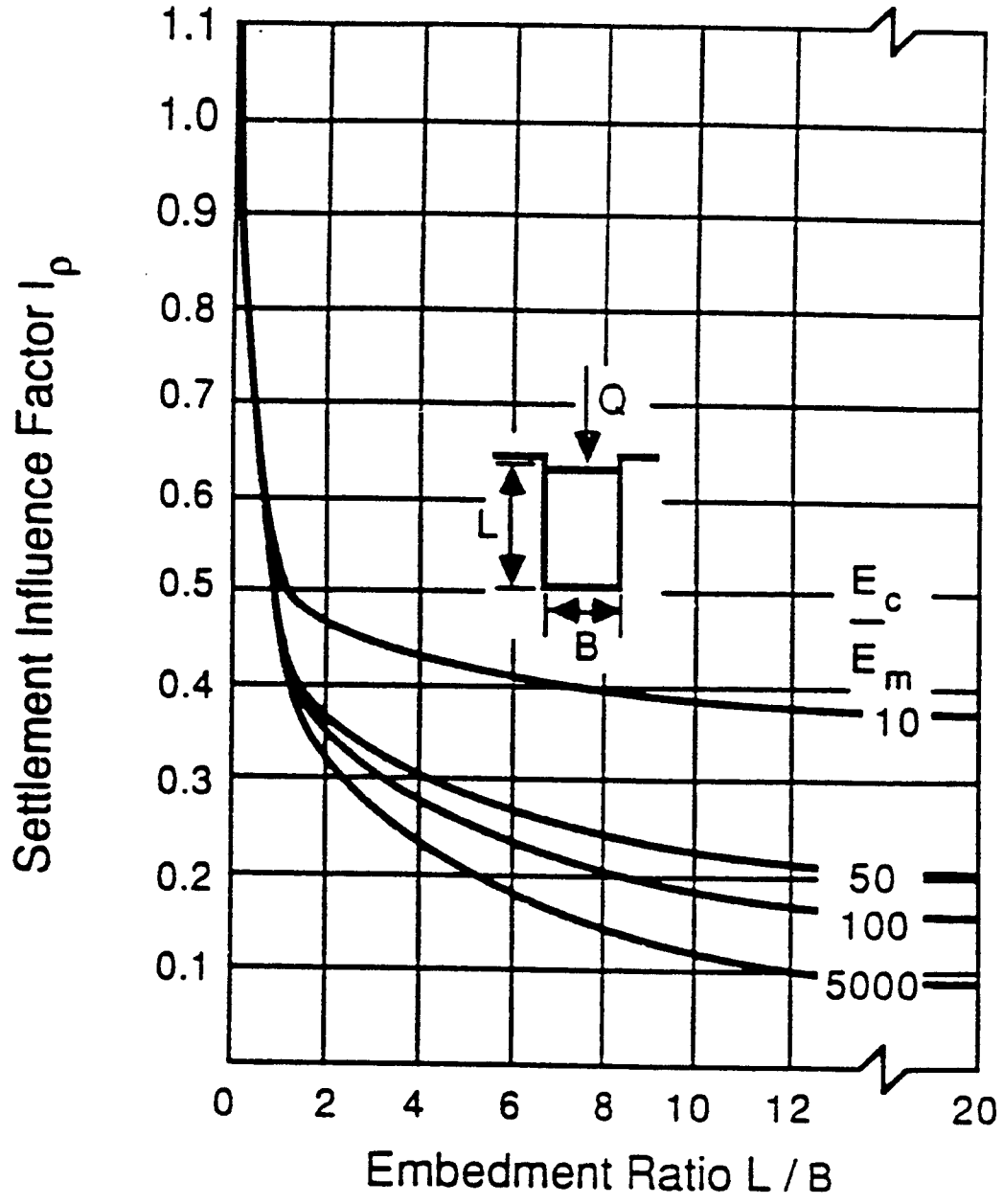

Figure 6 - Settlement Influence Factors as a Function of Embedment Ratio and Modular Ratio (Donald, Sloan, and Chiu, 1980)

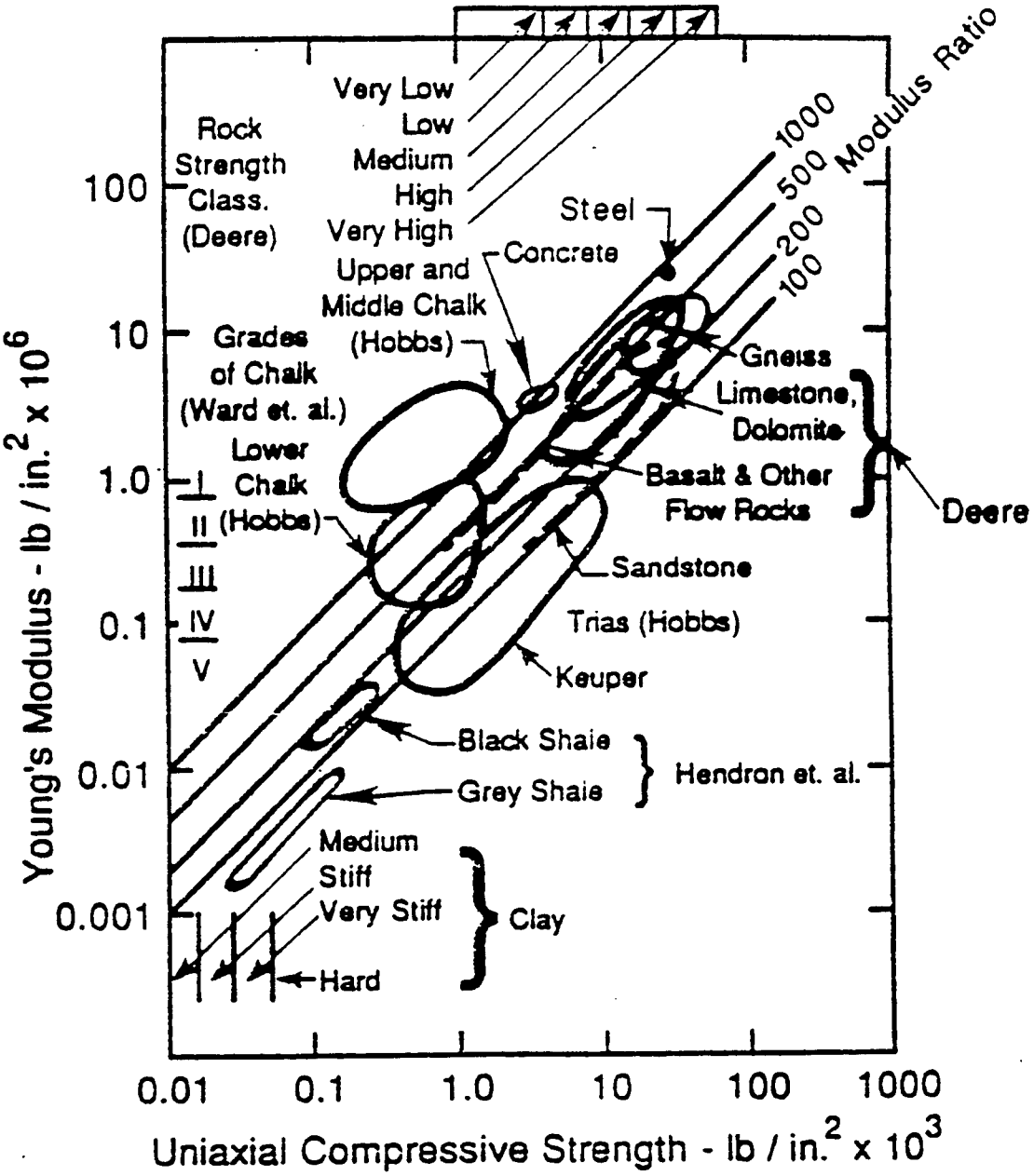

Figure 7 - Engineering Classification of Intact Rock (as presented by Horvath and Kenney, 1979)

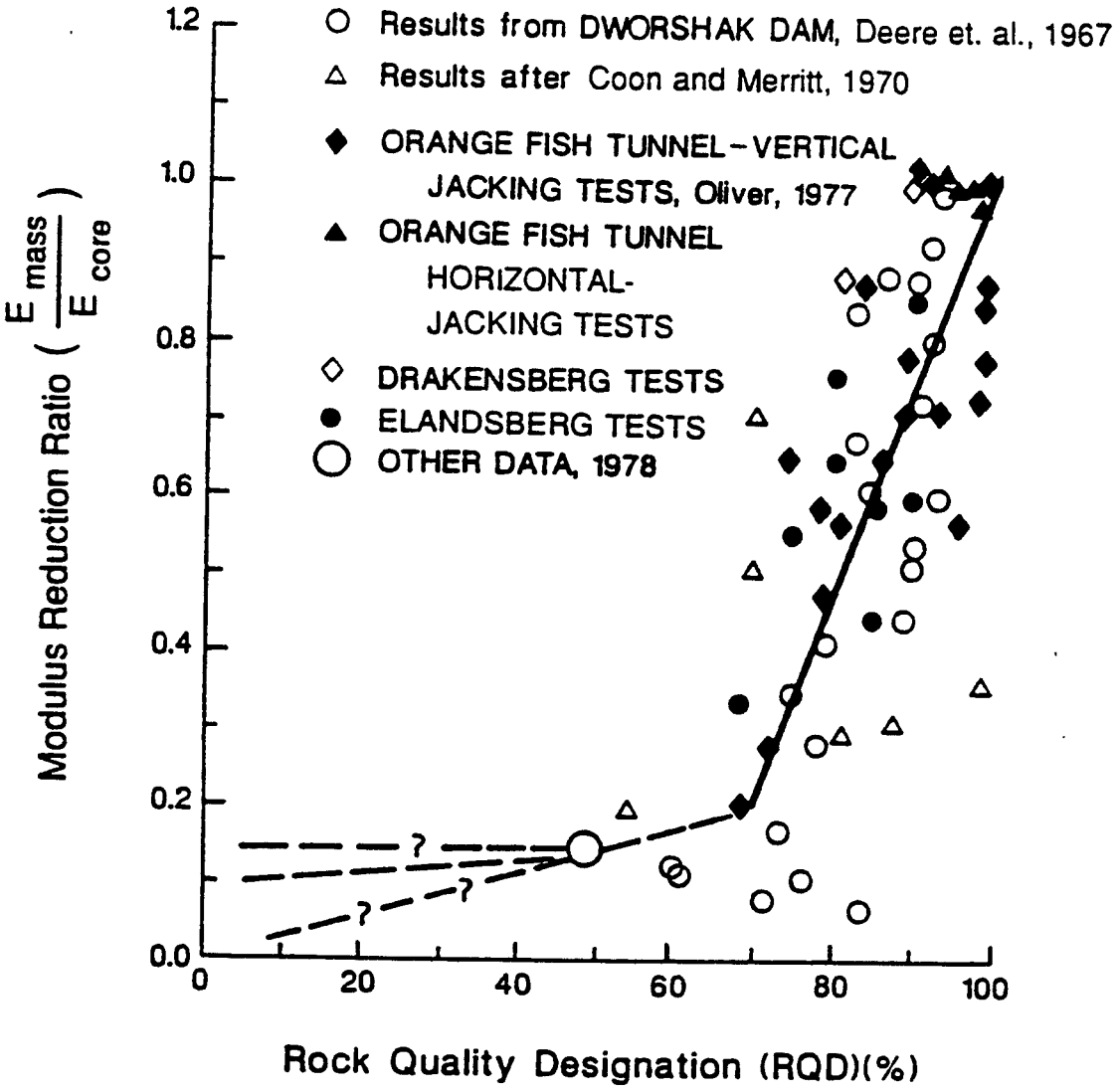

Figure 8 - Modulus Reduction as a Function of RQD (Bieniawski, 1984)

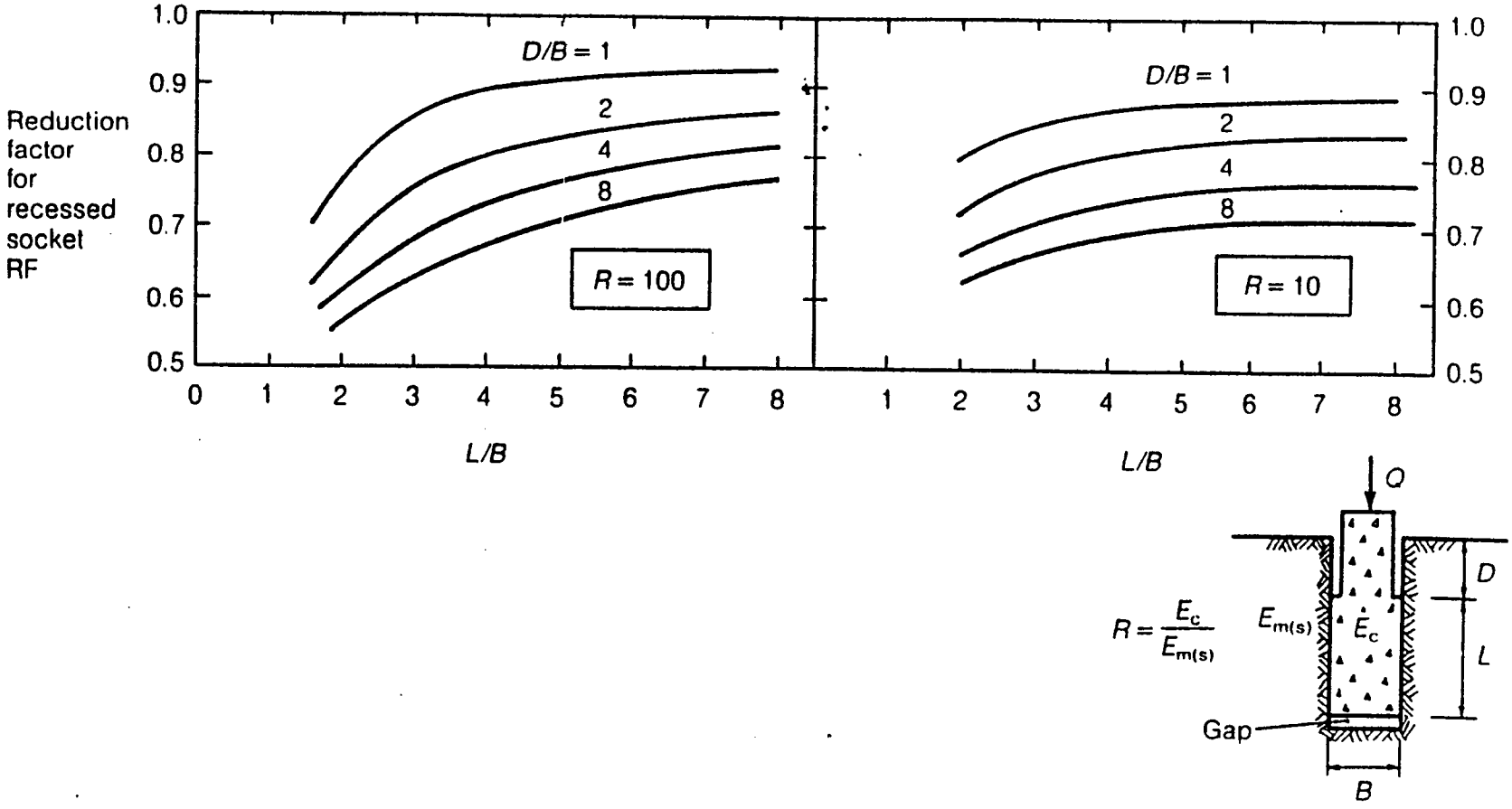

Figure 9 - Reduction Factors for a Recessed Socket (Pells and Turner, 1979)

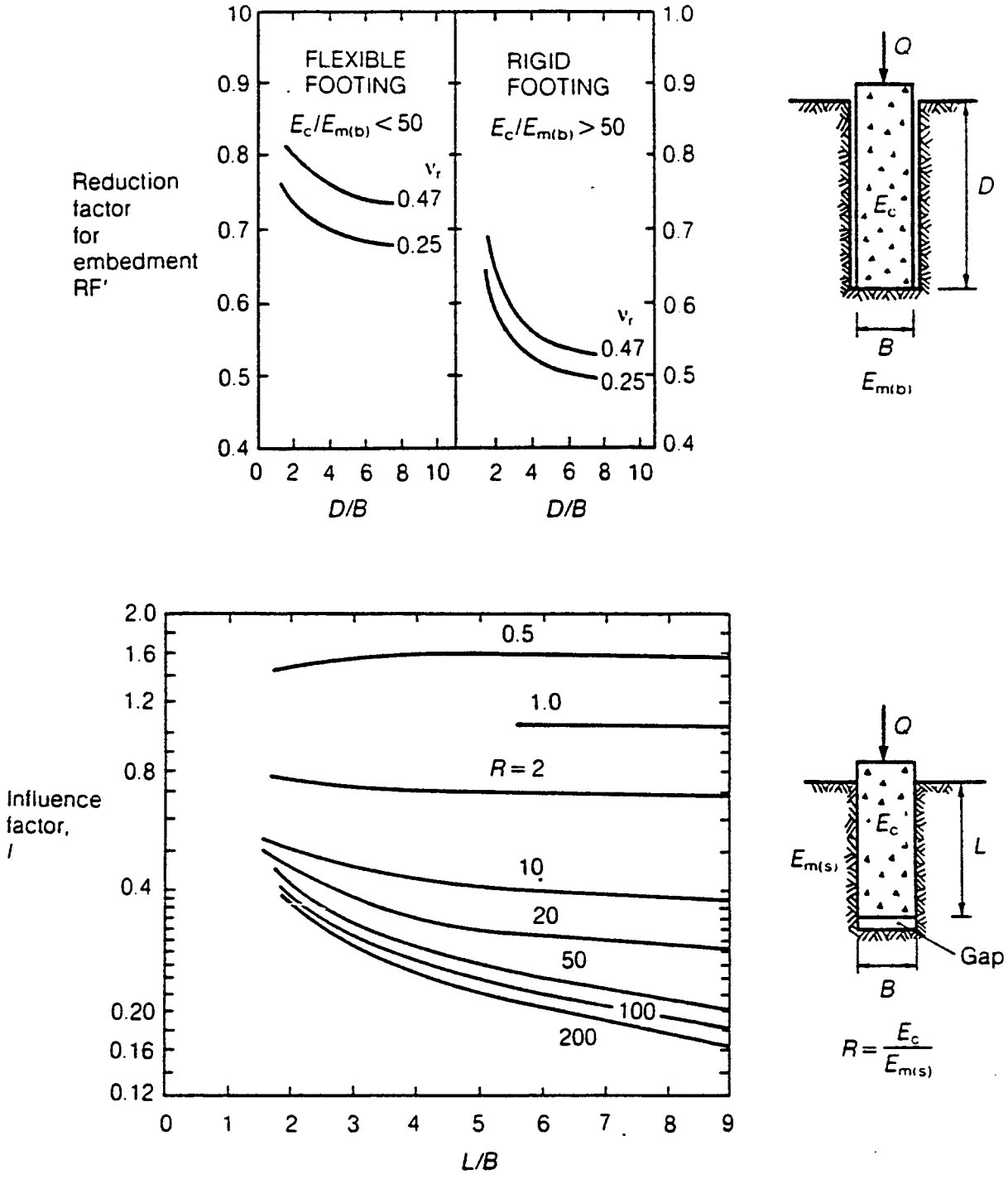

Figure 10 - (a) Reduction Factors for Calculation of Average Settlement of End Bearing Sockets (b) Elastic Settlement Influence Factors for Side Resistance Socketed Piers (Pells and Turner, 1979)

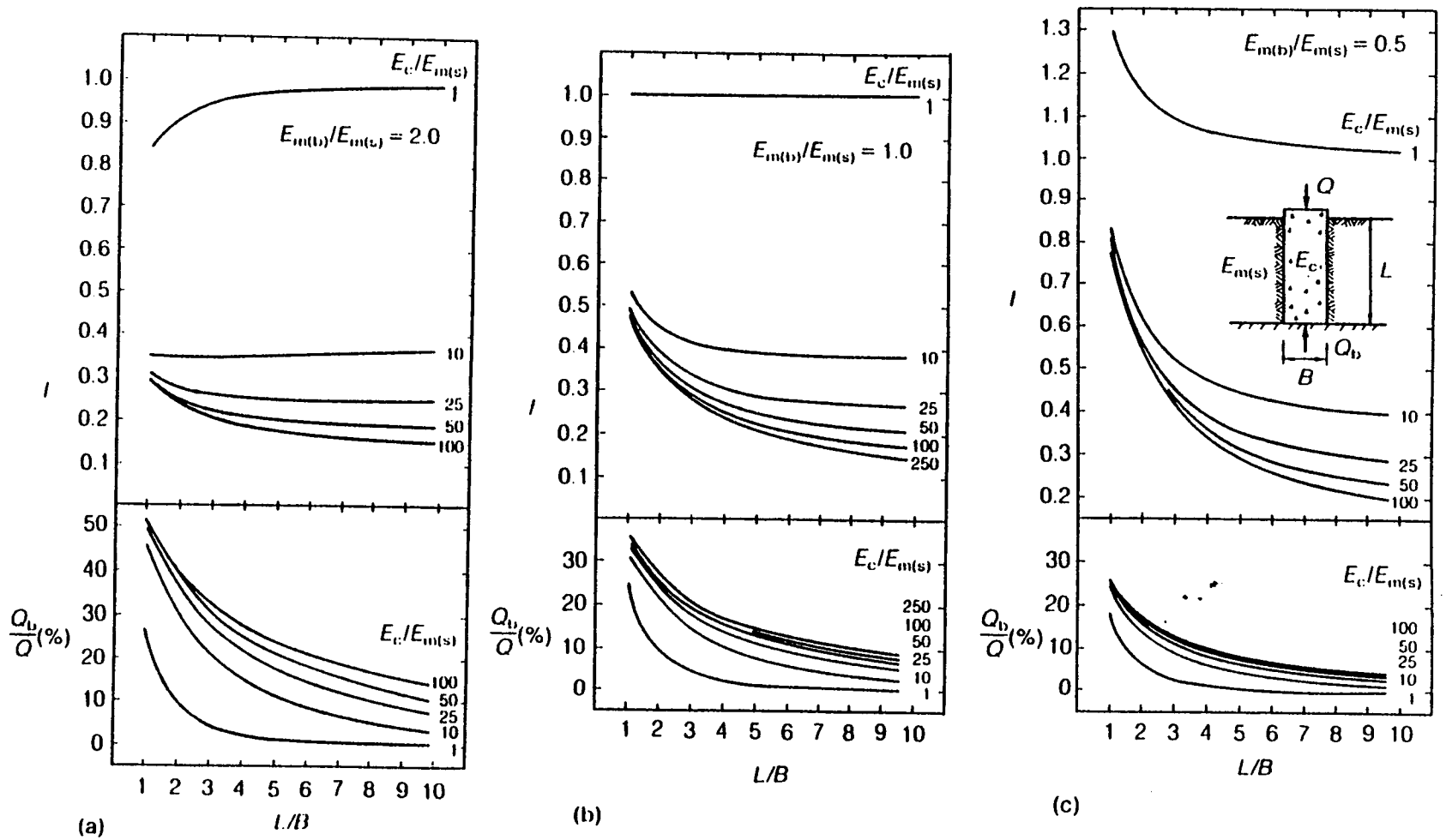

Figure 11 - Influence Factors and End Bearing Ratios for Complete Socketed Piers (Rowe and Armitage, 1987)

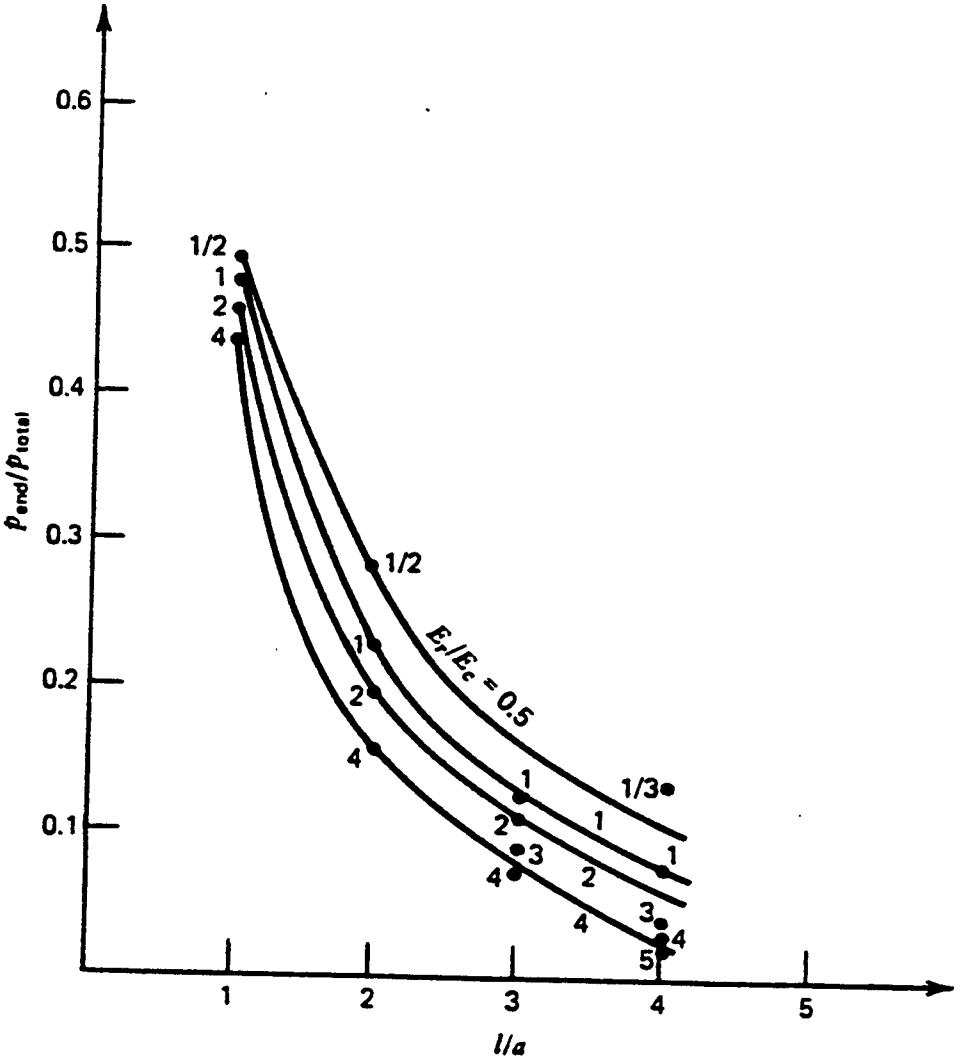

Figure 12 - Data on Load Transfer of Socketed Piers (Ladanyi, 1977)

Classification	RQD	Deformability (Ed/Et)
Very poor	0-25	under 0.20
Poor	25-50	under 0.20
Fair	50-75	0.20-0.50
Good	75-90	0.50-0.80
Excellent	90-100	0.80-1.00

Et = tangent modulus at 50% unconfined compression strength

Table 1 - Rock-Quality and Deformability Correlation (Merritt, 1983)

	Er/Ep		
Ls/ds	0.25	1	4
0.5	54	48	44
1	31	23	18
1.5	17	12	8
2	13	8	4

Table 2 - Percentage of Load in End Bearing (Merritt, 1983)

l/a	0	2	4	6	8	14
n: vr=0	1	1.4	2.1	2.2	2.3	2.4
n: vr=0.3	1	1.6	1.8	1.8	1.9	2
n: vr=0.5	1	1.4	1.6	1.6	1.7	1.8

Table 3 - Factors for Embedment Ratio (Goodman, 1989)

REFERENCES

Bowles, J. E. (1996), Foundation Analysis and Design. New York: Mcgraw Hill.

Bieniawski, Z. T. (1984), Rock Mechanics: Design in Mining and Tunneling. Boston: A. A. Balkema.

Canadian Geotechnical Society (1978), Canadian Foundation Engineering Manual, Part 2 Shallow Foundations. Montreal: Canadian Geotechnical Society.

Carter, J. P., & Kulhawy, F. H. (1988). Analysis and design of drilled shaft foundations socketed into rock. EPRI Report El-5918. Palo Alto, CA: Electric Power Research Institute.

Coduto, J. P. (1994), Foundation Design: Principles and Practices. Englewood Cliffs, New Jersey: Prentice Hall.

Donald, I. B., Chiu, H. K., & Sloan, S. W. (1980). Theoretical analysis of rock socketed piles. In P. J. N. Pells (Ed.), Proceedings of the International Conference on Structural Foundations on Rock (pp. 303-316), Sydney, Australia. Rotterdam, Netherlands: A. A. Balkema.

Goodman, R. E. (1989), Introduction to Rock Mechanics. New York: John Wiley & Sons.

Horvath, R. G., & Kenney, T. C. (1979). Shaft resistance of rock-socketed drilled piers. Proceedings of the Symposium on Deep Foundation. ASCE.

Kulhawy, F. H. (1983), Transmission Line Structures Foundations for Uplift-Compression Loading. EPRI Report El-5918. Palo Alto, CA: Electric Power Research Institute.

Ladanyi, B. (1977). Friction and end bearing tests on bedrock for high capacity socket design: Discussion. Canadian Geotechnical Journal, 14, 153-155.
363-373), Sydney, Australia. Rotterdam, Netherlands: A. A. Balkema.

Merritt, F. S. (1983), Standard Handbook for Civil Engineers. New York: McGraw Hill.

Pells, P. J. N. and Turner, R. M. (1979), Elastic solution for the design and analysis of rock socketed piles, Canadian Geotechnical Journal, 16: 481-7.

Reese, L. C., & O'Neill, M. W. (1987). Drilled shafts: construction procedures and design methods. Design Manual. McLean, VA: U.S. Department of Transportation, Federal Highway Administration.

Rowe, R. K., & Armitage, H. H. (1987). A design method for piers in soft rock. Canadian Geotechnical Journal, 24, 114-125.

Wyllie, D. C. (1992). Foundations on rock. New York: Chapman & Hall.

Appendix B

This appendix includes the calibration curves for the three Osterberg cells used in the field test of the rock socketed drilled shafts. The curves were provided by Loadtest Inc.

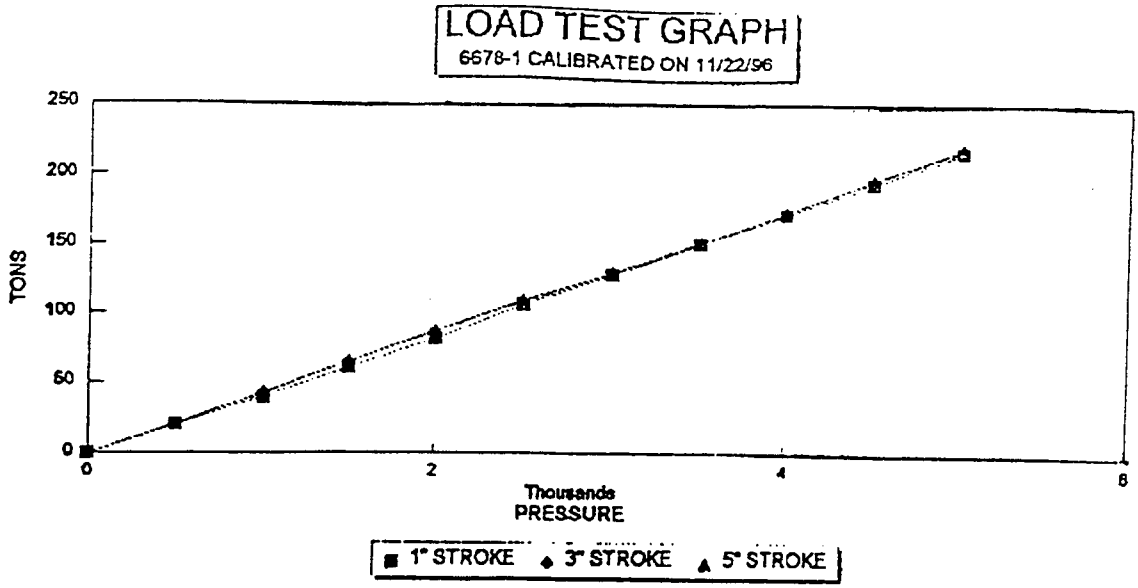

STROKE: 1 INCH 3 INCH 5 INCH

PRESSURE	TONS	TONS	TONS
0	0	0	0
500	19.70	20.08	20.45
1000	39.77	42.05	42.80
1500	60.23	64.77	64.77
2000	81.44	85.98	86.74
2500	106.06	107.58	109.09
3000	128.41	129.55	130.30
3500	151.52	151.52	152.65
4000	171.97	173.48	174.24
4500	193.94	196.21	196.97
5000	216.29	218.18	219.32
5500	237.88	239.77	241.67
6000	259.47	262.12	263.26
6500	280.68	284.85	285.98
7000	303.03	306.06	307.95
7500	324.24	328.79	329.92

Regression Output:		1 INCH
Constant		-3.76984
Std Err of Y Est		1.170223
R Squared		0.999868
No. of Observations		15
Degrees of Freedom		13
X Coefficient(s)	0.043853	
Std Err of Coef.	0.00014	

Regression Output:		3 INCH
Constant		-2.17893
Std Err of Y Est		0.451881
R Squared		0.99998
No. of Observations		15
Degrees of Freedom		13
X Coefficient(s)	0.044061	
Std Err of Coef.	0.000054	

Regression Output:		5 INCH
Constant		-1.76407
Std Err of Y Est		0.374181
R Squared		0.999987
No. of Observations		15
Degrees of Freedom		13
X Coefficient(s)	0.04421	
Std Err of Coef.	0.000045	

CALIBRATION STANDARDS:

All data presented is derived from 6" dia. certified hydraulic pressure gauges and electronic load transducer, manufactured and calibrated by the University of Illinois at Champaign, Illinois. All calibrations and certifications are traceable through the Laboratory Master Deadweight Gauges directly to the National Institute of Standards and Technology. No Specific guidelines exist for calibration of load test jacks and equipment but procedures comply with similar guidelines for calibration of gauges, ANSI specifications B40.1.

*AE & FC CUSTOMER:LOADTEST INC.
*AE & FC JOB NO.:6742
*CUSTOMER P.O.NO.:LT-8353

*CONTRACTOR:HAYES DRILLING
*JOB LOCATION:KANSAS CITY, MO
*DATED:11/21/96

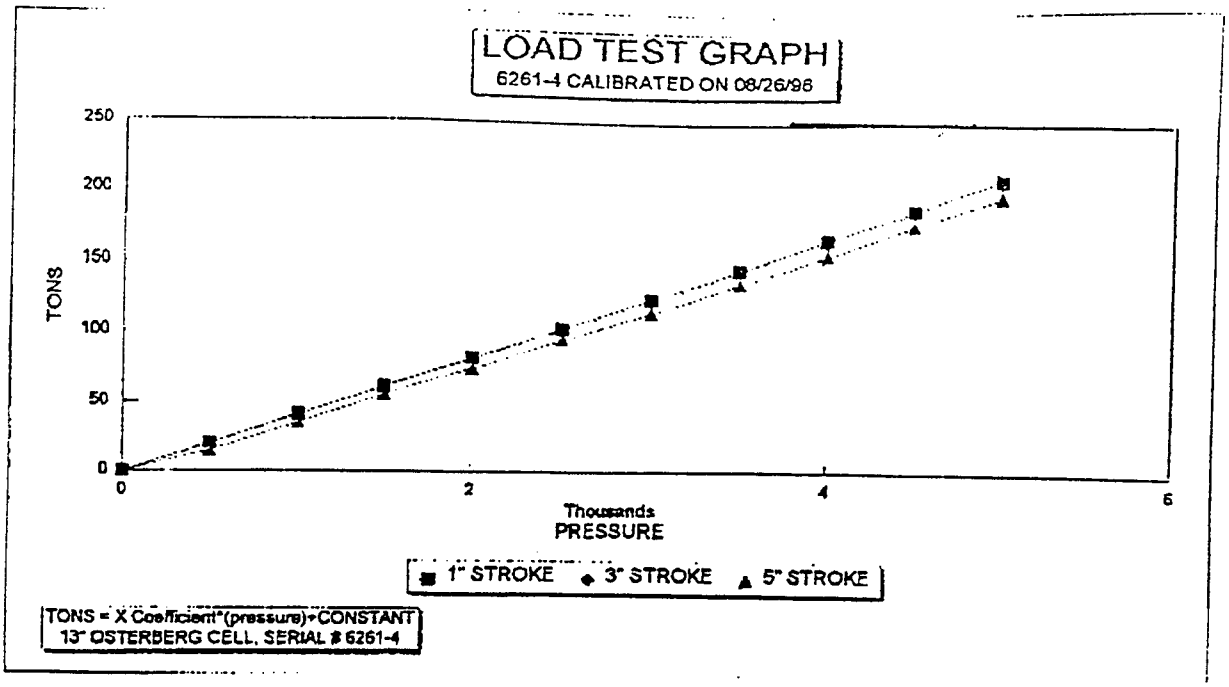

STROKE: 1 INCH 3 INCH 5 INCH

PRESSURE	TONS	TONS	TONS
0	0	0	0
500	20.83	20.08	15.91
1000	41.29	40.91	35.23
1500	61.74	60.98	56.06
2000	82.20	81.44	74.62
2500	103.41	102.27	95.08
3000	125.00	122.73	114.77
3500	145.08	143.94	134.85
4000	166.29	164.39	154.92
4500	186.74	185.61	175.38
5000	207.95	206.06	195.45
5500	229.55	227.65	215.91
6000	250.00	245.83	235.98
6500	271.21	265.15	255.68
7000	292.80	282.58	274.24
7500	313.64	308.33	300.00

CALIBRATION STANDARDS:

All data presented is derived from 6" dia. certified hydraulic pressure gauges and electronic load transducer, manufactured and calibrated by the University of Illinois at Champaign, Illinois. All calibrations and certifications are traceable through the Laboratory Master Deadweight Gauges directly to the National Institute of Standards and Technology. No Specific guidelines exist for calibration of load test jacks and equipment but procedures comply with similar guidelines for calibration of gauges, ANSI specifications B40.1.

Regression Output:		1 INCH
Constant		-1.00649
Std Err of Y Est		0.507227
R Squared		0.999973
No. of Observations		15
Degrees of Freedom		13
X Coefficient(s)	0.04188	
Std Err of Coef.	0.000061	

Regression Output:		3 INCH
Constant		0.12987
Std Err of Y Est		1.512639
R Squared		0.999746
No. of Observations		15
Degrees of Freedom		13
X Coefficient(s)	0.040933	
Std Err of Coef.	0.000181	

Regression Output:		5 INCH
Constant		-5.27056
Std Err of Y Est		1.287398
R Squared		0.99981
No. of Observations		15
Degrees of Freedom		13
X Coefficient(s)	0.040219	
Std Err of Coef.	0.000154	

*AE & FC CUSTOMER:LOADTEST INC.
*AE & FC JOB NO.:6742
*CUSTOMER P.O.NO.:LT-8353

*CONTRACTOR:HAYES DRILLING
*JOB LOCATION:KANSAS CITY, MO
*DATED:11/21/96

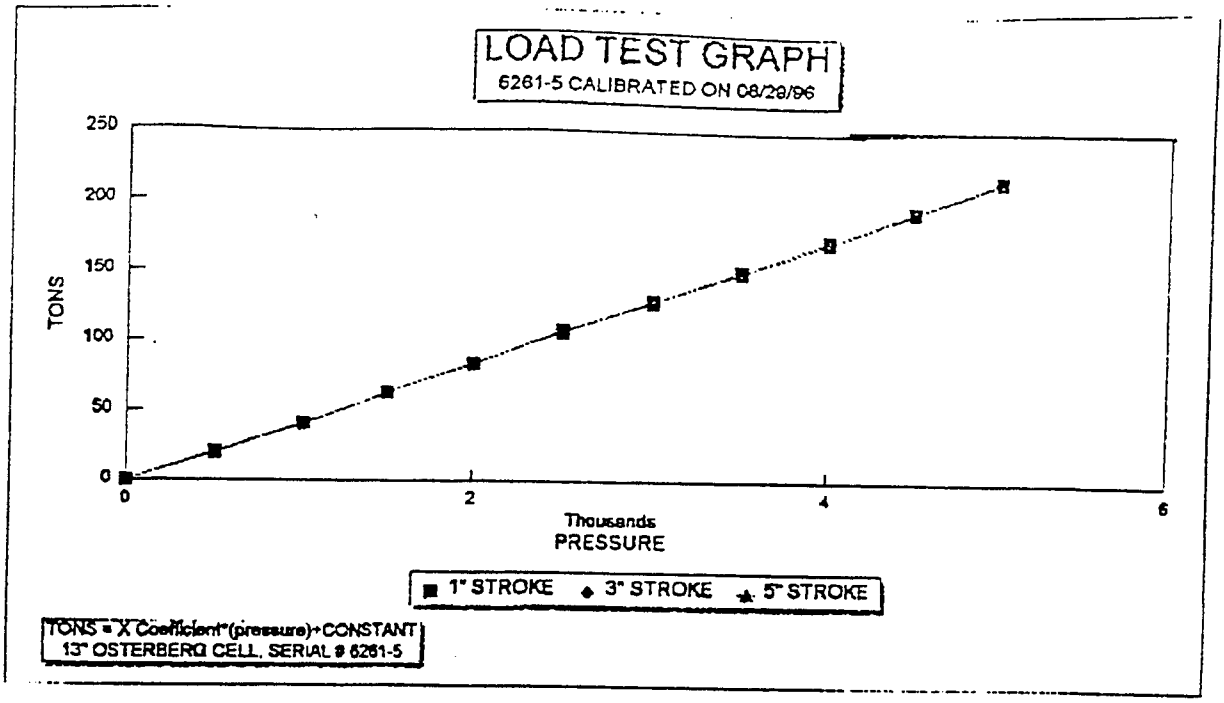

STROKE:	1 INCH	3 INCH	5 INCH
PRESSURE	TONS	TONS	TONS
0	0	0	0
500	20.08	18.94	19.32
1000	40.53	40.15	39.77
1500	61.36	62.12	61.36
2000	82.95	83.33	83.33
2500	107.20	105.68	105.68
3000	128.79	127.65	127.27
3500	151.14	149.62	148.86
4000	172.73	171.21	171.21
4500	193.56	192.80	191.67
5000	215.53	214.39	214.02
5500	237.12	235.61	235.98
6000	258.33	257.58	257.20
6500	280.30	279.55	279.55
7000	302.27	301.14	301.52
7500	324.24	323.48	323.48

Regression Output:		1 INCH
Constant		-2.58658
Std Err of Y Est		0.862308
R Squared		0.999927
No. of Observations		15
Degrees of Freedom		13
X Coefficient(s)	0.043582	
Std Err of Coef.	0.000103	

Regression Output:		3 INCH
Constant		-3.06638
Std Err of Y Est		0.334387
R Squared		0.999989
No. of Observations		15
Degrees of Freedom		13
X Coefficient(s)	0.043488	
Std Err of Coef.	0.00004	

Regression Output:		5 INCH
Constant		-3.40909
Std Err of Y Est		0.480283
R Squared		0.999977
No. of Observations		15
Degrees of Freedom		13
X Coefficient(s)	0.043523	
Std Err of Coef.	0.000057	

CALIBRATION STANDARDS:

All data presented is derived from 6" dia. certified hydraulic pressure gauges and electronic load transducer, manufactured and calibrated by the University of Illinois at Champaign, Illinois. All calibrations and certifications are traceable through the Laboratory Master Deadweight Gauges directly to the National Institute of Standards and Technology. No Specific guidelines exist for calibration of load test jacks and equipment but procedures comply with similar guidelines for calibration of gauges, ANSI specifications B40.1.

*AE & FC CUSTOMER:LOADTEST INC.
*AE & FC JOB NO.:6742
*CUSTOMER P.O.NO.:LT-8353

*CONTRACTOR:HAYES DRILLING
*JOB LOCATION:KANSAS CITY, MO
*DATED:11/21/96

Appendix C

This appendix includes the raw data collected during the field testing of the rock socketed drilled shafts. It includes the data collected by the laptop PC as well as the data collected manually during the test procedure.

Shaft #1 Test Data (PC Collected)

TIME		DIAL GAGE	DIAL GAGE	DIAL GAGE	DIAL GAGE	DIAL GAGE	DIAL GAGE	CELL
		A	B	C	D	E	F	PRESS.
1854	30	0.0004	0.0004	0.004	-99999	0.0002	0.0001	17.674
1855	0	0.0038	0.01	0.007	-99999	0.0002	0.0001	11.276
1855	30	0.0027	0.0032	0.0066	0.0011	0.0002	0.0001	0.0791
1856	0	0.003	0.0032	0.0017	0.0011	0.0003	0.0001	24.072
1856	30	0.003	0.0032	0.0017	0.0011	0.0003	0.0001	22.473
1857	0	0.003	0.0032	0.0019	0.0012	0.0003	0.0001	-54.243
1857	30	0.003	0.0032	0.0022	0.0013	0.0003	0.0001	89.719
1858	0	0.003	0.0032	0.0024	0.0015	0.0003	0.0001	20.938
1858	30	0.003	0.0032	0.0025	0.0018	0.0004	0.0001	19.338
1859	0	0.003	0.0032	0.0029	0.002	0.0004	0.0001	30.535
1859	30	0.0039	0.0032	0.0031	0.0023	0.0004	0.0001	38.533
1900	0	0.0039	0.0032	0.0032	0.0025	0.0004	0.0001	46.583
1900	30	0.0039	0.0032	0.0035	0.0027	0.0004	0.0001	86.573
1901	0	0.0039	0.0032	0.0037	0.0029	0.0004	0.0001	20.989
1901	30	0.0039	0.0032	0.0038	0.003	0.0004	0.0001	73.777
1902	0	0.0044	0.0032	0.0041	0.0035	0.0004	0.0001	22.589
1902	30	0.0044	0.0032	0.0041	0.0035	0.0004	0.0001	86.573
1903	0	0.0044	0.0032	0.0042	0.0036	0.0004	0.0001	88.216
1903	30	0.0044	0.0032	0.0043	0.0036	0.0004	0.0001	21.031
1904	0	0.0044	0.0032	0.0047	0.0038	0.0004	0.0001	22.63
1904	30	0.005	0.0032	0.0048	0.004	0.0004	0.0001	-47.754
1905	0	0.005	0.0032	0.0049	0.0041	0.0004	0.0001	-14.161
1905	30	0.005	0.0032	0.0049	0.0041	0.0004	0.0001	19.431
1906	0	0.005	0.0032	0.0049	0.0043	0.0004	0.0001	-3.0107
1906	30	0.005	0.0032	0.0052	0.0044	0.0004	0.0001	19.384
1907	0	0.005	0.0032	0.0052	0.0045	0.0004	0.0001	16.185
1907	30	0.0068	0.0068	0.0063	0.0053	0.0004	0.0001	0.18848
1908	0	0.0068	0.0068	0.0064	0.0054	0.0004	0.0001	19.384
1908	30	0.0068	0.0068	0.0064	0.0054	0.0004	0.0001	20.983
1909	0	0.0068	0.0068	0.0064	0.0054	0.0004	0.0001	24.144
1909	30	0.0068	0.0068	0.0064	0.0054	0.0004	0.0001	108.92
1910	0	0.0068	0.0068	0.0064	0.0059	0.0008	0.0007	326.47
1910	30	0.0068	0.0068	0.0065	0.006	0.0009	0.0007	481.63
1911	0	0.0068	0.0068	0.0065	0.006	0.0009	0.0007	484.82
1911	30	0.0068	0.0068	0.0068	0.006	0.0009	0.0007	462.43
1912	0	0.0068	0.0068	0.0068	0.0061	0.0009	0.0007	369.62
1912	30	0.0068	0.0068	0.0069	0.0061	0.0009	0.0007	479.99
1913	0	0.0068	0.0068	0.007	0.0061	0.0009	0.0007	476.79
1913	30	0.0068	0.0068	0.007	0.0061	0.0009	0.0007	296.04
1914	0	0.0068	0.0068	0.007	0.0062	0.0009	0.0007	532.78
1914	30	0.0068	0.0068	0.007	0.0062	0.0009	0.0007	342.4

1915	0	0.0068	0.0068	0.0078	0.0065	0.0009	0.0007	460.77
1915	30	0.0068	0.0068	0.0085	0.0077	0.0014	0.0015	1025.4
1916	0	0.0068	0.0068	0.0086	0.0078	0.0014	0.0015	956.63
1916	30	0.0068	0.0068	0.0087	0.0079	0.0014	0.0015	943.83
1917	0	0.0068	0.0068	0.0087	0.0079	0.0014	0.0015	943.83
1917	30	0.0068	0.0068	0.0087	0.008	0.0014	0.0015	937.41
1918	0	0.0068	0.0068	0.0087	0.008	0.0014	0.0015	939.01
1918	30	0.0068	0.0068	0.0089	0.0082	0.0014	0.0015	934.21
1919	0	0.0068	0.0068	0.009	0.0083	0.0014	0.0015	963
1919	30	0.0068	0.0068	0.009	0.0083	0.0014	0.0015	958.2
1920	0	0.0068	0.0068	0.0092	0.0084	0.0014	0.0015	964.6
1920	30	0.0054	0.0067	0.0112	0.0104	0.0022	0.0022	1447.6
1921	0	0.0054	0.0067	0.0112	0.0104	0.0022	0.0022	1404.4
1921	30	0.0054	0.0067	0.0112	0.0105	0.0022	0.0022	1458.8
1922	0	0.0054	0.0067	0.0114	0.0107	0.0022	0.0022	1454
1922	30	0.0054	0.0067	0.0115	0.0108	0.0022	0.0022	1386.9
1923	0	0.0054	0.0067	0.0115	0.0108	0.0022	0.0022	1434.8
1923	30	0.0054	0.0067	0.0115	0.0109	0.0022	0.0022	1433.2
1924	0	0.0054	0.0067	0.0115	0.0109	0.0022	0.0022	1401.2
1924	30	0.0054	0.0067	0.0119	0.011	0.0022	0.0022	1490.8
1925	0	0.0054	0.0067	0.0119	0.011	0.0022	0.0022	1426.8
1925	30	0.0054	0.0067	0.0119	0.011	0.0022	0.0022	1418.8
1926	0	0.0015	0.0044	0.0143	0.0141	0.0035	0.0032	1977.1
1926	30	0.0015	0.0034	0.0147	0.0144	0.0035	0.0032	1895.5
1927	0	0.0015	0.0034	0.0147	0.0144	0.0035	0.0032	1881.1
1927	30	0.0015	0.0034	0.0148	0.0145	0.0035	0.0032	1873.1
1928	0	0.0015	0.0034	0.0149	0.0147	0.0035	0.0032	1842.7
1928	30	0.0015	0.0034	0.0152	0.0148	0.0035	0.0032	1935.5
1929	0	0.0015	0.0034	0.0153	0.0149	0.0035	0.0032	1849.1
1929	30	0.0015	0.0034	0.0153	0.0149	0.0035	0.0032	1845.9
1930	0	0.0015	0.0034	0.0154	0.015	0.0035	0.0032	1818.7
1930	30	0.0015	0.0034	0.0154	0.015	0.0035	0.0032	1833.1
1931	0	-0.01	-0.0028	0.0214	0.0213	0.0052	0.0048	2463.3
1931	30	-0.0104	-0.0028	0.0216	0.0215	0.0052	0.0048	2442.5
1932	0	-0.0155	-0.0054	0.0234	0.0234	0.0057	0.0054	2570.4
1932	30	-0.0161	-0.0054	0.024	0.0238	0.0057	0.0054	2519.2
1933	0	-0.0161	-0.0054	0.0243	0.0239	0.0057	0.0055	2484.1
1933	30	-0.0161	-0.0054	0.0247	0.0242	0.0056	0.0055	2474.5
1934	0	-0.0161	-0.0054	0.0247	0.0244	0.0056	0.0055	2455.3
1934	30	-0.0161	-0.0054	0.0247	0.0245	0.0056	0.0055	2448.9
1935	0	-0.0166	-0.0062	0.0254	0.025	0.0057	0.0055	2359.3
1935	30	-0.017	-0.0062	0.0257	0.0253	0.0057	0.0055	2565.6
1936	0	-0.0219	-0.0102	0.0311	0.031	0.0067	0.0065	3095.1
1936	30	-0.0226	-0.0103	0.032	0.0319	0.0067	0.0065	3024.7
1937	0	-0.0226	-0.0103	0.0325	0.0322	0.0066	0.0065	2981.5
1937	30	-0.0226	-0.0103	0.0326	0.0324	0.0066	0.0065	2994.3
1938	0	-0.0226	-0.0103	0.0328	0.0326	0.0067	0.0065	3061.6
1938	30	-0.024	-0.0127	0.0337	0.0335	0.0067	0.0066	3053.6

1939	0	-0.0242	-0.0127	0.0342	0.0338	0.0067	0.0066	3026.4
1939	30	-0.0243	-0.0127	0.0344	0.0342	0.0067	0.0066	3024.8
1940	0	-0.025	-0.0127	0.0353	0.0346	0.0067	0.0066	3149.6
1940	30	-0.025	-0.0136	0.0358	0.036	0.0074	0.0074	3042.4
1941	0	-0.0295	-0.0167	0.0422	0.042	0.0076	0.008	3562.2
1941	30	-0.0298	-0.0168	0.0433	0.0429	0.0076	0.008	3543.1
1942	0	-0.0304	-0.0203	0.0443	0.0437	0.0075	0.008	3515.9
1942	30	-0.0305	-0.0203	0.0443	0.0437	0.0075	0.008	3485.5
1943	0	-0.0312	-0.0212	0.0449	0.0441	0.0076	0.008	3563.8
1943	30	-0.0312	-0.0212	0.0449	0.0444	0.0076	0.008	3538.3
1944	0	-0.0312	-0.0212	0.0451	0.0445	0.0076	0.008	3459.8
1944	30	-0.0312	-0.0212	0.0453	0.0446	0.0076	0.008	3504.6
1945	0	-0.0312	-0.0212	0.0454	0.0446	0.0076	0.008	3317.5
1945	30	-0.0312	-0.0212	0.0455	0.0447	0.0076	0.008	3415.1
1946	0	-0.0356	-0.0222	0.0525	0.0522	0.0085	0.0089	4040.5
1946	30	-0.0367	-0.0229	0.0547	0.0543	0.0086	0.009	4034.1
1947	0	-0.0367	-0.0229	0.0552	0.0548	0.0085	0.009	3992.4
1947	30	-0.0367	-0.0229	0.0555	0.055	0.0084	0.009	3965.3
1948	0	-0.0371	-0.024	0.0557	0.0551	0.0084	0.009	3926.9
1948	30	-0.0371	-0.024	0.0559	0.0553	0.0084	0.009	3981.3
1949	0	-0.0377	-0.0245	0.0565	0.0559	0.0084	0.009	3989.3
1949	30	-0.0377	-0.0245	0.0567	0.0562	0.0084	0.009	3933.3
1950	0	-0.0377	-0.0245	0.0568	0.0564	0.0084	0.009	3949.2
1950	30	-0.0382	-0.0245	0.0572	0.0567	0.0084	0.009	3986
1951	0	-0.0436	-0.0287	0.0674	0.067	0.0095	0.0104	4462.7
1951	30	-0.0442	-0.0293	0.0688	0.0684	0.0093	0.0104	4563.5
1952	0	-0.0442	-0.0293	0.0695	0.069	0.0093	0.0104	4493.1
1952	30	-0.0442	-0.0293	0.0698	0.0693	0.0092	0.0104	4381.1
1953	0	-0.0448	-0.0295	0.0702	0.0695	0.0092	0.0104	4398.7
1953	30	-0.0448	-0.0295	0.0703	0.0696	0.0092	0.0104	4376.3
1954	0	-0.0448	-0.0295	0.0705	0.0698	0.0091	0.0104	4355.5
1954	30	-0.0448	-0.0295	0.0706	0.07	0.0091	0.0104	4331.5
1955	0	-0.0448	-0.0295	0.0707	0.07	0.0091	0.0104	4318.7
1955	30	-0.0448	-0.0295	0.0707	0.0701	0.0091	0.0104	4272.3
1956	0	-0.049	-0.034	0.0774	0.0771	0.0101	0.0112	5054.5
1956	30	-0.052	-0.0367	0.0819	0.0815	0.0103	0.0119	5147.2
1957	0	-0.052	-0.0367	0.0831	0.0825	0.01	0.0119	4932.9
1957	30	-0.0522	-0.0367	0.0836	0.0829	0.0099	0.0119	4905.7
1958	0	-0.0528	-0.0368	0.0846	0.0839	0.01	0.0119	4876.9
1958	30	-0.0528	-0.0368	0.0848	0.0843	0.0099	0.0119	4942.5
1959	0	-0.0536	-0.0374	0.0856	0.085	0.01	0.0119	4851.3
1959	30	-0.0536	-0.0375	0.086	0.0853	0.01	0.0119	4932.9
2000	0	-0.0536	-0.0375	0.0862	0.0854	0.0099	0.0119	5038.4
2000	30	-0.0542	-0.0379	0.0864	0.0856	0.0099	0.0119	4795.3
2001	0	-0.0578	-0.0407	0.092	0.0917	0.0107	0.0123	5406.3
2001	30	-0.0593	-0.0407	0.0949	0.0943	0.0107	0.0126	5503.9
2002	0	-0.06	-0.0407	0.0958	0.0951	0.0106	0.0126	5375.9
2002	30	-0.0603	-0.0407	0.0969	0.0962	0.0106	0.0127	5427.1

2003	0	-0.0603	-0.0407	0.0973	0.0966	0.0106	0.0127	5377.5
2003	30	-0.0617	-0.0407	0.0986	0.0981	0.0107	0.0127	5529.5
2004	0	-0.0617	-0.0407	0.0992	0.0984	0.0106	0.0127	5467.1
2004	30	-0.0624	-0.0407	0.0997	0.0989	0.0106	0.0127	5462.3
2005	0	-0.0624	-0.0407	0.0998	0.099	0.0106	0.0127	5561.5
2005	30	-0.0632	-0.0405	0.1006	0.0998	0.0107	0.0127	5572.7
2006	0	-0.0671	-0.0339	0.1071	0.1068	0.0113	0.0136	5958.1
2006	30	-0.0688	-0.0307	0.1111	0.1104	0.0114	0.0137	5998.1
2007	0	-0.0699	-0.0286	0.1128	0.1122	0.0114	0.0137	6026.9
2007	30	-0.0705	-0.0278	0.1135	0.1127	0.0113	0.0137	5889.3
2008	0	-0.0711	-0.0276	0.1143	0.1135	0.0113	0.0137	6129.3
2008	30	-0.0711	-0.0275	0.1147	0.114	0.0113	0.0137	5970.9
2009	0	-0.0718	-0.0264	0.1151	0.1142	0.0112	0.0137	5991.7
2009	30	-0.0725	-0.0261	0.1161	0.1153	0.0113	0.0138	6113.3
2010	0	-0.0726	-0.0261	0.1166	0.1157	0.0113	0.0138	5927.7
2010	30	-0.0731	-0.0252	0.1168	0.1159	0.0113	0.0138	5948.5
2011	0	-0.0776	-0.0173	0.1242	0.1238	0.0118	0.0149	6581.9
2011	30	-0.0785	-0.0158	0.1266	0.1261	0.0117	0.015	6509.9
2012	0	-0.0793	-0.0147	0.1282	0.1276	0.0116	0.0151	6417.2
2012	30	-0.0806	-0.0133	0.1295	0.1288	0.0116	0.0151	6446
2013	0	-0.0815	-0.0124	0.1307	0.13	0.0117	0.0151	6444.4
2013	30	-0.0815	-0.0124	0.1311	0.1304	0.0116	0.0151	6476.3
2014	0	-0.0821	-0.011	0.1322	0.1316	0.0116	0.0151	6282.8
2014	30	-0.0821	-0.0109	0.1326	0.1318	0.0116	0.0151	6383.6
2015	0	-0.0831	-0.0088	0.1334	0.1326	0.0116	0.0151	6476.3
2015	30	-0.0831	-0.0088	0.1336	0.1328	0.0116	0.0151	6386.8
2016	0	-0.0877	-0.0016	0.1412	0.1412	0.0123	0.0161	7028.2
2016	30	-0.0904	0.0026	0.1463	0.1459	0.0123	0.0162	7037.8
2017	0	-0.0913	0.005	0.1481	0.1477	0.0123	0.0167	7042.6
2017	30	-0.093	0.0068	0.151	0.1507	0.0123	0.0167	7068.2
2018	0	-0.0943	0.0087	0.1533	0.1529	0.0123	0.0168	7084.2
2018	30	-0.0952	0.0098	0.1546	0.1541	0.0122	0.0168	6986.6
2019	0	-0.0961	0.012	0.1567	0.1563	0.0123	0.0168	7050.6
2019	30	-0.0969	0.0126	0.1575	0.1568	0.0122	0.0168	6909.8
2020	0	-0.0972	0.0137	0.1586	0.1581	0.0122	0.0169	7015.4
2020	30	-0.0984	0.0144	0.1601	0.1597	0.0123	0.017	7215.3
2021	0	-0.1054	0.0274	0.1742	0.1742	0.0129	0.0184	7588
2021	30	-0.1073	0.0308	0.1779	0.1779	0.0127	0.0184	7583.2
2022	0	-0.109	0.033	0.1807	0.1805	0.0128	0.0184	7628
2022	30	-0.1106	0.0354	0.1834	0.1833	0.0128	0.0186	7618.4
2023	0	-0.1113	0.0395	0.1851	0.185	0.0127	0.0186	7645.6
2023	30	-0.1129	0.0411	0.1876	0.1876	0.0128	0.0187	7568.8
2024	0	-0.1137	0.0425	0.1885	0.1884	0.0127	0.0188	7549.6
2024	30	-0.1142	0.0436	0.1896	0.1894	0.0126	0.0188	7580
2025	0	-0.1143	0.0436	0.1902	0.19	0.0125	0.0189	7540
2025	30	-0.1143	0.0436	0.1904	0.1902	0.0124	0.0189	7677.6
2026	0	-0.1208	0.0537	0.2006	0.2014	0.0132	0.02	8027.8
2026	30	-0.1238	0.0573	0.2063	0.2068	0.013	0.0201	8010.2

2027	0	-0.1256	0.0608	0.209	0.2094	0.013	0.0201	7970.3
2027	30	-0.1273	0.0632	0.2115	0.2119	0.013	0.0202	8069.4
2028	0	-0.1282	0.0649	0.2132	0.2135	0.0129	0.0202	8002.2
2028	30	-0.1288	0.065	0.2149	0.215	0.0129	0.0203	8024.6
2029	0	-0.1299	0.0668	0.2161	0.2165	0.0129	0.0206	8016.6
2029	30	-0.1304	0.068	0.2174	0.2176	0.0129	0.0207	8050.2
2030	0	-0.1315	0.0688	0.2184	0.2188	0.0129	0.0207	8013.4
2030	30	-0.1323	0.0699	0.2192	0.2192	0.0127	0.0207	8023
2031	0	-0.1394	0.08	0.2308	0.2317	0.0132	0.0216	8552.8
2031	30	-0.1435	0.085	0.2375	0.2384	0.0132	0.0218	8517.6
2032	0	-0.1465	0.0893	0.243	0.2439	0.0131	0.0219	8418.5
2032	30	-0.1489	0.0941	0.2479	0.2487	0.0132	0.0223	8488.8
2033	0	-0.1511	0.0972	0.2515	0.2524	0.0132	0.0223	8573.6
2033	30	-0.1536	0.101	0.2554	0.2564	0.0132	0.0224	8557.6
2034	0	-0.1562	0.1044	0.2597	0.2605	0.0133	0.0225	8554.3
2034	30	-0.159	0.1084	0.2637	0.2645	0.0136	0.0226	8538.4
2035	0	-0.1611	0.112	0.2673	0.2682	0.0136	0.023	8421.6
2035	30	-0.164	0.1149	0.271	0.2718	0.0137	0.0231	8629.5
2036	0	-0.1656	0.1172	0.2737	0.2746	0.0137	0.0231	8615.1
2036	30	-0.1834	0.1411	0.2991	0.3012	0.0147	0.0242	8960.6
2037	0	-0.2279	0.1821	0.3485	0.3501	0.0153	0.0258	9034.1
2037	30	-0.3129	0.2573	0.4352	0.434	0.0147	0.0289	8539.9
2038	0	-0.4164	0.3404	0.5327	0.5261	0.0132	0.0313	8023.3
2038	30	-0.5343	0.4155	0.6221	0.6069	0.0124	0.0322	7716.1
2039	0	-0.6456	0.4824	0.6976	0.6687	0.0129	0.0323	7322.7
2039	30	-0.706	0.5133	0.7343	0.6982	0.0124	0.0314	6956.4
2040	0	-0.708	0.5161	0.7385	0.702	0.0121	0.0312	6794.8
2040	30	-0.7082	0.5172	0.7402	0.7039	0.0117	0.0307	6705.2
2041	0	-0.7083	0.5184	0.7418	0.7051	0.0115	0.0306	6601.2
2041	30	-0.7083	0.5188	0.7429	0.7061	0.0114	0.0305	6697.2
2042	0	-0.6937	0.5194	0.7391	0.7062	0.0091	0.0273	4549.1
2042	30	-0.6663	0.5103	0.7266	0.6965	0.005	0.0224	3122.3
2043	0	-0.6144	0.4849	0.7039	0.6774	0.0002	0.0168	1433.2
2043	30	-0.5547	0.4577	0.6798	0.6574	-0.0029	0.013	148.79
2044	0	-0.532	0.4497	0.672	0.6512	-0.0036	0.0121	-54.35
2044	30	-0.5238	0.4468	0.6696	0.6493	-0.0037	0.0119	33.623
2045	0	-0.5201	0.446	0.6688	0.6487	-0.0038	0.0119	33.623
2045	30	-0.5179	0.4458	0.6684	0.6485	-0.0038	0.0119	27.218
2046	0	-0.5162	0.4457	0.6681	0.6485	-0.0038	0.0116	-70.352
2046	30	-0.515	0.4455	0.668	0.6484	-0.0038	0.0115	30.417
2047	0	-0.5137	0.4453	0.668	0.6484	-0.0038	0.0114	27.218
2047	30	-0.5128	0.4452	0.6679	0.6484	-0.0039	0.0114	43.213
2048	0	-0.5121	0.4449	0.6679	0.6484	-0.0039	0.0114	27.218_

Shaft #2 Test Data (PC Collected)

TIME		DIAL GAGE	DIAL GAGE	DIAL GAGE	DIAL GAGE	DIAL GAGE	DIAL GAGE	CELL
		A	B	C	D	E	F	PRESS.
1502	30	0.0005	0.0088	0.0021	0.0017	0.0001	0	38.392
1503	0	0.0005	0.0088	0.0021	0.0017	0.0001	0	38.392
1503	30	0.0005	0.0088	0.0021	0.0017	0.0001	0	35.193
1504	0	0.0005	0.0088	0.002	0.0019	0.0001	0	63.984
1504	30	0.0005	0.0088	0.002	0.0019	0.0001	0	68.782
1505	0	0.0005	0.0088	0.002	0.0019	0.0001	0	78.379
1505	30	0.0005	0.0088	0.002	0.0019	0.0001	0	47.906
1506	0	0.0005	0.0088	0.002	0.0019	0.0001	0	27.113
1506	30	0.0005	0.0088	0.0019	0.0019	0.0001	0	35.111
1507	0	0.0005	0.0088	0.0019	0.0019	0.0001	0	35.111
1507	30	0.0005	0.0088	0.0019	0.0019	0.0001	0	43.108
1508	0	0.0005	0.0088	0.0019	0.0019	0.0001	0	28.713
1508	30	0.0005	0.0088	0.0018	0.0019	0.0001	0	19.212
1509	0	0.0005	0.0088	0.0018	0.0019	0	0	56
1509	30	-0.0008	0.0088	0.0039	0.0033	0.0011	0.0007	590.23
1510	0	-0.0019	0.0096	0.0043	0.0038	0.0011	0.0007	625.42
1510	30	-0.0018	0.0103	0.0044	0.0046	0.0011	0.0007	619.02
1511	0	-0.0018	0.0103	0.0045	0.0046	0.0011	0.0007	604.72
1511	30	-0.0018	0.0103	0.0045	0.0046	0.0011	0.0007	588.73
1512	0	-0.0018	0.0103	0.0045	0.0046	0.0011	0.0007	598.33
1512	30	-0.0018	0.0103	0.0045	0.0046	0.0011	0.0007	625.52
1513	0	-0.0018	0.0103	0.0045	0.0046	0.0011	0.0007	587.13
1513	30	-0.0018	0.0103	0.0045	0.0046	0.0011	0.0007	571.13
1514	0	-0.0018	0.0103	0.0046	0.0046	0.0011	0.0007	575.91
1514	30	-0.0043	0.0103	0.0108	0.0107	0.0025	0.0014	1071.8
1515	0	-0.0043	0.0103	0.0112	0.0111	0.0025	0.0014	1019
1515	30	-0.0049	0.0114	0.012	0.0113	0.0025	0.0014	1006.2
1516	0	-0.0049	0.0114	0.012	0.0113	0.0025	0.0014	986.99
1516	30	-0.0049	0.0114	0.012	0.0113	0.0025	0.0014	978.99
1517	0	-0.0049	0.0114	0.012	0.0113	0.0025	0.0014	959.78
1517	30	-0.0051	0.0114	0.0121	0.0114	0.0025	0.0014	969.37
1518	0	-0.0051	0.0114	0.0121	0.0115	0.0025	0.0014	970.97
1518	30	-0.0053	0.0082	0.0156	0.0154	0.0032	0.0014	1070.1
1519	0	-0.0053	0.0082	0.0159	0.0157	0.0032	0.0014	1031.8
1519	30	-0.0079	0.0059	0.0319	0.0326	0.0048	0.0014	1514.8
1520	0	-0.0089	0.0054	0.0364	0.0372	0.0049	0.0016	1575.6
1520	30	-0.0093	0.0041	0.037	0.0377	0.0047	0.0016	1524.4
1521	0	-0.0094	0.0039	0.0378	0.038	0.0046	0.0016	1506.8
1521	30	-0.0094	0.0039	0.0379	0.038	0.0046	0.0016	1486
1522	0	-0.0094	0.0039	0.0379	0.0381	0.0045	0.0015	1474.8
1522	30	-0.0094	0.0039	0.0387	0.0385	0.0045	0.0015	1546.8

1523	0	-0.0099	0.0037	0.0391	0.039	0.0045	0.0015	1514.8
1523	30	-0.0099	0.0035	0.0391	0.039	0.0045	0.0015	1498.8
1524	0	-0.0099	0.0033	0.0393	0.0391	0.0045	0.0015	1497.2
1524	30	-0.0124	0.0017	0.0616	0.0623	0.006	0.0024	2047.4
1525	0	-0.0131	-0.0002	0.0657	0.0654	0.0059	0.0025	1932.3
1525	30	-0.0134	-0.0004	0.0672	0.0666	0.0059	0.0025	1959.4
1526	0	-0.0138	-0.0008	0.0682	0.0682	0.0059	0.0025	1988.1
1526	30	-0.0138	-0.0008	0.0686	0.0686	0.0059	0.0025	1956.1
1527	0	-0.0138	-0.0008	0.0696	0.0697	0.0059	0.0026	2007.3
1527	30	-0.0138	-0.0008	0.0699	0.0702	0.0059	0.0026	1988.1
1528	0	-0.0146	-0.0008	0.072	0.0724	0.0061	0.0027	2024.9
1528	30	-0.0146	-0.0008	0.0722	0.0727	0.0061	0.0027	2013.7
1529	0	-0.0146	-0.0008	0.0724	0.073	0.006	0.0027	1975.3
1529	30	-0.0178	-0.0031	0.0999	0.1029	0.0074	0.0029	2522.3
1530	0	-0.0193	-0.0051	0.1111	0.1129	0.0073	0.0027	2573.5
1530	30	-0.0193	-0.0051	0.112	0.1132	0.0069	0.0026	2467.9
1531	0	-0.0195	-0.0057	0.1132	0.1145	0.0068	0.0021	2423.1
1531	30	-0.0195	-0.0057	0.1156	0.1166	0.0073	0.0019	2579.9
1532	0	-0.0201	-0.0059	0.1163	0.1174	0.0069	0.0019	2445.6
1532	30	-0.0201	-0.006	0.1168	0.1175	0.0068	0.0019	2440.8
1533	0	-0.0201	-0.006	0.1185	0.1194	0.0069	0.0019	2501.5
1533	30	-0.0201	-0.006	0.1188	0.1199	0.0068	0.0019	2493.5
1534	0	-0.0201	-0.006	0.119	0.12	0.0068	0.0019	2452
1534	30	-0.022	-0.0083	0.1347	0.1399	0.0079	0.0021	2794.3
1535	0	-0.0238	-0.0098	0.1461	0.1484	0.0072	0.002	2751.1
1535	30	-0.0245	-0.0104	0.1472	0.1488	0.0069	0.0019	2693.5
1536	0	-0.0245	-0.0104	0.1474	0.1493	0.0068	0.0019	2711.1
1536	30	-0.0245	-0.0104	0.1476	0.1495	0.0068	0.0019	2648.7
1537	0	-0.0245	-0.0104	0.1479	0.1496	0.0067	0.0018	2635.9
1537	30	-0.0245	-0.0104	0.1481	0.1498	0.0066	0.0018	2603.9
1538	0	-0.0245	-0.0104	0.1481	0.1501	0.0066	0.0018	2611.9
1538	30	-0.0245	-0.0104	0.1482	0.1502	0.0066	0.0018	2608.7
1539	0	-0.0245	-0.0104	0.1483	0.1504	0.0066	0.0018	2611.9
1539	30	-0.0245	-0.0104	0.1485	0.1505	0.0066	0.0018	2640.7
1540	0	-0.0245	-0.0104	0.1487	0.1508	0.0065	0.0017	2589.5
1540	30	-0.025	-0.0122	0.149	0.1511	0.0065	0.0014	2587.8
1541	0	-0.025	-0.0122	0.1492	0.1511	0.0065	0.0014	2594.2
1541	30	-0.025	-0.0122	0.1496	0.1513	0.0065	0.0014	2551
1542	0	-0.025	-0.0122	0.1497	0.1515	0.0065	0.0014	2567
1542	30	-0.025	-0.0122	0.1497	0.1516	0.0065	0.0014	2562.2
1543	0	-0.025	-0.0122	0.1497	0.1516	0.0065	0.0014	2559
1543	30	-0.025	-0.0122	0.1497	0.1517	0.0065	0.0014	2583
1544	0	-0.0246	-0.0123	0.1499	0.1517	0.0065	0.0014	2507.8
1544	30	-0.0246	-0.0123	0.1499	0.1518	0.0065	0.0014	2547.8
1545	0	-0.0232	-0.0123	0.1461	0.1483	0.0049	-0.0006	1772.1
1545	30	-0.0224	-0.0121	0.1458	0.1477	0.0055	-0.0006	1991.2
1546	0	-0.0226	-0.0121	0.1461	0.1479	0.0055	-0.0006	2120.8
1546	30	-0.0226	-0.0121	0.1466	0.1485	0.0057	-0.0006	2220

1547	0	-0.0233	-0.0121	0.1467	0.1485	0.0057	-0.0006	2212
1547	30	-0.0233	-0.0121	0.1467	0.1486	0.0057	-0.0006	2202.4
1548	0	-0.0233	-0.0121	0.1467	0.1486	0.0057	-0.0006	2183.2
1548	30	-0.0233	-0.0121	0.1467	0.1486	0.0056	-0.0006	1986.5
1549	0	-0.0226	-0.0121	0.1449	0.1473	0.0047	-0.0019	1690.6
1549	30	-0.0218	-0.0114	0.143	0.1454	0.0043	-0.0022	1530.2
1550	0	-0.0214	-0.0113	0.1416	0.1439	0.0041	-0.0027	1466.3
1550	30	-0.0212	-0.0111	0.1412	0.1438	0.0041	-0.0027	1466.3
1551	0	-0.0194	-0.0091	0.1352	0.1374	0.0027	-0.005	1087.2
1551	30	-0.0092	-0.0003	0.0918	0.0925	-0.0007	-0.0106	63.683
1552	0	-0.0085	0.0003	0.089	0.0898	-0.0007	-0.0107	
1728	0	-0.0012	0.011	0.0817	0.0836	-0.0003	-0.0109	0.01025
1728	30	-0.0014	0.011	0.0816	0.0832	-0.0004	-0.0109	27.202
1729	0	-0.0014	0.011	0.0815	0.0832	-0.0004	-0.0109	3.207
1729	30	-0.0014	0.011	0.0815	0.0832	-0.0004	-0.011	8.0056
1730	0	-0.0014	0.011	0.0815	0.0832	-0.0004	-0.011	16.003
1730	30	-0.0014	0.011	0.0815	0.0832	-0.0004	-0.011	27.199
1731	0	-0.0014	0.011	0.0815	0.0832	-0.0004	-0.011	97.577
1731	30	-0.0018	0.011	0.0815	0.0832	-0.0004	-0.011	115.17
1732	0	-0.0018	0.011	0.0814	0.0832	-0.0004	-0.011	27.279
1732	30	-0.0018	0.011	0.0812	0.0831	-0.0005	-0.011	12.883
1733	0	-0.0018	0.011	0.0811	0.0831	-0.0005	-0.011	43.274
1733	30	-0.0018	0.011	0.0811	0.0831	-0.0005	-0.011	46.473
1734	0	-0.0018	0.011	0.0811	0.0831	-0.0005	-0.011	41.674
1734	30	-0.0018	0.011	0.0811	0.0831	-0.0005	-0.011	112.05
1735	0	-0.0018	0.011	0.0811	0.0831	-0.0005	-0.011	27.261
1735	30	-0.0018	0.011	0.0809	0.0831	-0.0005	-0.011	11.266
1736	0	-0.0018	0.011	0.0809	0.0831	-0.0005	-0.011	12.865
1736	30	-0.0019	0.011	0.0809	0.0831	-0.0005	-0.011	43.257
1737	0	-0.0019	0.011	0.0809	0.0831	-0.0006	-0.011	41.657
1737	30	-0.0019	0.011	0.0809	0.0831	-0.0006	-0.011	38.458
1738	0	-0.0019	0.011	0.0809	0.0831	-0.0006	-0.011	14.451
1738	30	-0.0019	0.011	0.0809	0.0831	-0.0006	-0.011	57.638
1739	0	-0.0019	0.011	0.0809	0.0831	-0.0006	-0.011	59.238
1739	30	-0.0019	0.011	0.0809	0.0831	-0.0006	-0.011	57.638
1740	0	-0.0019	0.011	0.0809	0.0831	-0.0006	-0.011	3.2542
1740	30	-0.0016	0.011	0.0809	0.083	-0.0006	-0.011	16.05
1741	0	-0.0016	0.011	0.081	0.083	-0.0007	-0.011	22.518
1741	30	-0.0016	0.011	0.081	0.083	-0.0007	-0.011	22.518
1742	0	-0.0016	0.011	0.081	0.083	-0.0007	-0.011	28.916
1742	30	-0.0016	0.011	0.081	0.083	-0.0007	-0.011	56.109
1743	0	-0.0016	0.011	0.081	0.083	-0.0007	-0.011	27.317
1743	30	-0.0016	0.0104	0.081	0.083	-0.0007	-0.011	20.918
1744	0	-0.0016	0.0104	0.081	0.083	-0.0007	-0.011	14.575
1744	30	-0.0016	0.0104	0.081	0.083	-0.0008	-0.011	4.9778
1745	0	-0.0068	0.0085	0.0965	0.0976	0.0022	-0.0098	929.55
1745	30	-0.0074	0.0077	0.0968	0.098	0.0021	-0.0098	875.16
1746	0	-0.0074	0.0077	0.0981	0.0992	0.0023	-0.0097	939.15

1746	30	-0.0074	0.0077	0.0983	0.0995	0.0022	-0.0097	943.9
1747	0	-0.0074	0.0077	0.0984	0.0996	0.0021	-0.0097	951.89
1747	30	-0.0074	0.0077	0.0984	0.0997	0.0021	-0.0097	910.3
1748	0	-0.0074	0.0072	0.0984	0.0998	0.0021	-0.0097	911.9
1748	30	-0.0078	0.0072	0.0984	0.0999	0.002	-0.0097	942.3
1749	0	-0.0078	0.0056	0.0985	0.0999	0.002	-0.0097	910.3
1749	30	-0.0078	0.0056	0.0985	0.0999	0.002	-0.0097	887.87
1750	0	-0.0078	0.0056	0.0985	0.0999	0.002	-0.0097	873.47
1750	30	-0.0147	0.0007	0.1347	0.1371	0.0052	-0.0094	1996.4
1751	0	-0.015	0.0005	0.1365	0.139	0.0052	-0.0094	2010.8
1751	30	-0.015	0.0005	0.137	0.1392	0.0052	-0.0094	2009.2
1752	0	-0.015	0.0005	0.1371	0.1394	0.0051	-0.0094	1967.6
1752	30	-0.0154	-0.0003	0.1372	0.1397	0.0051	-0.0094	1957.9
1753	0	-0.0154	-0.0003	0.1372	0.1397	0.0051	-0.0094	1924.3
1753	30	-0.016	-0.0008	0.1381	0.1405	0.0051	-0.0094	2041.1
1754	0	-0.016	-0.0008	0.1382	0.1406	0.0051	-0.0094	2034.7
1754	30	-0.0164	-0.0009	0.1383	0.1407	0.0051	-0.0094	1964.3
1755	0	-0.0164	-0.0009	0.1385	0.1407	0.0051	-0.0094	1989.9
1755	30	-0.0183	-0.0027	0.1497	0.1542	0.0065	-0.0084	2359.4
1756	0	-0.0201	-0.0048	0.1556	0.1598	0.0064	-0.0083	2517.7
1756	30	-0.0201	-0.0048	0.1566	0.1599	0.0062	-0.0083	2477.8
1757	0	-0.0201	-0.0048	0.1569	0.1599	0.0061	-0.0083	2449
1757	30	-0.0201	-0.0048	0.157	0.1599	0.0061	-0.0083	2449
1758	0	-0.0201	-0.0048	0.1586	0.1623	0.0062	-0.0083	2498.5
1758	30	-0.0204	-0.0048	0.1597	0.163	0.0062	-0.0082	2527.3
1759	0	-0.0204	-0.005	0.16	0.163	0.0062	-0.0082	2498.5
1759	30	-0.0204	-0.005	0.16	0.163	0.0062	-0.0082	2530.5
1800	0	-0.0204	-0.005	0.1601	0.163	0.0062	-0.0082	2476.1
1800	30	-0.0251	-0.0098	0.1891	0.1931	0.007	-0.0059	2988
1801	0	-0.0259	-0.0107	0.1925	0.1937	0.0068	-0.0059	2943.2
1801	30	-0.0274	-0.0123	0.196	0.1937	0.0068	-0.0054	2994.2
1802	0	-0.0281	-0.013	0.1979	0.1937	0.0067	-0.0054	2986.2
1802	30	-0.0287	-0.0136	0.1992	0.1938	0.0066	-0.0054	2986.2
1803	0	-0.0287	-0.0136	0.1995	0.1938	0.0066	-0.0054	2992.6
1803	30	-0.0287	-0.0136	0.1998	0.1938	0.0065	-0.0054	2931.8
1804	0	-0.0293	-0.0144	0.2009	0.1938	0.0065	-0.0054	2994.2
1804	30	-0.0294	-0.0145	0.2011	0.1938	0.0065	-0.0054	2919
1805	0	-0.0294	-0.0145	0.2014	0.1938	0.0065	-0.0054	2914.2
1805	30	-0.0347	-0.0203	0.2512	0.2529	0.0067	-0.0027	3531.6
1806	0	-0.0379	-0.0235	0.2695	0.2704	0.0061	-0.0021	3570
1806	30	-0.0398	-0.0258	0.2799	0.2807	0.0057	-0.002	3494.8
1807	0	-0.0404	-0.0263	0.2866	0.2871	0.0054	-0.0019	3506
1807	30	-0.0414	-0.0289	0.2888	0.2894	0.0052	-0.0019	3493.2
1808	0	-0.0421	-0.0299	0.294	0.295	0.0052	-0.0014	3592.4
1808	30	-0.0426	-0.0299	0.2979	0.2992	0.0051	-0.0014	3549.2
1809	0	-0.0426	-0.0299	0.2987	0.2999	0.005	-0.0014	3485.2
1809	30	-0.0428	-0.0299	0.3003	0.3017	0.0049	-0.0014	3549.2
1810	0	-0.0428	-0.0299	0.3011	0.3024	0.0048	-0.0014	3480.4

1810	30	-0.0651	-0.0563	0.433	0.4401	0.0041	0.0021	4016.3
1811	0	-0.1065	-0.1036	0.617	0.6288	0.001	0.0036	3941.1
1811	30	-0.1489	-0.1521	0.7986	0.8129	-0.0025	0.005	3909.1
1812	0	-0.1994	-0.2159	-1.5116	0.9892	-0.0061	0.0058	3870.7
1812	30	-0.2539	-0.285	-1.5114	1.159	-0.0097	0.0061	3864.3
1813	0	-0.3116	-0.3571	-1.5116	1.3262	-0.0133	0.0067	3752.4
1813	30	-0.378	-0.4404	-1.5116	1.4894	-0.0159	0.0067	3787.6
1814	0	-0.457	-0.5393	-1.5116	1.6522	-0.0181	0.0069	3702.8
1814	30	-0.5437	-0.6568	-1.5117	1.8318	-0.0192	0.007	3707.6
1815	0	-0.6148	-0.7514	-1.5117	2.0173	-0.0199	0.0066	3640.4
1815	30	-0.6185	-0.7543	-1.5117	2.0241	-0.0206	0.0055	3213.3
1816	0	-0.6183	-0.7543	-1.5117	2.0261	-0.0207	0.0052	3200.6
1816	30	-0.612	-0.7524	-1.5117	2.0268	-0.023	0.0023	2456.8
1817	0	-0.604	-0.7451	-1.5117	2.0214	-0.0239	0.0011	2023.3
1817	30	-0.6034	-0.7445	-1.5117	2.0213	-0.0239	0.0011	2058.5
1818	0	-0.6028	-0.7442	-1.5117	2.0213	-0.0239	0.0011	2053.7
1818	30	-0.602	-0.7429	-1.5117	2.0213	-0.0239	0.001	2056.9
1819	0	-0.577	-0.7172	-1.5117	1.9897	-0.0286	-0.006	991.67
1819	30	-0.5752	-0.7155	-1.5117	1.9893	-0.0284	-0.006	1065.2
1820	0	-0.5737	-0.7143	-1.5117	1.9884	-0.0284	-0.006	1038.1
1820	30	-0.5725	-0.7131	-1.5118	1.9879	-0.0287	-0.0069	1062
1821	0	-0.5204	-0.665	-1.5118	1.9175	-0.03	-0.0147	97.56
1821	30	-0.4816	-0.645	-1.5118	1.8969	-0.0284	-0.0157	27.182
1822	0	-0.4748	-0.6405	-1.5118	1.8921	-0.0278	-0.0158	28.783
1822	30	-0.4713	-0.6372	-1.5118	1.8897	-0.0277	-0.0163	27.184
1823	0							

Shaft #3Test Data (PC Collected)

TIME		DIAL GAGE	DIAL GAGE	DIAL GAGE	DIAL GAGE	DIAL GAGE	DIAL GAGE	CELL
		A	B	C	D	E	F	PRESS.
2143	30	-0.0002	0	0.0015	0.001	0	0.0007	25.611
2144	0	-0.0002	0	0.0015	0.001	0	0.0007	6.4167
2144	30	-0.0002	0	0.0015	0.001	0	0.0007	25.607
2145	0	-0.0002	0	0.0015	0.001	0	0.0007	27.206
2145	30	-0.0002	0	0.0015	0.001	0	0.0007	-4.7834
2146	0	-0.0002	0	0.0015	0.001	0	0.0007	-103.95
2146	30	-0.0002	0	0.0015	0.001	-0.0001	0.0007	32.005
2147	0	-0.0002	0	0.0015	0.001	-0.0002	0.0007	38.4
2147	30	-0.0002	0	0.0015	0.001	-0.0002	0.0007	-19.182
2148	0	-0.0002	0	0.0015	0.001	-0.0003	0.0007	219.14
2148	30	-0.0002	0	0.0015	0.001	-0.0003	0.0007	25.604
2149	0	-0.0002	0	0.0015	0.001	-0.0003	0.0008	505.45
2149	30	-0.0002	0	0.0018	0.001	-0.0003	0.0008	508.65
2150	0	-0.0002	0	0.0018	0.001	-0.0003	0.0008	467.06
2150	30	-0.0002	0	0.002	0.0011	-0.0003	0.0008	652.6
2151	0	-0.0002	0	0.002	0.0011	-0.0003	0.0009	526.24
2151	30	-0.0002	0	0.002	0.0012	-0.0003	0.0009	649.4
2152	0	-0.0002	0	0.0021	0.0012	-0.0003	0.0009	547.04
2152	30	-0.0002	0	0.0021	0.0013	-0.0003	0.0009	585.42
2153	0	-0.0002	0	0.0021	0.0013	-0.0003	0.0009	566.23
2153	30	-0.0002	0	0.0022	0.0017	-0.0003	0.0013	510.25
2154	0	-0.0204	0	0.0055	0.004	0.0003	0.0017	945.31
2154	30	-0.0504	0	0.0061	0.0046	0.0007	0.0022	1009.3
2155	0	-0.0523	0	0.0062	0.0048	0.0007	0.0022	1010.9
2155	30	-0.0529	0	0.0063	0.0049	0.0007	0.0022	985.3
2156	0	-0.0564	0	0.0065	0.005	0.0007	0.0022	1039.7
2156	30	-0.0564	0	0.0066	0.005	0.0007	0.0022	1007.7
2157	0	-0.0585	0	0.0067	0.0052	0.0007	0.0022	950.1
2157	30	-0.0587	0	0.0067	0.0052	0.0007	0.0022	1031.7
2158	0	-0.0587	0	0.0068	0.0053	0.0007	0.0022	962.9
2158	30	-0.0593	0	0.0068	0.0053	0.0007	0.0022	878.13
2159	0	-0.0907	0	0.0074	0.0062	0.0009	0.0023	1348.4
2159	30	-0.1458	0	0.0081	0.0067	0.001	0.0025	1406
2200	0	-0.2009	0	0.0087	0.0073	0.0013	0.0025	1575.5
2200	30	-0.2066	0	0.0088	0.0074	0.0013	0.0025	1519.5
2201	0	-0.2155	0	0.0089	0.0075	0.0013	0.0025	1621.9
2201	30	-0.2172	0	0.009	0.0076	0.0013	0.0025	1495.5
2202	0	-0.2189	0	0.009	0.0076	0.0013	0.0025	1476.3
2202	30	-0.2197	0	0.009	0.0076	0.0013	0.0025	1484.3
2203	0	-0.2215	0	0.0091	0.008	0.0013	0.0025	1455.5
2203	30	-0.221	0	0.0109	0.0093	0.0022	0.0025	1466.7

2204	0	-0.2217	0	0.0109	0.0093	0.0022	0.0025	1604.3
2204	30	-0.2222	0	0.0109	0.0093	0.0022	0.0025	1441.1
2205	0	-0.2237	0	0.0109	0.0093	0.0022	0.0025	1593.2
2205	30	-0.2243	0	0.0109	0.0093	0.0022	0.0025	1574
2206	0	-0.2243	0	0.0109	0.0093	0.0022	0.0025	1455.7
2206	30	-0.2265	0	0.0109	0.0095	0.0022	0.0025	1390.1
2207	0	-0.221	0.0078	0.0171	0.0153	0.0019	0.0028	1510.1
2207	30	-0.222	0.0078	0.0171	0.0153	0.0019	0.0029	1505.3
2208	0	-0.2641	0.0078	0.0171	0.0153	0.0021	0.0029	1687.6
2208	30	-0.3541	0.0078	0.0182	0.0161	0.0025	0.0031	1970.7
2209	0	-0.3916	0.0078	0.0192	0.017	0.0026	0.0032	1953.1
2209	30	-0.3978	0.0078	0.0194	0.0174	0.0026	0.0032	1905.1
2210	0	-0.4019	0.0078	0.0198	0.0175	0.0026	0.0032	1994.7
2210	30	-0.4046	0.0078	0.0198	0.0177	0.0026	0.0032	2053.8
2211	0	-0.4065	0.0078	0.0199	0.0177	0.0026	0.0032	1972.3
2211	30	-0.4075	0.0078	0.02	0.0178	0.0026	0.0032	2009.1
2212	0	-0.408	0.0078	0.02	0.0178	0.0026	0.0032	1997.9
2212	30	-0.4097	0.0078	0.0201	0.0182	0.0026	0.0032	2007.5
2213	0	-0.41	0.0078	0.0201	0.0182	0.0026	0.0032	1887.5
2213	30	-0.4892	0.0089	0.0223	0.0204	0.0031	0.0039	2421.7
2214	0	-0.5276	0.0105	0.0238	0.0218	0.0031	0.004	2616.8
2214	30	-0.5354	0.0111	0.0243	0.0224	0.0032	0.0041	2527.3
2215	0	-0.5417	0.0113	0.0248	0.0228	0.0032	0.0041	2618.4
2215	30	-0.5444	0.0116	0.0249	0.0229	0.0032	0.0041	2504.9
2216	0	-0.5453	0.0116	0.0249	0.0229	0.0032	0.0041	2514.5
2216	30	-0.547	0.0117	0.0251	0.0233	0.0032	0.0041	2437.7
2217	0	-0.5489	0.0122	0.0254	0.0234	0.0032	0.0041	2751.2
2217	30	-0.5498	0.0122	0.0254	0.0235	0.0032	0.0041	2482.5
2218	0	-0.5501	0.0122	0.0255	0.0235	0.0032	0.0045	2480.9
2218	30	-0.5854	0.0151	0.0281	0.0265	0.0035	0.0048	3016.7
2219	0	-0.5985	0.0161	0.0293	0.0274	0.0037	0.0048	3093.5
2219	30	-0.6024	0.0166	0.0296	0.0279	0.0037	0.0048	2942.9
2220	0	-0.6051	0.0169	0.03	0.0281	0.0037	0.0048	2920.6
2220	30	-0.6074	0.0174	0.0303	0.0284	0.0037	0.0049	3253.2
2221	0	-0.6081	0.0174	0.0303	0.0284	0.0037	0.0049	2989.3
2221	30	-0.6094	0.0174	0.0305	0.0288	0.0037	0.0049	2950.9
2222	0	-0.6101	0.0176	0.0306	0.0288	0.0037	0.0049	3000.5
2222	30	-0.6105	0.0176	0.0306	0.029	0.0037	0.0049	2975
2223	0	-0.6124	0.0178	0.0312	0.0298	0.004	0.0054	2947.8
2223	30	-0.6401	0.0225	0.035	0.0334	0.0043	0.0056	3649.9
2224	0	-0.6434	0.0232	0.0355	0.0338	0.0043	0.0056	3464.4
2224	30	-0.6468	0.0235	0.0361	0.0345	0.0043	0.0056	3605.1
2225	0	-0.6488	0.0239	0.0365	0.0347	0.0044	0.0056	3550.8
2225	30	-0.6497	0.0239	0.0367	0.0352	0.0044	0.0056	3494.8
2226	0	-0.6508	0.0243	0.0369	0.0353	0.0044	0.0056	3365.2
2226	30	-0.6514	0.0243	0.0369	0.0353	0.0044	0.0056	3322.1
2227	0	-0.6525	0.0247	0.0372	0.0355	0.0044	0.0056	3475.6
2227	30	-0.6538	0.025	0.0375	0.036	0.0045	0.0056	3728.3

2228	0	-0.6544	0.0251	0.0376	0.036	0.0045	0.0056	3526.8
2228	30	-0.6707	0.0303	0.0422	0.0409	0.0052	0.0064	4013
2229	0	-0.6754	0.0313	0.043	0.0412	0.0052	0.0064	4133
2229	30	-0.678	0.0319	0.0437	0.0418	0.0052	0.0064	3905.9
2230	0	-0.6797	0.0322	0.044	0.0423	0.0052	0.0064	3977.9
2230	30	-0.6818	0.0329	0.0446	0.0428	0.0052	0.0064	4096.2
2231	0	-0.6833	0.0335	0.0449	0.0433	0.0053	0.0064	4185.8
2231	30	-0.6842	0.0335	0.0452	0.0434	0.0053	0.0064	4125
2232	0	-0.6856	0.0338	0.0455	0.0438	0.0053	0.0064	4121.8
2232	30	-0.6858	0.0338	0.0456	0.044	0.0053	0.0064	4062.6
2233	0	-0.6871	0.0344	0.046	0.0443	0.0054	0.0065	4160.2
2233	30	-0.6987	0.0406	0.0512	0.0498	0.006	0.0071	4622.5
2234	0	-0.7034	0.0419	0.0526	0.0512	0.006	0.0071	4528.1
2234	30	-0.7055	0.0425	0.0532	0.0517	0.006	0.0071	4577.7
2235	0	-0.707	0.043	0.0536	0.0521	0.006	0.0071	4614.5
2235	30	-0.7085	0.0435	0.0541	0.0524	0.006	0.0071	4571.3
2236	0	-0.7093	0.0438	0.0543	0.0526	0.006	0.0071	4552.1
2236	30	-0.7105	0.0441	0.0546	0.053	0.006	0.0071	4617.7
2237	0	-0.7107	0.0442	0.055	0.0531	0.006	0.0072	4523.3
2237	30	-0.7118	0.0447	0.0551	0.0535	0.006	0.0072	4580.9
2238	0	-0.7124	0.0447	0.0552	0.0536	0.006	0.0072	4443.3
2238	30	-0.7133	0.045	0.0556	0.0539	0.0061	0.0072	4596.9
2239	0	-0.7139	0.0453	0.0558	0.054	0.0061	0.0072	4662.5
2239	30	-0.721	0.0511	0.0607	0.0594	0.0067	0.0079	5099.1
2240	0	-0.7244	0.0527	0.0622	0.0609	0.0068	0.0079	5286.3
2240	30	-0.7268	0.0538	0.0632	0.0618	0.0068	0.0079	5182.3
2241	0	-0.7278	0.0542	0.0637	0.0623	0.0068	0.0079	5032
2241	30	-0.729	0.0545	0.064	0.0626	0.0068	0.0079	4979.2
2242	0	-0.7303	0.0552	0.0646	0.0633	0.0068	0.0079	5195.1
2242	30	-0.7317	0.0559	0.0652	0.0638	0.0071	0.0081	5177.5
2243	0	-0.7323	0.0561	0.0655	0.0641	0.0071	0.0081	5092.7
2243	30	-0.7326	0.0562	0.0656	0.0642	0.0071	0.0081	5028.8
2244	0	-0.733	0.0562	0.0657	0.0643	0.0071	0.0081	4876.8
2244	30	-0.7389	0.0623	0.071	0.0699	0.0075	0.0086	5612.6
2245	0	-0.7426	0.0647	0.073	0.0721	0.0075	0.0087	5596.6
2245	30	-0.7443	0.0656	0.0741	0.073	0.0076	0.0087	5737.3
2246	0	-0.7458	0.0666	0.0751	0.0738	0.0076	0.0087	5614.2
2246	30	-0.7471	0.0674	0.0759	0.0746	0.0076	0.0087	5564.6
2247	0	-0.7483	0.0683	0.0767	0.0755	0.0077	0.0087	5619
2247	30	-0.7493	0.0695	0.0776	0.0766	0.0078	0.0087	5694.2
2248	0	-0.75	0.0702	0.0782	0.0771	0.0078	0.0087	5476.6
2248	30	-0.751	0.071	0.0791	0.0779	0.0079	0.0087	5611
2249	0	-0.7514	0.0712	0.0793	0.0784	0.0079	0.0087	5579
2249	30	-0.7592	0.0832	0.0901	0.0896	0.0088	0.0096	6143.6
2250	0	-0.7616	0.0854	0.0922	0.0914	0.0088	0.0096	6006.1
2250	30	-0.7633	0.0865	0.0935	0.0928	0.0088	0.0096	5999.7
2251	0	-0.765	0.0882	0.0951	0.0945	0.0088	0.0096	6052.4
2251	30	-0.7666	0.0896	0.0965	0.096	0.0089	0.0096	6095.6

2252	0	-0.7676	0.091	0.0975	0.0969	0.0089	0.0096	6113.2
2252	30	-0.7688	0.0918	0.0984	0.0977	0.0089	0.0096	6006.1
2253	0	-0.7698	0.0925	0.0991	0.0985	0.0089	0.0096	6025.3
2253	30	-0.77	0.0929	0.0996	0.0989	0.0089	0.0096	6102
2254	0	-0.7705	0.093	0.0999	0.0992	0.0089	0.0096	6034.9
2254	30	-0.7761	0.1026	0.1081	0.1079	0.0097	0.0104	6557.9
2255	0	-0.7787	0.1062	0.1116	0.1113	0.0097	0.0104	6417.1
2255	30	-0.781	0.1088	0.1141	0.1138	0.0098	0.0105	6701.8
2256	0	-0.7821	0.1104	0.1157	0.1153	0.0098	0.0105	6578.7
2256	30	-0.7832	0.1119	0.117	0.1168	0.0098	0.0105	6479.5
2257	0	-0.7846	0.1136	0.1189	0.1186	0.0098	0.0105	6546.7
2257	30	-0.7857	0.1158	0.1207	0.1206	0.0099	0.0106	6615.5
2258	0	-0.7866	0.1175	0.1224	0.1224	0.01	0.0106	6517.9
2258	30	-0.7874	0.1187	0.1237	0.1234	0.0101	0.0106	6596.3
2259	0	-0.7881	0.1199	0.1247	0.1244	0.0101	0.0106	6500.3
2259	30	-0.7938	0.1328	0.1366	0.1369	0.011	0.0115	7007.3
2300	0	-0.7978	0.1407	0.1442	0.1442	0.0111	0.0118	7175.3
2300	30	-0.7997	0.1439	0.1477	0.1474	0.0111	0.0118	7119.3
2301	0	-0.8014	0.1466	0.1505	0.1504	0.0112	0.0118	6876.2
2301	30	-0.8025	0.148	0.152	0.1519	0.0112	0.0118	7044.1
2302	0	-0.8037	0.1502	0.1542	0.1538	0.0112	0.0118	6975.4
2302	30	-0.805	0.1516	0.1557	0.1553	0.0112	0.0118	7096.9
2303	0	-0.8058	0.1527	0.1568	0.1564	0.0112	0.0118	7117.7
2303	30	-0.8067	0.1542	0.1583	0.1579	0.0112	0.0118	7094
2304	0	-0.8071	0.1545	0.159	0.1585	0.0112	0.0118	7006.1
2304	30	-0.8113	0.1618	0.1657	0.1662	0.0119	0.0122	7634.7
2305	0	-0.8153	0.1713	0.175	0.1747	0.012	0.0126	7599.5
2305	30	-0.8176	0.175	0.1784	0.1781	0.012	0.0126	7551.5
2306	0	-0.8193	0.1776	0.1814	0.1809	0.012	0.0126	7421.9
2306	30	-0.8206	0.1797	0.1836	0.1831	0.012	0.0126	7615.4
2307	0	-0.8218	0.1814	0.1853	0.1848	0.012	0.0126	7580.2
2307	30	-0.8229	0.183	0.187	0.1864	0.012	0.0126	7525.8
2308	0	-0.8241	0.184	0.1881	0.1874	0.012	0.0127	7668.2
2308	30	-0.8243	0.1847	0.1887	0.1881	0.012	0.0127	7509.8
2309	0	-0.8245	0.1849	0.1895	0.189	0.0121	0.0127	7396.3
2309	30	-0.8339	0.2048	0.2078	0.2074	0.0128	0.0134	8111.2
2310	0	-0.837	0.2114	0.2145	0.2138	0.0129	0.0134	8045.6
2310	30	-0.8387	0.2144	0.2176	0.2169	0.0129	0.0134	8128.8
2311	0	-0.8401	0.2165	0.2199	0.2196	0.0129	0.0136	8108
2311	30	-0.8418	0.2193	0.2226	0.2217	0.0129	0.0136	8128.8
2312	0	-0.8429	0.2209	0.2245	0.2234	0.0129	0.0136	8213.6
2312	30	-0.8438	0.2224	0.226	0.2249	0.0129	0.0136	8053.9
2313	0	-0.8454	0.2248	0.2285	0.2274	0.0129	0.0136	8113.1
2313	30	-0.8461	0.226	0.2297	0.2288	0.0129	0.0136	8149.9
2314	0	-0.8466	0.2267	0.2306	0.2296	0.0129	0.0136	7977.1
2314	30	-0.8515	0.2364	0.2398	0.239	0.0133	0.0137	8364.2
2315	0	-0.8554	0.2439	0.247	0.246	0.0135	0.0142	8588.1
2315	30	-0.8574	0.2481	0.2518	0.2507	0.0135	0.0142	8423.3

2316	0	-0.861	0.2543	0.2573	0.2563	0.0135	0.0142	8727.2
2316	30	-0.8614	0.2558	0.2591	0.2578	0.0135	0.0142	8452.1
2317	0	-0.8635	0.2594	0.2628	0.2617	0.0135	0.0142	8536.9
2317	30	-0.8656	0.2631	0.2663	0.2651	0.0135	0.0142	8552.9
2318	0	-0.867	0.2658	0.2693	0.268	0.0136	0.0142	8548
2318	30	-0.8674	0.2665	0.2701	0.2688	0.0135	0.0142	8312.9
2319	0	-0.8692	0.2695	0.2729	0.2721	0.0136	0.0143	8759.1
2319	30	-0.8755	0.2818	0.2849	0.2841	0.0138	0.0145	9082.2
2320	0	-0.8814	0.2931	0.2962	0.2953	0.0139	0.0146	9152.6
2320	30	-0.8851	0.2999	0.303	0.3016	0.0139	0.0149	9218.2
2321	0	-0.8881	0.3051	0.3083	0.3067	0.0139	0.015	9168.6
2321	30	-0.8898	0.3081	0.3114	0.3098	0.0139	0.015	9117.4
2322	0	-0.891	0.3101	0.3136	0.3121	0.0138	0.015	9135
2322	30	-0.8918	0.3115	0.3153	0.3137	0.0138	0.015	9021.4
2323	0	-0.8939	0.3144	0.3183	0.3167	0.0138	0.015	9202.1
2323	30	-0.8948	0.3161	0.32	0.3185	0.0138	0.015	9079
2324	0	-0.8955	0.3175	0.3214	0.3201	0.0138	0.015	9053.3
2324	30	-0.9033	0.331	0.3345	0.3337	0.0143	0.0153	9547.6
2325	0	-0.9094	0.3423	0.3459	0.3445	0.0144	0.0154	9701.1
2325	30	-0.9143	0.3512	0.3554	0.3542	0.0143	0.0157	9525.2
2326	0	-0.9197	0.3607	0.3655	0.3645	0.014	0.0158	9346
2326	30	-0.926	0.3702	0.3753	0.3735	0.0137	0.0158	9560.4
2327	0	-0.931	0.3774	0.383	0.381	0.0136	0.0158	9704.3
2327	30	-0.9337	0.3819	0.3883	0.3867	0.0135	0.0158	9581.1
2328	0	-0.9395	0.3903	0.3967	0.3948	0.0135	0.0159	9587.5
2328	30	-0.9446	0.3979	0.4049	0.4028	0.0132	0.0159	9491.5
2329	0	-0.9493	0.4052	0.4126	0.4112	0.0131	0.0159	9685.1
2329	30	-0.9753	0.4441	0.4548	0.4546	0.0128	0.0167	9442
2330	0	-1.0218	0.4933	0.5247	0.5241	0.0127	0.0174	8909.3
2330	30	-1.0654	0.4935	0.5801	0.5794	0.0118	0.0175	8981.3
2331	0	-1.1148	0.4935	0.6522	0.6506	0.0106	0.0175	9155.6
2331	30	-1.1701	0.4935	0.7209	0.7199	0.0095	0.0175	8862.9
2332	0	-1.2285	0.4935	0.7867	0.7848	0.0079	0.0174	8930.1
2332	30	-1.2691	0.0969	0.8669	0.8635	0.0055	0.0166	8910.9
2333	0	-1.319	0.0968	0.9428	0.9388	0.0031	0.0153	8914.1
2333	30	-1.3757	0.0968	1.0196	1.0145	0.0002	0.0142	8698.1
2334	0	-1.3805	0.0968	1.0327	1.025	-0.0009	0.0129	8079.1
2334	30	-1.3785	0.0968	1.0369	1.0289	-0.0014	0.0127	7909.6
2335	0	-1.3772	0.0968	1.0395	1.0314	-0.0016	0.0126	7946.4
2335	30	-1.3755	0.0968	1.0423	1.0335	-0.0017	0.0126	7927.2
2336	0	-1.3638	0.0968	1.0409	1.0333	-0.0031	0.0105	6127.7
2336	30	-1.3447	0.0968	1.034	1.0249	-0.0055	0.0081	4248.3
2337	0	-1.3195	0.0968	1.0174	1.008	-0.0086	0.0054	3231
2337	30	-1.2756	0.0968	0.9979	0.9892	-0.0113	0.0023	2272.9
2338	0	-1.2324	0.0968	0.9773	0.9692	-0.0135	0	1612.3
2338	30	-1.1702	0.0968	0.9452	0.9377	-0.0153	-0.0024	897.33
2339	0	-1.0979	0.0968	0.8702	0.8641	-0.0167	-0.0042	113.58
2339	30	-1.0745	0.0968	0.8503	0.8457	-0.0167	-0.0042	17.61

2340	0	-1.0674	0.0968	0.8449	0.8408	-0.0167	-0.0042	35.205
2340	30	-1.0636	0.0968	0.8419	0.8378	-0.0167	-0.0042	25.608
2341	0	-1.0604	0.0968	0.8398	0.8361	-0.0167	-0.0043	41.603
2341	30	-1.0587	0.0968	0.8381	0.8346	-0.0167	-0.0043	27.285
2342	0	-1.0569	0.0968	0.8369	0.8335	-0.017	-0.0043	27.285
2342	30	-1.0558	0.0968	0.8358	0.8323	-0.0173	-0.0043	28.884
2343	0	-1.0545	0.0968	0.835	0.8314	-0.0174	-0.0044	-91.082_

Shaft #1Test Data (Manually Collected)

Load	Starting	Ending	Time	Interval	Dial Gage	Dial Gage	Dial Gage	Dial Gage	Dial Gage	Dial Gage
Interval	Press.	Press.	Start	(min.)	A	B	C	D	E	F
1L0			18:56:30		0.003	0.0032	0.0017	0.0011	0.0003	0.0001
1L1	481	342	19:10:30	4	0.0068	0.0068	0.007	0.0062	0.0009	0.0007
1L2	1025	958	19:15:30	4	0.0068	0.0068	0.009	0.0083	0.0014	0.0015
1L3	1447	1490	19:20:30	4	0.0054	0.0067	0.0119	0.011	0.0022	0.0022
1L4	1977	1818	19:26:00	4	0.0051	0.0034	0.0154	0.015	0.0035	0.0032
1L5	2463	2359	19:31:00	4	-0.0166	-0.0062	0.0254	0.025	0.0057	0.0055
1L6	3095	3149	19:36:00	4	-0.025	-0.0127	0.0353	0.0346	0.0067	0.0066
1L7	3562	3317	19:41:00	4	-0.0312	-0.0212	0.0454	0.0446	0.0076	0.008
1L8	4040	3949	19:46:00	4	-0.0377	-0.0245	0.0568	0.0564	0.0084	0.09
1L9	4462	4318	19:51:00	4	-0.0448	-0.0295	0.0707	0.07	0.0091	0.0104
1L10	5054	5038	19:56:00	4	-0.0536	-0.0375	0.0862	0.0854	0.0099	0.0119
1L11	5406	5561	20:01:00	4	-0.0624	-0.0407	0.0998	0.099	0.0106	0.0127
1L12	5958	5927	20:06:00	4	-0.0726	-0.0261	0.1166	0.1157	0.00113	0.0138
1L13	6581	6476	20:11:00	4	-0.0831	-0.0088	0.1334	0.1326	0.0116	0.0151
1L14	7028	7015	20:16:00	4	-0.0972	0.0137	0.1586	0.1581	0.0122	0.0169
1L15	7587	7539	20:21:00	4	-0.1143	0.0436	0.1902	0.19	0.0125	0.0189
1L16	8027	8013	20:26:00	4	-0.1315	0.0688	0.2184	0.2188	0.0129	0.0207
1L17	8552	8629	20:31:00	4	-0.1611	0.112	0.2673	0.2682	0.0136	0.023
1L18	8960	6600	20:36:30	4	-0.7083	0.5184	0.7418	0.7051	0.0115	0.0306
1L19	33	27	20:45:00	2	-0.5137	0.4453	0.668	0.6484	-0.0038	0.0014

Shaft #2 First Loading Test Data (Manually Collected)

Load	Starting	Ending	Time	Interval	Dial Gage	Dial Gage	Dial Gage	Dial Gage	Dial Gage	Dial Gage
Interval	Press.	Press.	Start	(min.)	A	B	C	D	E	F
1L0			15:09:30		0.0005	0.0088	0.0021	0.0017	0.0001	0
1L1	590	571	15:13:30	4	-0.0018	0.0103	0.0045	0.0046	0.0011	0.0007
1L2	1000	1070	15:14:00	4	-0.0053	0.0082	0.0156	0.0154	0.0032	0.0014
1L3	1500	1498	15:19:45	4	-0.0099	0.0035	0.0391	0.039	0.0045	0.0015
1L4	2000	2013	15:24:30	4	-0.0146	-0.0008	0.0722	0.0727	0.0061	0.0027
1L5	2500	2493	15:29:30	4	-0.0201	-0.006	0.1188	0.0119	0.0068	0.0019
1L6	2711	2608	15:34:30	4	-0.0245	-0.0114	0.1483	0.1504	0.0066	0.0018

Shaft #2 Second Loading Test Data (Manually Collected)

Load	Starting	Ending	Time	Interval	Dial Gage	Dial Gage	Dial Gage	Dial Gage	Dial Gage	Dial Gage
Interval	Press.	Press.	Start	(min.)	A	B	C	D	E	F
2L0			17:29:00		-0.0014	0.011	0.0815	0.0832	-0.0004	-0.011
2L1	929	910	17:45:00	4	-0.0078	0.0056	0.0985	0.0999	0.002	-0.0097
2L2	1996	1964	17:50:30	4	-0.0164	-0.0009	0.1385	0.1407	0.0051	-0.0094
2L3	2517	2530	17:55:30	4	-0.0204	-0.005	0.16	0.163	0.0062	-0.0082
2L4	2987	2919	18:00:30	4	-0.0294	-0.0145	0.2011	0.1938	0.0065	-0.0054
2L5	3531	3549	18:05:30	4	-0.0428	-0.0299	0.3003	0.3017	0.0049	-0.0014
2L6	4016	3707	18:10:30	4	-0.5437	-0.6568		1.831	-0.0192	-0.007

Shaft #3 Test Data (Manually Collected)

Load	Starting	Ending	Time	Interval	Dial Gage	Dial Gage	Dial Gage	Dial Gage	Dial Gage	Dial Gage
Interval	Press.	Press.	Start	(min.)	A	B	C	D	E	F
1L0					-0.0002	0	0.0015	0.001	-0.0002	0.0007
1L1	505	566	21:49:00	4	-0.0002	0	0.0021	0.0013	-0.0003	0.0009
1L2	1009	963	21:54:00	4	-0.0587	0	0.0068	0.0053	0.0007	0.0022
1L3	1575	1455	22:00:00	4	-0.2243	0	0.0109	0.0093	0.0022	0.0025
1L4	1970	2007	22:08:30	4	-0.4097	0.078	0.0201	0.0182	0.0026	0.0032
1L5	2421	2482	22:13:30	4	-0.5498	0.0122	0.0254	0.0235	0.0032	0.0041
1L6	3016	2974	22:18:30	4	-0.6105	0.0176	0.0306	0.029	0.0037	0.0049
1L7	3649	3728	22:23:30	4	-0.6538	0.025	0.0375	0.036	0.0045	0.0056
1L8	4013	4062	22:28:30	4	-0.6858	0.0338	0.0456	0.044	0.0053	0.0064
1L9	4622	4596	22:33:30	4	-0.7133	0.045	0.0556	0.0539	0.0061	0.0072
1L10	5099	5028	22:39:30	4	-0.7325	0.0562	0.0656	0.0642	0.0071	0.0081
1L11	5612	5610	22:44:30	4	-0.751	0.071	0.0791	0.0729	0.0079	0.0087
1L12	6143	6102	22:49:30	4	-0.77	0.0929	0.0996	0.0989	0.0089	0.0096
1L13	6143	6596	22:54:30	4	-0.7873	0.1187	0.1237	0.1234	0.0101	0.0106
1L14	7007	7094	22:59:30	4	-0.8067	0.1542	0.1583	0.1579	0.0112	0.0118
1L15	7634	7509	23:04:30	4	-0.8243	0.1847	0.1887	0.1881	0.012	0.0127
1L16	8111	8149	23:09:30	4	-0.8461	0.226	0.2297	0.2288	0.0129	0.0136
1L17	864	8312	23:14:30	4	-0.8674	0.2665	0.2701	0.2688	0.0135	0.0142
1L18	9082	9078	23:19:30	4	-0.8948	0.3161	0.32	0.3185	0.0138	0.015
1L19	9547	9491	23:24:30	4	-0.9446	0.3979	0.4049	0.402	0.0132	0.0159
	35		23:40:00	2	-1.056	0.0968	0.8368	0.8346	-0.017	-0.0043

APPENDIX D

This appendix contains photographs taken during shaft construction and testing. The photograph descriptions are as follows:

Photo		Page
D1	Shaft excavation using a truck mounted rotary drill.	134
D2	Spinning the flight auger to remove the drill cuttings.	134
D3	Core barrel used for excavating rock.	135
D4	An Osterberg cell during the assembly of the test apparatus.	135
D5	Osterberg cells attached to the placement channels.	136
D6	Placing the Osterberg cell assembly into the shaft via a boom truck.	136
D7	Placing the concrete into the shaft	137
D8	Placing the concrete into the shaft	137
D9	Dial gages attached to the telltale rods and reference beam	138
D10	Dial gages attached to the telltale rods and reference beam	138
D11	The PC data collector during the testing process.	139
D12	The tent surrounding the test site.	139

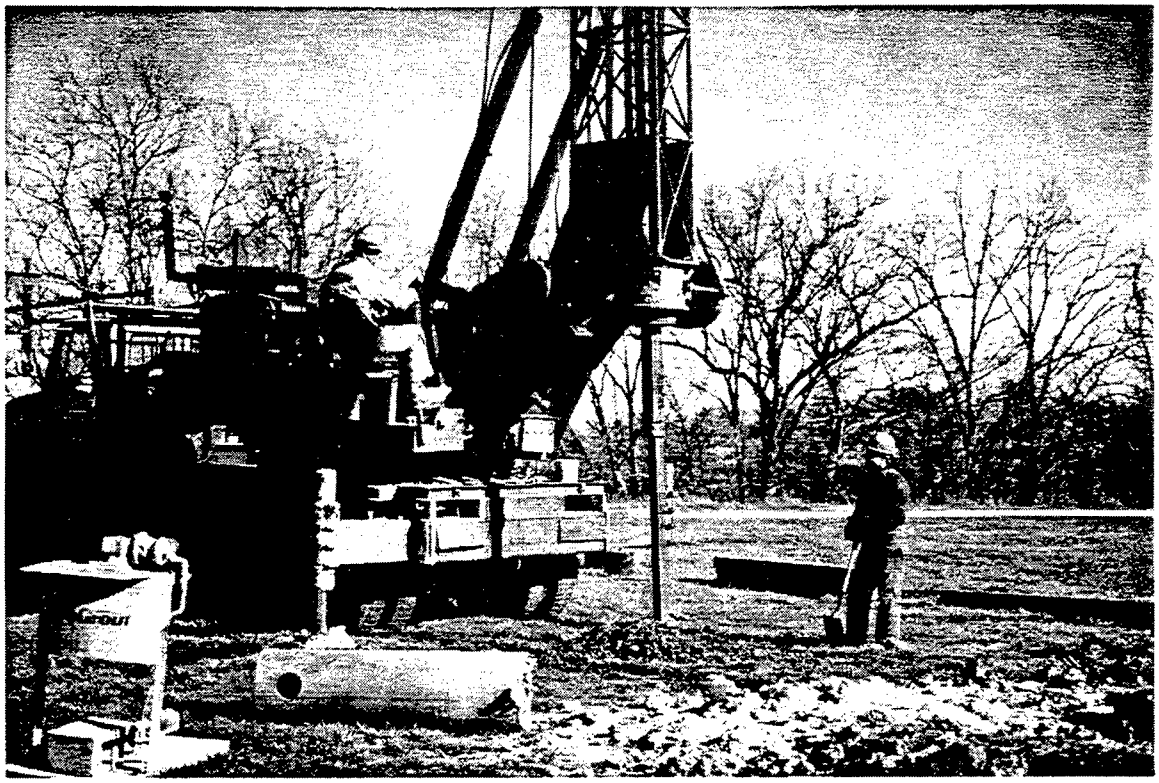

D1

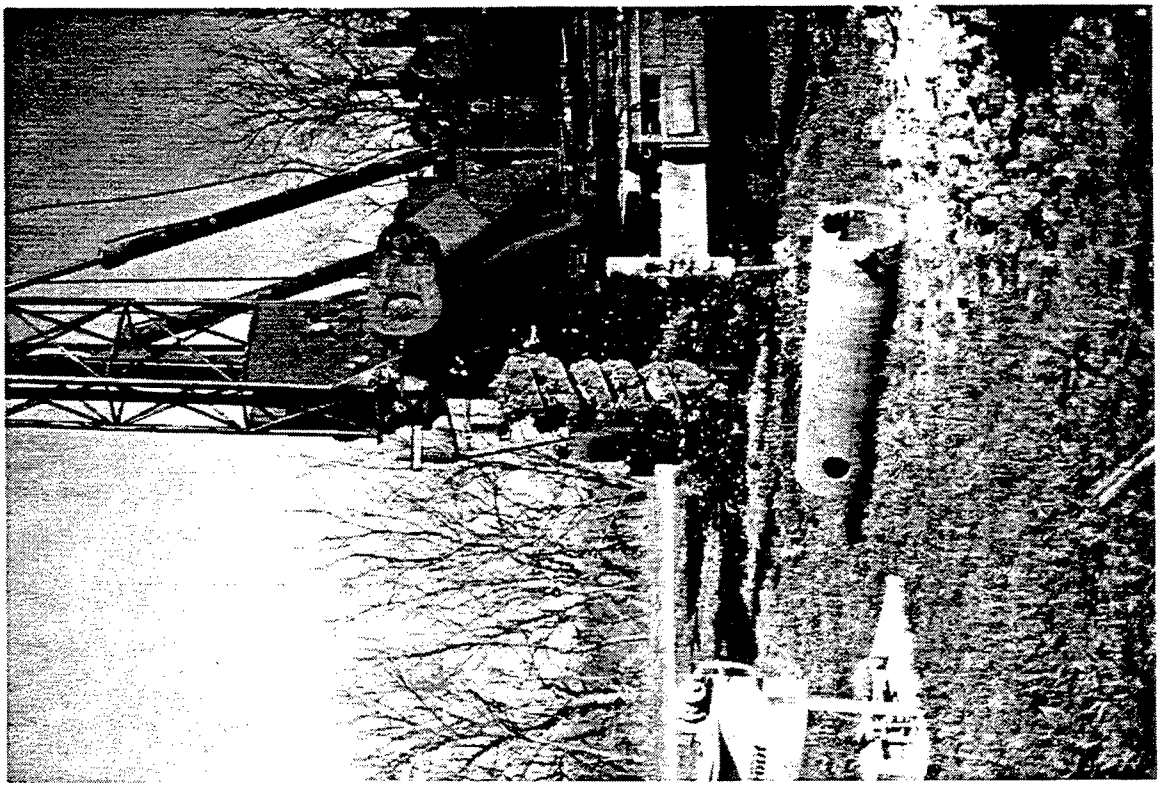

D2

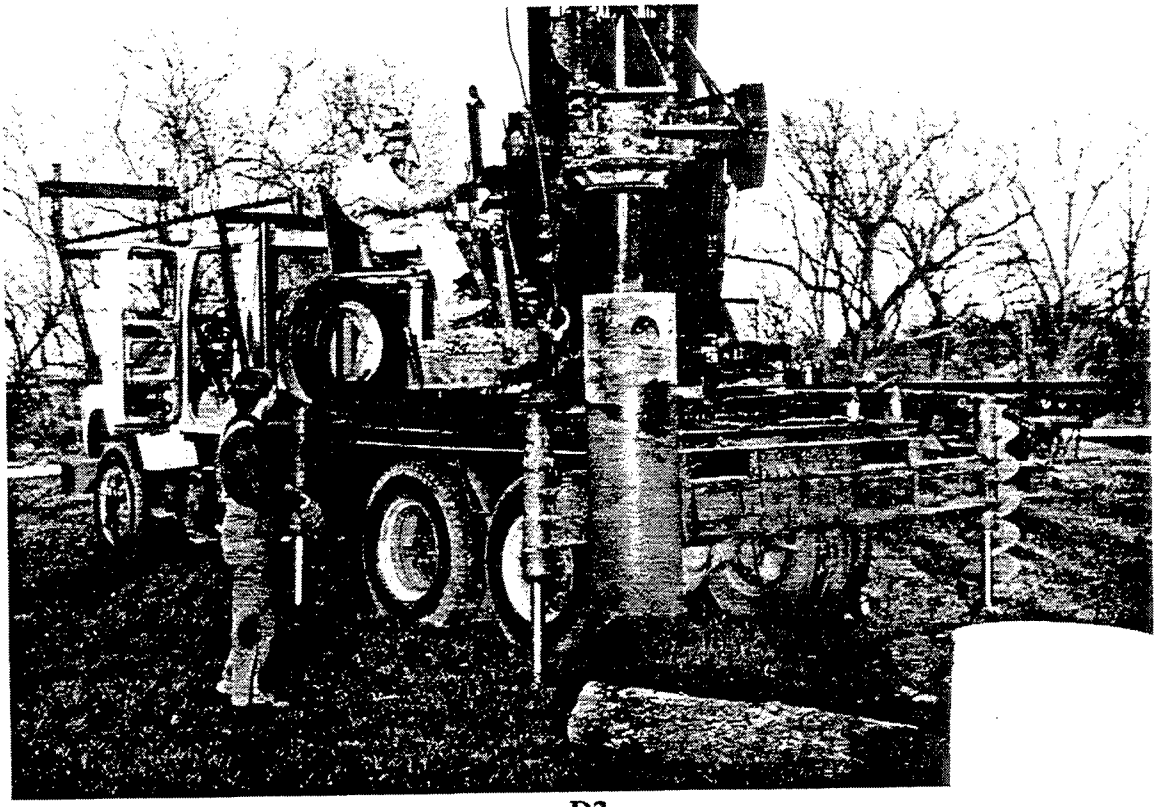

D3

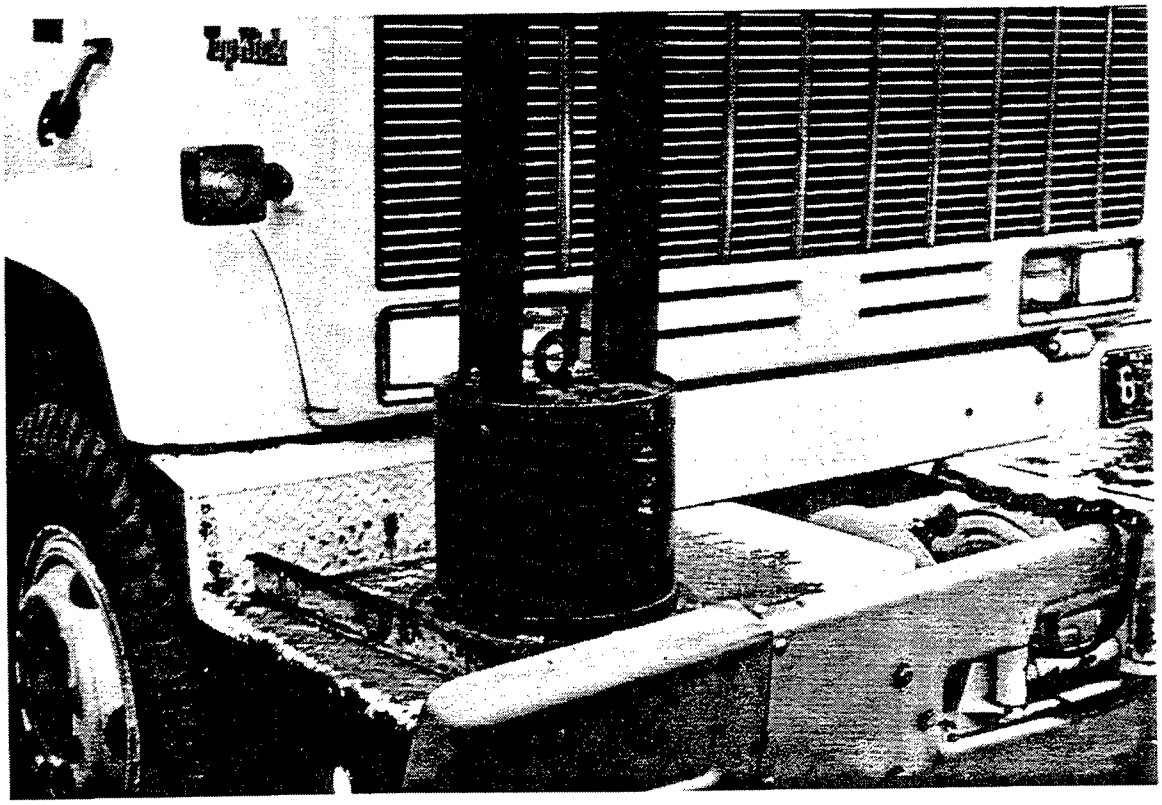

D4

D5

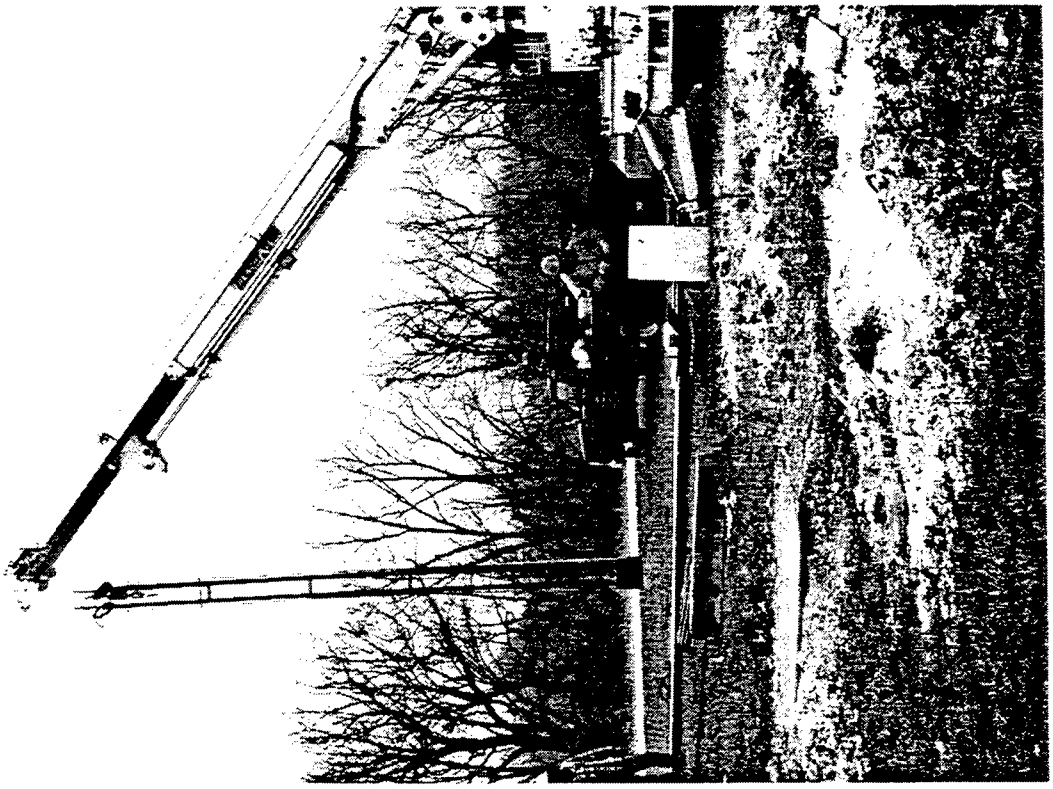

D6

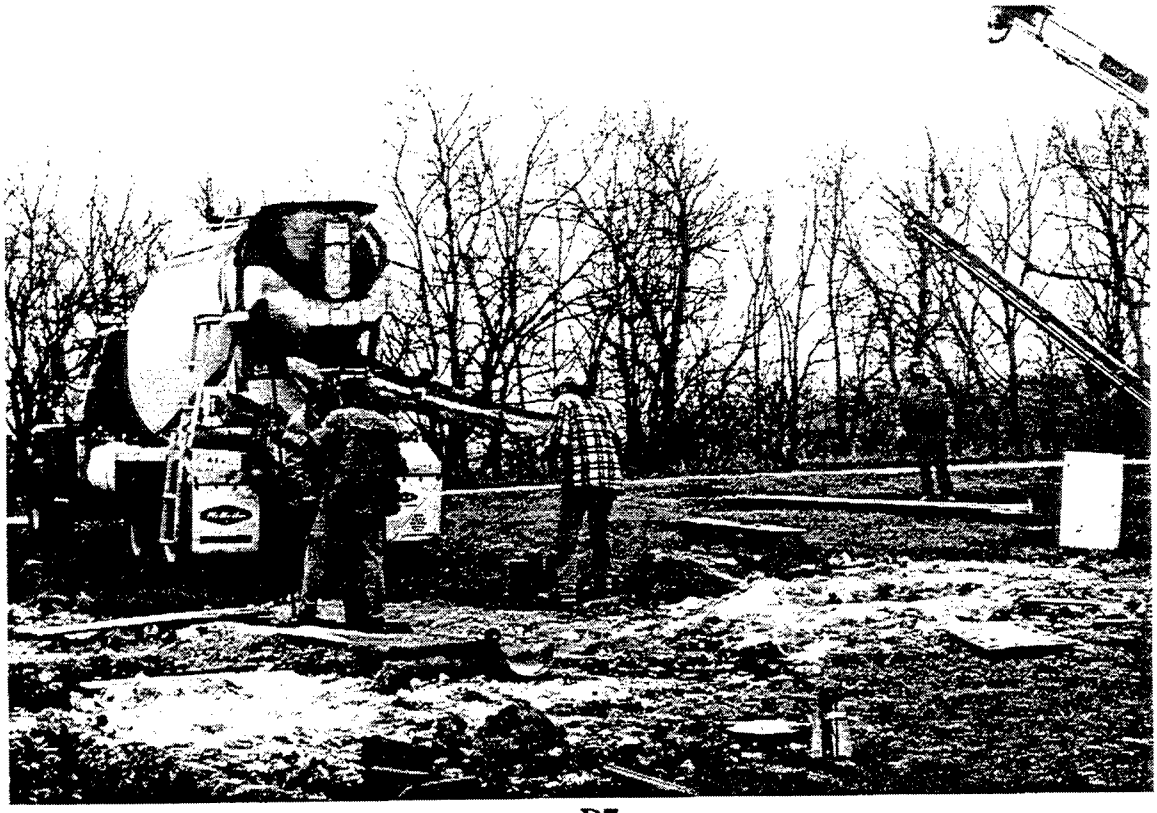

D7

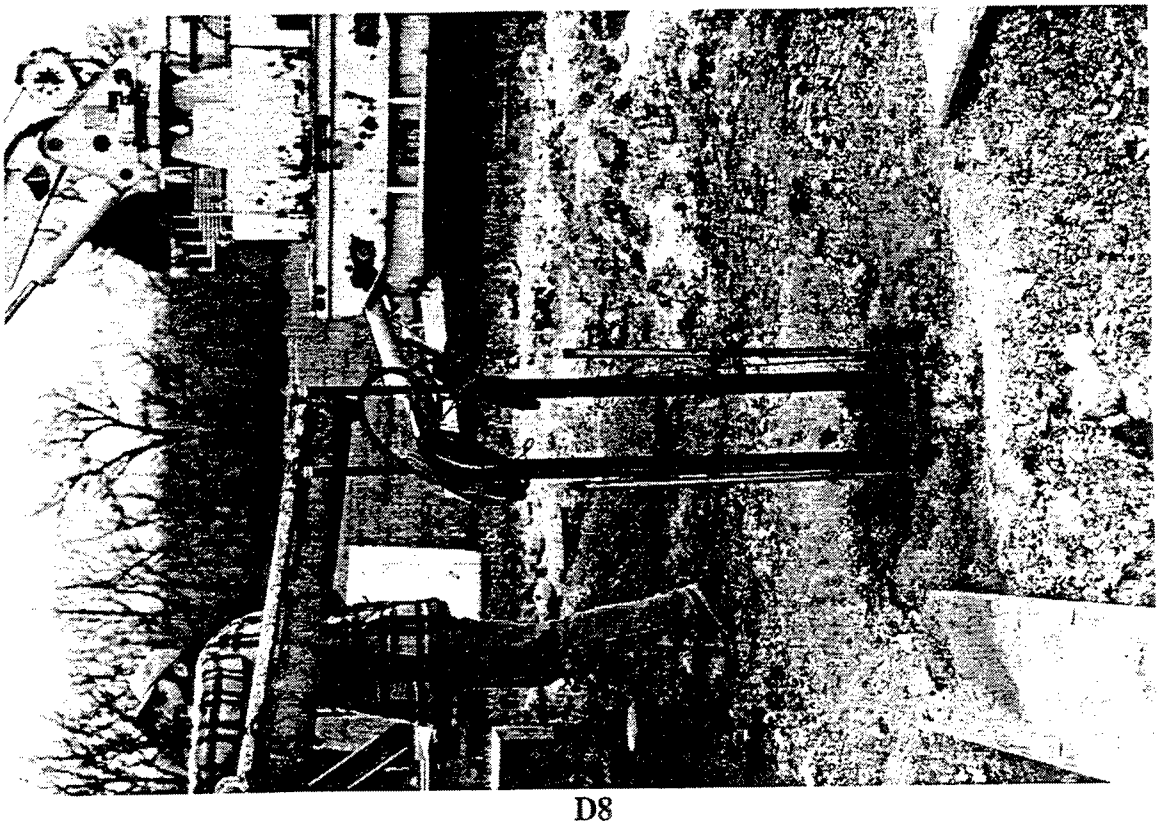

D8

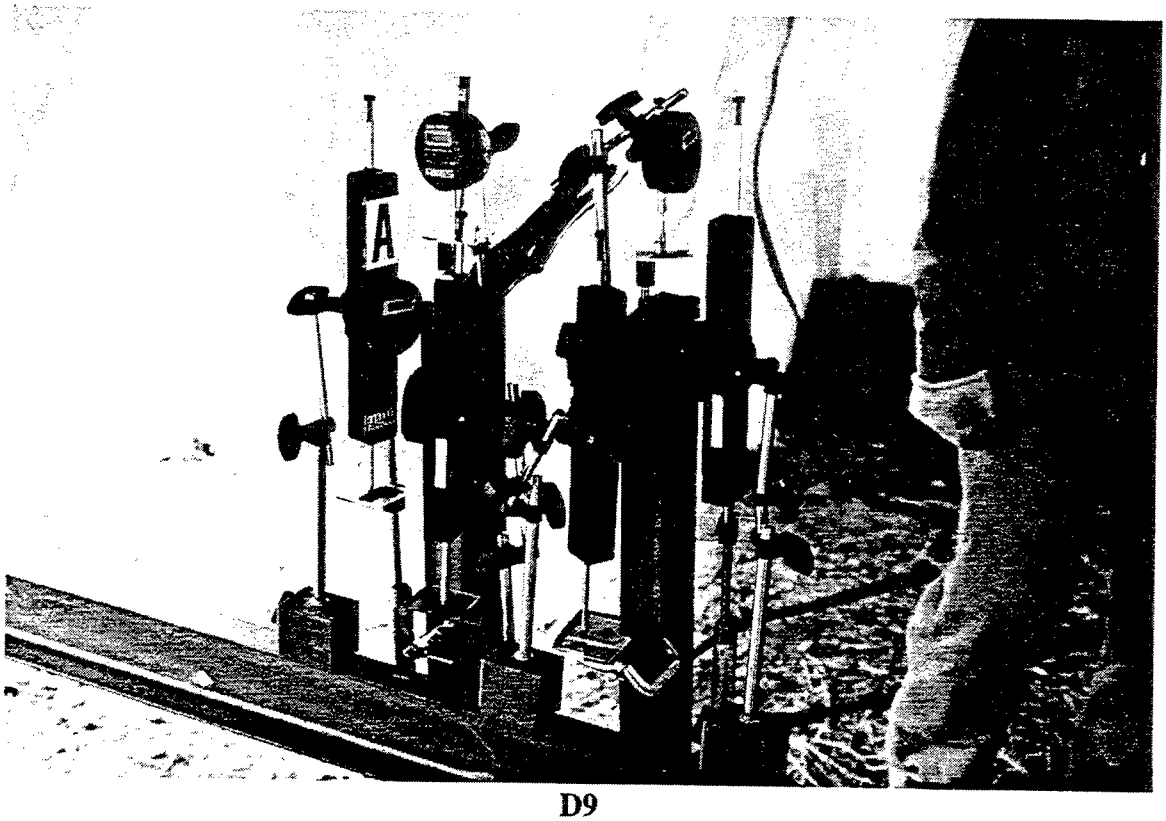

D9

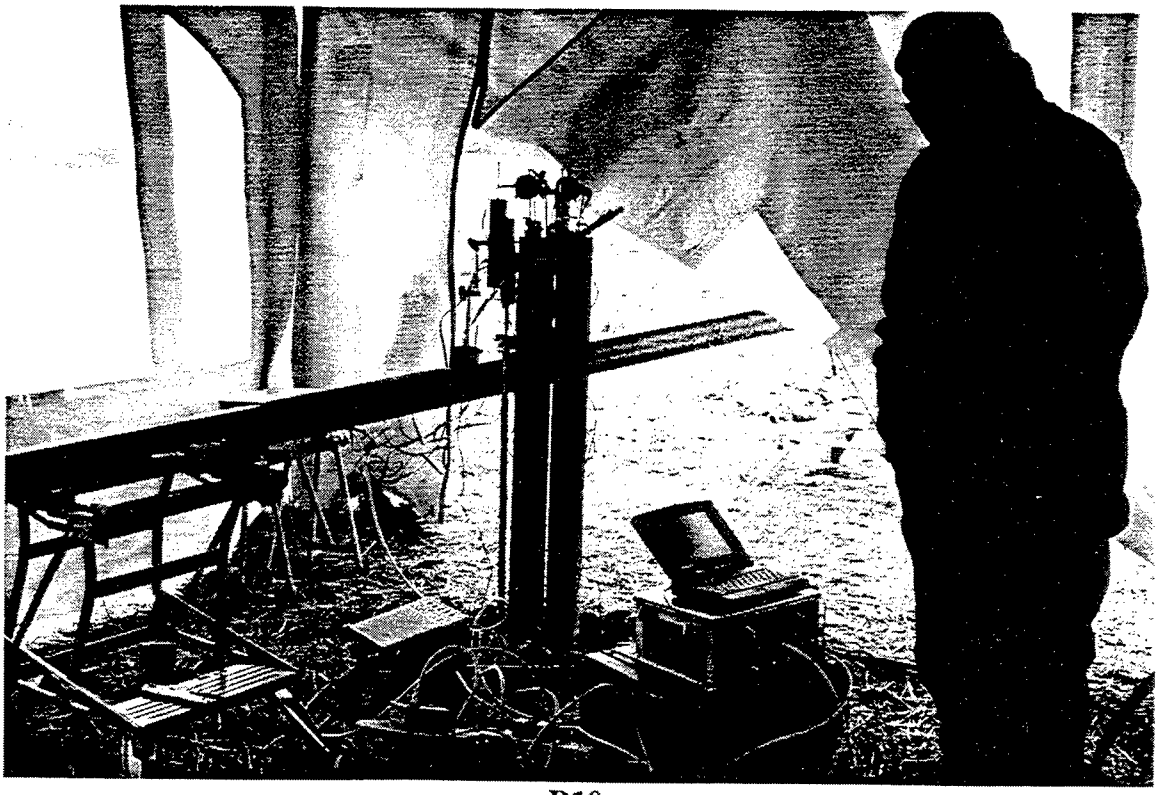

D10

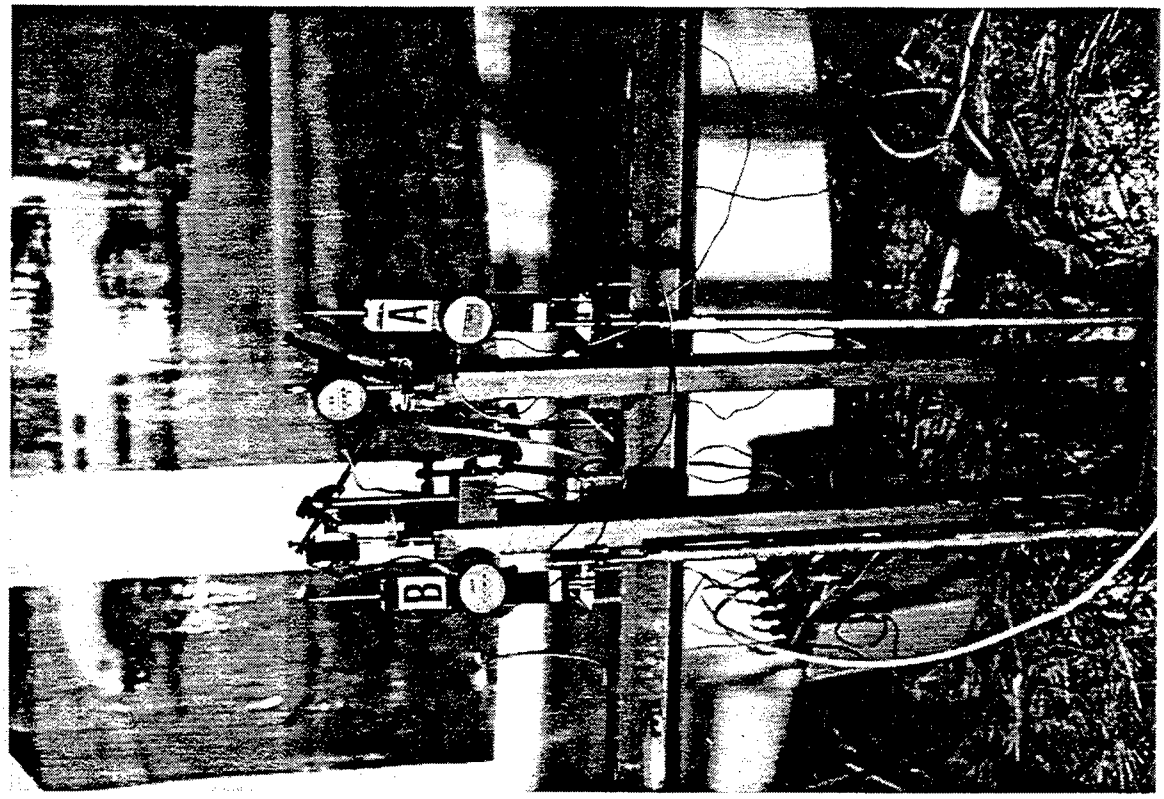

D11

D12